

For Takeshi B.

Acknowledgements

I wish to thank my thesis supervisor Dr. Rüdiger Klein who gave me the opportunity to do my PhD work in his lab and directed my scientific work all these years.

Special thanks to Dr. Tomoko Iwata for offering me a fruitful collaboration and for supervising the first part of my PhD studies.

I thank all my collaborators, especially Guido Panté and Lu Qun for providing tools to do my studies and interesting discussion. Special thanks also to lab members Joaquim Egea and Jenny Köhler who very kindly provided DNA constructs and antibodies.

I thank Angel Nebreda at EMBL as member of my thesis committee for his precious suggestions.

Special Thanks to Sidney Cambridge for critically reading and proofreading this thesis and for his friendship.

I acknowledge all members of the Klein lab for providing a great environment both in the lab and in the Biergarten. Especially I am grateful to Svetla Dimitrova, Joaquim Egea, Jenny Köhler, Archana Mishra, Laura Knott, Elsa Martinez, Taija Mäkinen, Stefan Weinges and Manuel Zimmer, for their help, critical discussions and friendship.

I would like to thank all the people at the Max-Planck Institute of Neurobiology who have supported and encouraged my work, especially the members of the labs of Amparo Acker-Palmer and Gaia Tavosanis for their discussions during our joint group meetings.

**A DNA-Microarray screening: δ -Catenin, a new
mediator of Eph-ephrin signaling**

Dissertation

Der Fakultät für Biologie der
Ludwig-Maximilians Universität München

Eingereicht am 20.5.2005 von
Luca Dolce

First “Gutachter“: Dr. Rüdiger Klein

Second “Gutachter“: Dr. Angelika Böttger

The work presented in this thesis was performed from March 2001 to August 2001 in the laboratory of Dr. Rüdiger Klein at the European Molecular Biology Laboratories (EMBL) Heidelberg, Germany; and from September 2001 to April 2005 at the Max-Planck Institute of Neurobiology Munich, Germany.

Erklärung

Ich versichere, daß ich meine Dissertation selbstständig, ohne unerlaubte Hilfe angefertigt, und mich dabei keiner anderen als der von mir ausdrücklich bezeichneten Hilfen und Quellen bedient habe.

Die Dissertation wurde in der jetzigen oder ähnlichen Form bei keiner anderen Hochschule eingereicht und hat noch keinen sonstigen Prüfungszwecken gedient.

(Ort, Datum)

(Luca Dolce)

1. TABLE OF CONTENTS

1. TABLE OF CONTENTS	6
2. ABBREVIATIONS	9
3. PREFACE	14
4. SUMMARY	16
5. INTRODUCTION	17
5.1 Introduction outline.....	18
5.2 The generation of the dendritic tree.....	19
5.2.1 Dendrite outgrowth.....	20
5.2.2 Dendrite guidance.....	21
5.2.3 Dendrite branching.....	21
5.2.3.1 Role of Rho family GTPases in dendrite branching.....	23
5.2.3.2 Downstream cellular effectors of Rho family GTPases	25
5.2.3.3 Extracellular cues that trigger Rho family GTPases signalling cascade.....	28
5.2.3.4 Spine formation.....	29
5.3 Eph receptors and their ephrin ligands.....	33
5.3.1 The Eph class of receptor tyrosine kinases.....	33
5.3.2 Ephrin ligands.....	34
5.3.3 Signaling mechanisms by Eph receptors and ephrin ligands.....	36
5.3.3.1 Mechanisms of Eph receptor forward signaling.....	46
5.3.3.2 Mechanisms of ephrin ligand reverse signalling.....	40
5.3.4 Effects of Eph-ephrin signaling.....	43
5.3.4.1 Forward and reverse signaling during axon guidance.....	43
5.3.4.2 Eph/ephrins and synaptic plasticity.....	45
5.4 cDNA Microarrays.....	47
5.5 New candidate molecules for dendritic development: δ -Catenin.....	50
5.5.1 Molecular structure.....	50
5.5.2 Expression pattern.....	52
5.5.3 The biological functions of δ -Catenin.....	56
5.5.3.1 δ -Catenin in cell junctions.....	56
5.5.3.2 δ -Catenin in dendrites and synapses.....	59

5.5.3.3 δ -Catenin and actin cytoskeleton dynamics.....	60
6. RESULTS.....	64
6.1 Identification of novel Eph-ephrin downstream effectors using a cDNA microarray screening: δ -Catenin.....	65
6.2 δ -Catenin and Eph-ephrin signaling.....	76
6.2.1 δ -Catenin is phosphorylated by Eph-forward signaling but not by ephrin-reverse.....	76
6.2.2 δ -Catenin and EphA4 interact physically.....	79
6.3 Eph receptor forward signaling, but not ephrin reverse signaling, leads to the formation of δ -Catenin aggregates	87
6.4 δ -Catenin and Eph-ephrin signaling are required for the establishment of proper dendritic morphology.....	92
6.4.1 δ -Catenin and the dynamics of filopodia formation.....	109
6.5. δ -Catenin and HeLa cell migration.....	116
7. DISCUSSION.....	120
7.1 Outlook.....	134
8. MATERIALS AND METHODS.....	135
8. 1 Buffers and solutions.....	135
8.2 Media and antibiotics for bacterial culture	136
8.3 Bacterial strains.....	137
8.4 Media and supplements for tissue culture.....	137
8.5 Media and supplements for primary culture of neurons.....	138
8.6 Cell lines.....	138
8.7 Solutions for cell Transfection.....	139
8.8 Solutions for Biochemistry.....	139
8.9 Plasmids.....	140
8.9.1 Expression constructs.....	140
8.10 Antibodies.....	141
8.11 Chemicals and commercial kits.....	143
8.12 Molecular biology.....	144
8.12.2 Enzymatic treatment of DNA.....	144
8.12.3 Separation of DNA on agarose gels.....	145
8.12.4 Purification of DNA.....	145
8.12.5 Transformation of competent E. coli by electroporation.....	145
8.13 Semi-quantitative real-time PCR.....	146
8.13.1 cDNA preparation.....	146
8.13.2 PCR primers and templates.....	146
8.13.3 LightCycler RT-PCR.....	146

8.14 Primary culture of cortical neurons for biochemistry	147
8.14.1 Stimulation of cells.....	147
8.15 Primary culture of neurons for immunocytochemistry, cell imaging and time lapse imaging.....	148
8.15.1 Transfection of cell lines and primary neurons.....	148
8.15.2 Time-lapse imaging.....	149
8.15.3 Immunocytochemistry and cell imaging.....	149
8.16 Microarray.....	150
8.16.1 Microarray production.....	150
8.16.2 RNA extraction and preparation of fluorescent probes.....	151
8.16.3 Microarray hybridization.....	151
8.16.4 Microarray analysis.....	151
8.16.5 Insert cloning and generation of probes for various uses.....	152
8.17 Boyden chamber assay.....	152
8.18 Sholl analysis.....	153
8.19 Biochemistry.....	153
8.19.1 Cell lysis.....	153
8.19.2 Immunoblotting and immunoprecipitation.....	154
8.20 Histology.....	154
8.20.1 Vibratome sections for <i>in situ</i> hybridization.....	154
8.20.2 <i>In situ</i> hybridization.....	155
9. BIBLIOGRAPHY.....	157
10. CURRICULUM VITAE.....	174

2. ABBREVIATIONS

Abi-1 Abl interacting protein-1

Abl Abelson kinase

ACp Anterior Commissure, posterior

AMP Adenosin-5'-monophosphate

AMPA D-2-amino-3-hydroxy-5-methyl-4-isoxazole-propionic acid

AP Adaptor protein

APS Ammonium-persulfate

Arg Abelson related gene

ARP2/3 Actin related protein 2/3

ATP Adenosin-5'-triphosphate

BBS BES buffered saline

BDNF Brain-derived neurotrophic factor

BES N,N-bis[2-hydroxyethyl]-2-aminoethanesulfonic acid

Borax Sodium tetraborate

bFGF Basic fibroblast growth factor

BSA Bovine serum albumine

CAM Cell adhesion molecule

CamKII Ca²⁺/Calmodulin-dependent kinase II

cAMP Cyclic AMP

CAP Cbl associated protein

Cbp Csk binding protein

Cdc42 Cell division cycle 42

cDNA Complementary DNA

CNS Central nervous system

CREB Ca²⁺/cAMP-response element binding protein

Csk C-terminal Src kinase

CXCR CXC motif receptor

DIV Days *in vitro*

DMEM Dulbecco's modified Eagles medium

DNA Deoxyribonucleic acid

D-PBS Dulbecco's phosphate buffered saline

E Embryonic day

EDTA Ethylenediamine-tetra acetic acid

EGFP Enhanced green fluorescent protein

Eph Erythropoietin-producing hepatocellular

Ephexin Eph-interacting exchange protein

Ephrin Eph family receptor interacting protein

ERK Extracellular regulated kinase

EYFP Enhanced yellow fluorescent protein

FAK Focal adhesion kinase

FBS Fetal bovine serum

FNIII Fibronectin type III

Fyn Fgr/Yes-related Novel gene

G Protein GTP binding protein

GAP GTPase activating protein

GDP Guanosine diphosphate

GEF Guanine nucleotide exchange factor

Glob Globular (domain)

GluR Glutamate receptor subunit

GPI Glycosylphosphatidylinositol

GRIP Glutamate receptor interacting protein

HBSS Hank's balanced salt solution

Hepes (Hydroxyethyl)-piperazine-ethane sulfonic acid

HGF Hepatocyte growth factor

IF Immunofluorescence

Ig Immunoglobulin

IH Immunohistochemistry

IP Immunoprecipitation

KD Kinase dead

LB Luria-Bertani

LTD Long-term depression

LTP Long-term potentiation

MAPK Mitogen-activated protein kinase

Nck Noncatalytic region of tyrosine kinase

NGF Nerve growth factor

Nik Nck interacting kinase

NMDA N-methyl-D-aspartate

N-WASP Neural Wiskott-Aldrich syndrome protein

PAGE Polyacrylamid gel electrophoresis

PAK P21-activated kinase

PARG PTPL1-associated RhoGAP

PCR Polymerase chain reaction

PDB PDZ binding (domain)

PDGF Platelet-derived growth factor

PDZ PSD95/Discs large/ZO-1

PFA Paraformaldehyde

PI3K Phosphatidylinositol 3-kinase

PICK Protein interacting with C kinase

PKA Protein kinase A

PKC Protein kinase C

PRK2 PKC related kinase 2

PSD Postsynaptic density

PSD-95 Postsynaptic density protein 95

PTP-BL Phosphotyrosine phosphatase-basophile like

PY Phospho-tyrosine

Rac Ras-related C3 botulinum toxin substrate

Rap Ras related protein

Ras Rat sarcoma

RGC Retinal ganglion cell

RGS Regulator of G-protein signaling

Rho Ras homologous member

RNA Ribonucleic acid

Robo Roundabout

ROCK Rho-associated, coiled-coil containing protein kinase

Rpm Round per minute

RT Room temperature

RT-PCR Real time PCR

RTK Receptor tyrosine kinase

SAM Sterile- α -motif

SC Superior colliculus

SDF-1 Stromal cell-derived factor 1

SDS Sodium dodecyl sulfate

SFK Src family kinase

SH Src homology

Src Sarcoma virus transforming gene product

TEMED N,N,N',N'-Tetra-methylethylenediamine

VASP Vasodilator-stimulated phosphoprotein

WB Western blot

Wnt Wntless-type mmtv integration site family

ZO1 Zona-occludens

3. PREFACE

During the development of multicellular organisms cells divide, migrate, differentiate and die in a spatially and temporally coordinated manner. One impressive example of morphogenesis is the development of the brain. Billions of neuronal cells begin to form a precise network of nerves and synaptic connections. Neurons are highly polarized cells, with an axon that transmits information from the cell to the environment and a dendritic tree that receives and decodes the signals arriving to the cell from the environment. During development, the establishment of neuronal polarity is a crucial event and it normally follows precise steps. Axonogenesis, or axon generation, is the first event of neuronal polarization. An axon arises from young, undifferentiated neurons, and then extends away from the cell to cover specific territories, often enduring particularly long journeys in order to establish the right connection and finally take up to delivering a specific electric message. The process of “dendritogenesis” or dendrite generation, immediately follows, and it consists of the outgrowth of tiny single processes that elongate, branch and further increase their complexity overtime resulting in the formation of an extensive and intricate dendritic “tree”. Mature neurons come in contact with axons of a number of other neurons through the complex dendritic network, receiving and integrating electric input messages, and then further transmitting the packages of information to the rest of the neuron and further.

The complex processes of axonogenesis, dendritogenesis and the establishment of the proper neuronal networks require that cells communicate with other cells and with their environment, the correct wiring of the nervous system relying on the ability of neurons to find and to recognize their appropriate synaptic partners during development. A growing axon with its highly dynamic growth cone encounters, for example, several environmental cues on its way, each bearing a message that directs the growing process in a defined direction. Extracellular information is received for example, via surface receptors that recognize specific stimuli and transduce signals into the interior of the cell

in order to evoke the proper responses, which may translate in a “stop” message or a “go”. Similar mechanisms govern the generation, correct extension and branching of the dendritic tree. The molecular mechanisms and the environmental cues driving axonogenesis and axonal guidance have been partially uncovered in the last years whereas less is known about the processes leading to dendritogenesis. The identification of new molecular players in dendritogenesis, both at a cellular level and as extracellular cues, is therefore a particularly interesting and challenging field.

4. SUMMARY

Signaling between ephrin ligands and their Eph receptors is crucial for several developmental processes. During the development of the nervous system some growth factors like the neurotrophins have been shown to be key regulators of dendritogenesis and dendritic architecture. Eph-ephrin signalling instead, has been mostly shown to be crucial for axon guidance and local events like the promotion of spine formation and maintenance, and synaptic plasticity, at later stages of neuronal development. Very little evidence is available that shows involvement of Eph-ephrin signalling in earlier stages of neuronal morphogenesis and their role as modulators of dendritic development in a broader structural way.

In the first part of the project, a microarray screening was carried out in order to identify new players in the Eph-ephrin signalling pathway. δ -Catenin, a developmental protein was found to be strongly induced by the activation of the Eph-ephrin system. δ -Catenin is a member of the Catenin family, proteins that are mainly involved in the formation and reinforcement of adherens junctions. Some members of this family, like β -Catenin and the nervous system-specific δ -Catenin, have recently been found to be crucial players in dendritic morphogenesis.

The second part of the project was aimed at elucidating the activity of δ -Catenin in dendritogenesis, characterising its potential role as a new effector in Eph-ephrin signalling, and establishing a biochemical link between the two.

5. INTRODUCTION

5.1 Introduction outline

The first part of this introduction will cover specific aspects of dendritogenesis, its chronology, what it is known about the extracellular cues directing it and the molecular mechanisms that lie downstream.

The second part will cover more specifically the nature of Eph-ephrin signalling, some of the neuronal developmental processes influenced by it and the molecular machinery downstream.

The third part will review the available information on candidate gene δ -Catenin: from protein structure to the known biological functions.

5.2 The generation of the dendritic tree

Although the processes of the generation of a dendritic tree are complex and diverse, they can be separated broadly into a few essential steps. First, dendrites grow out from morphologically immature and unpolarized young neurons and attain characteristic growth rates, lengths, diameters and molecular compositions, different from those neurites which will later be defined as axons. Second, dendrites extend in a defined direction and increase in diameter. Third, they start forming branches at defined intervals. Fourth, as dendrites elaborate, many also generate filopodia and small specialized protrusions called spines that are the major synaptic sites in the mammalian brain (see **figure 5.1**)

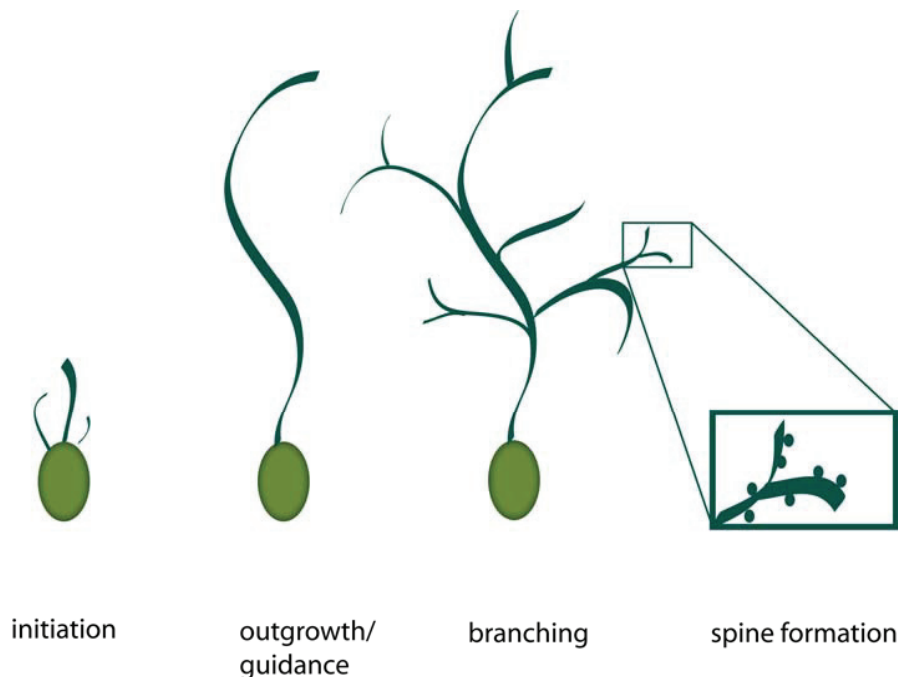


Figure 5.1 The four major steps of dendritogenesis. Initiation, outgrowth and guidance, branching and spine formation (modified from Scott and Luo, 2003).

5.2.1 Dendrite outgrowth

To form connections with the correct presynaptic axon, dendrites must sprout, and extend away from the neuronal cell body into their target field. The outgrowth is initiated by a local event of subcortical actin polymerization in an organized manner, similar to the formation of lamellipodia. Bundles of actin filaments push the cellular membrane forming a protrusion that is almost simultaneously invaded by microtubules, polymerizing in an oriented manner, and contributing to the elongation and stabilization of the process.

Several extracellular factors have been shown to contribute to dendritic sprouting and elongation. One example is a GPI-linked candidate plasticity gene 15 (CPG 15) that promotes tectal projection neurons to extend their dendrites when over-expressed in *Xenopus* tectal cells (Nedivi et al., 1998). Another is osteogenic protein 1 (OP-1), a member of the transforming growth factor- β (TGF- β) superfamily, which has been demonstrated to stimulate dendrite growth from sympathetic neurons in culture with nerve growth factor (NGF) as a cofactor and to promote primary dendrite elongation in E18 mouse cortical neurons (Lein et al., 1995; Le Roux et al., 1999).

NGF, together with brain derived neurotrophic factor (BDNF), neurotrophin 3 (NT3) and NT4/5, belongs to the family of neurotrophins; they are dimeric secretory proteins that signal through receptor tyrosine kinases, known as TrkA, TrkB, TrkC and the co-receptor p75NTR.

Neurotrophins have also been shown to increase dendritic length and complexity in several studies *in vivo* and *in vitro*, in cultures and in brain slices. (McAlister et al., 1995; McAlister et al., 1996). Time lapse imaging of live rat hippocampal neurons in slice cultures (Horch et al., 1999) showed that BDNF induces dendritic sprouting.

The dynamics of dendritic sprouting and elongation and especially the cellular pathways through which extracellular signals exert their effects have not yet been fully understood and it is not clear whether these factors act directly by locally regulating the cytoskeleton or if they turn on a specific genetic program for dendritic sprouting from undifferentiated neurons. Rho family GTPases whose roles are much better characterized in later dendrite development, could also be involved in dendritic sprouting.

5.2.2 Dendrite guidance

Similar to axonal processes, a growing dendrite has to steer toward its target and cross territories in order to establish the right connections. Not so much is known about dendritic guidance, whereas axonal guidance has been more extensively studied. In this process diffusible proteins like semaphorins, for example, are important. These molecules have been shown to be crucial for axonal growth cone guidance but they also seem to be involved in dendritic growth cone guidance.

Semaphorin (Sema) 3A normally causes repulsion or collapse of axonal growth cones. Interestingly, knock-out mice for Sema 3A also display defects in dendrite guidance of cortical pyramidal neurons (Polleux et al., 1998; Polleux et al., 2000) together with the expected axonal phenotypes. Sema 3A appears to serve as an attractant for the apical dendrites of pyramidal neurons in cortical slices (Polleux et al., 2000) because cortical pyramidal neurons send dendrites towards the source of endogenous Sema 3A (Giger et al., 1996). This asymmetric mechanism could be dependent on different concentrations, in dendrites and axons, of Guanylate cyclase (GCS), the enzyme that synthesizes cyclic nucleotide guanosine 3'/5'-monophosphate (cGMP) (Luo et al., 1993; Messersmith et al., 1995). cGMP seems to be necessary for Sema 3A-mediated dendritic attraction and a higher concentration in growing dendrites has been reported (Giger et al., 1996). Axonal

and dendritic growth cones may therefore share similar guidance mechanisms and transduction machinery even if they are differentially regulated.

5.2.3 Dendrite branching

To cover the correct target fields and reach the final neuronal “complexity”, most dendrites need to form an extensive set of dendritic branches. Two major mechanisms of dendrite branch formation have so far been described: one is the ‘splitting’ of growth cones which was first observed predominantly in *in vitro* studies (Bray et al., 1973), and second, the so called ‘interstitial’ branching, a process in which new branches arise along the sides of established dendritic shafts. This latter mechanism appears to be predominant in physiological conditions.

Time lapse studies of live pyramidal neurons from rat hippocampus slices have demonstrated that each branch initially appears in the form of a single filopodium and then it elongates assuming its defined morphology (Dailey and Smith, 1996).

Most filopodia emerge from and quickly retract into the dendritic shaft; some develop further into growth cone-like structures which then mature into branches (Daley et al., 1996). Stabilized branches extend and become substrate for further branch addition and stabilization, so that the final complexity is reached by iterative cycles of branch addition, stabilization and extension (see **figure 5.2**).

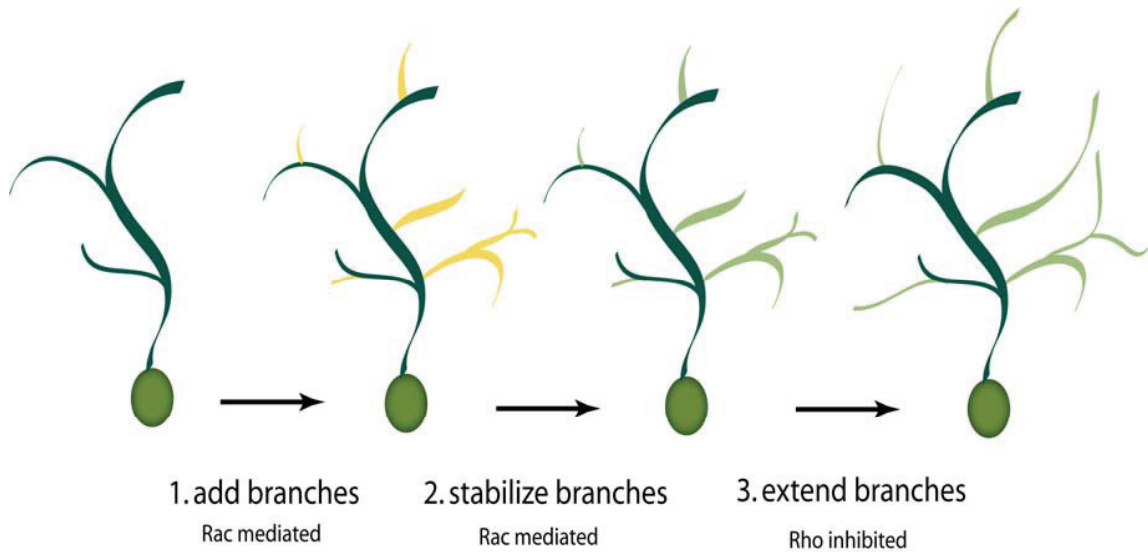


Figure 5.2. Rho GTPase-dependent stages of dendritic branching. For the correct development of dendrites, three distinct processes are required. Branches must be first added to the arbor and Rac plays a key role. Newly formed branches must then be stabilized and the process is also Rac-mediated. Finally, stabilized branches extend and these branches then support further branch additions in an iterative process. Branch extension is mediated by a decrease in RhoA activity. High levels of RhoA repress branch stabilization (modified from Cline and Van Aelst, 2004).

Newly generated filopodia arise mainly as bundles of actin filaments and F-actin seems to be the main component until the filopodium is committed to form a new branch and is therefore stabilized by the invasion of microtubules. The elongation is then elicited by a dual process involving dynamic F-actin structures at the leading edge of the growth cone and tubulin to stabilize and reinforce the newly formed process.

Similar to dendritic branch formation, the emergence of dendritic spines involves lateral protrusions of membrane and cytoskeleton: some of the newly formed filopodia are not stabilized in branches but mature into spines suggesting that the initial steps of the formation of both spines and branches could be similarly regulated but then differ later according to extracellular cues or neuronal activity (Altman et al., 1972; O’Leary et al., 1988; Yu et al., 1994; Daley et al., 1996).

5.2.3.1 Role of Rho family GTPases in dendrite branching

Because of the crucial role played by actin in the early stages of dendritic branching, the regulators of the actin cytoskeleton have been the most studied molecules, and specifically the Rho family of small GTPases have emerged as key integrators of environmental cues regulating actin dynamics in the dendritic cytoskeleton (see **figure 5.2**). The Rho family of small GTPases are low molecular weight guanine nucleotide binding proteins. They alternate between an ‘active’ GTP-bound state and an ‘inactive’ GDP-bound state. Only in their GTP bound state can those GTPases interact with downstream molecules that mediate their effect. The ratio of the two forms is regulated by a set of other molecules, for example the GTPase activating proteins (GAPs) which increase the hydrolysis rate of bound GTP and thereby inactivate Rho. Other regulating molecules are the guanine nucleotide exchange factors (GEFs) that instead favor the exchange of hydrolyzed GDP for GTP and thereby activate Rho. The level of activity of such regulators alternately favors one side of the equilibrium (see **figure 5.3**).

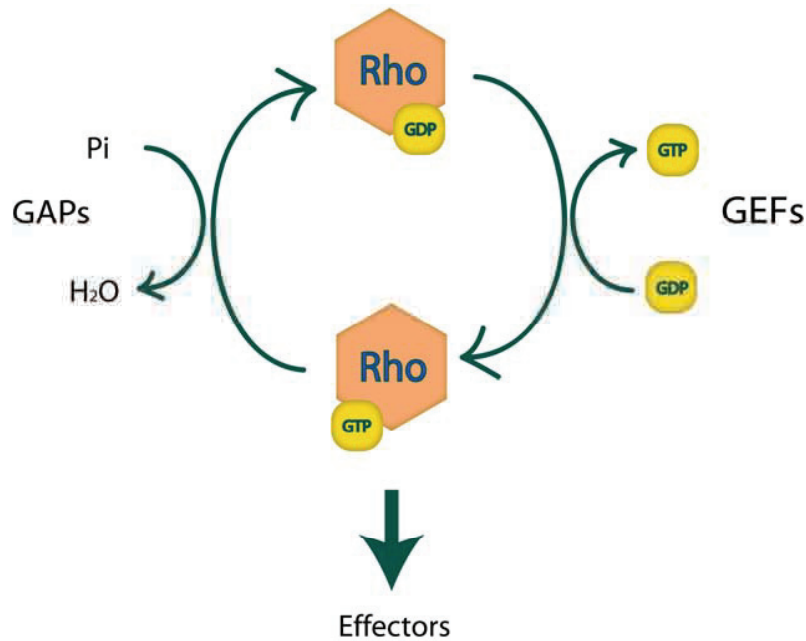


Figure 5.3. Molecular switch of Rho family GTPases. Inactive Rho bound to GDP is transformed into its active GTP bound state by a guanosine nucleotide exchange factor (GEF). Rho bound to GTP activates effector molecules. GTPase activity is promoted by a GTPase activating protein (GAP) that turns back Rho into its inactive GDP bound state.

The best studied members of the Rho family GTPases are cell division cycle 42 (Cdc42), Ras-related C3 botulinum toxin substrate 1 (Rac1) and Ras homologous member A (Rho A). Of the three molecules, Rac 1 and to some extent Cdc42, are key regulators of dendritic branching and dendritic remodelling. Rho A instead, appears to play a key role in regulating overall dendritic and branch lengths (see **figure 5.2**).

It has been shown in *Xenopus* retinal ganglion cells that the expression of dominant negative mutants of Cdc42 and Rac1 reduces dendritic complexity whereas RhoA mutants has no noticeable effect; conversely a dominant active form of Rac1 but not of Cdc42 favours dendritic branching (Ruchhoeft et al., 1999). Other studies with *Xenopus* neurons showed that Rac1 promotes branch addition whereas Rho A mostly seems to affect branch extension (Li et al., 2000) and interestingly, in chick retinal ganglion cells, constitutively active mutants of Rac1 promote the addition of tertiary branches.

Differently to Cdc42 and Rac 1, RhoA activity appears to be mostly inhibitory, as active RhoA functions as a repressor of dendritic growth when bound to GTP while allowing

dendritic growth when inactive. Under physiological conditions the Rho A pathway is normally repressed and is locally activated when dendritic growth needs to be limited. Expression of a constitutively active Rho A mutant in several neuronal systems generally results in a decrease in dendritic growth. Conversely, dominant negative versions of Rho A or RhoA selective inhibitors result in the opposite phenotype, i.e. a marked increase in total dendritic length. (Nakayama et al., 2000; Ruchhoeft et al., 1999; Wong et al., 2000; Lee et al., 2000).

Not surprisingly, Rho family GTPases are also important for dendritic spine formation; in particular, dominant active forms of Rac1 promote the formation and maturation of dendritic spines in Purkinje cells of transgenic mice and in rat hippocampal and cortical neurons (Luo et al., 1996; Nakayama et al., 2000; Tashiro et al., 2000). In contrast, Rho A activity seems to block spine formation, maintenance and elongation.

Experimental evidence thus suggests that a differential engagement of GTPases controls different structural changes to attain the final dendritic architecture and plasticity. In fact the situation may even be more complex, given recent evidence that there could be a cross talk between Rho GTPases and their upstream and downstream effectors, in the form of feedback loops which ultimately determine the final architectural outcome.

Interestingly, recent studies have shown that intracellular distributions of RhoA, Cdc42 and Rac1 differ according to the neuronal developmental stage in rat hippocampal cultures. During the early stages of process formation, that is during axon and dendritic sprouting, the three GTPases are evenly distributed throughout the cell, suggesting a possible interplay of the three different modulators, in a joint manner.

In fully developed neurons though, RhoA enriches in dendrites, Rac1 in axons, and Cdc42 is equally abundant in both domains, so that at later stages, a polarized segregation of the actin regulatory machinery might play an important role in axonal and dendritic architectural plasticity (Da Silva et al., 2004).

5.2.3.2 Downstream cellular effectors of Rho family GTPases

Members of the Rho family GTPase exert their function through the activation of a cascade of factors all of which tend to affect the dynamics of the actin and/or microtubule cytoskeleton.

Well-known effectors that can be activated by both Rac and Cdc42 belong to the p21-activated kinase (PAK) family of serine/threonine kinases. PAK proteins have been ascribed roles in regulating actin cytoskeleton dynamics and gene expression (Jaffer and Chernoff 2002; Bokoch et al., 2003). These kinases exist in an inactive state in the cytoplasm as a result of their N-terminal autoinhibitory region. Upon binding to Rac-GTP or Cdc42-GTP, the auto-inhibition is relieved, resulting in PAK activation and its auto-phosphorylation. One mechanism by which PAKs affect the actin cytoskeleton involves phosphorylation and activation of the Lin-11, Isl-1, and Mec-3 (LIM) domain-containing kinases (Yang et al. 1998; Edwards et al. 1999; Dan et al. 2001). Once active, these kinases phosphorylate and inhibit cofilin, an actin filament depolymerising factor, with the result of stabilizing actin filaments and promote actin polymerization (Bamburg 1999; Sanyon and Bernard 1999). The regulation of myosins is likely to be another component of PAK-mediated cytoskeletal signalling. There is evidence that PAK1 can interfere with myosin light chain (MLC) function via direct phosphorylation and inhibition of myosin light chain kinase (MLCK) (Sanders et al. 1999; Bokoch 2003). This action of PAK may assist in the disassembly of actin stress fibers triggered by PAK.

Another key mechanism by which Rac and Cdc42 relay signals to the actin cytoskeleton involves the Wiskott-Aldrich-syndrome family of scaffolding proteins. The Wiskott-Aldrich-syndrome protein (WASP) and its closest relative neuronal WASP (N-WASP) are regulated by Cdc42 (Rohatgi et al. 1999). Three other members of this family, WAVE1–3 (also known as Scar proteins) mediate actin-based processes triggered by Rac (Miki et al. 1998; Machesky et al. 1999; Suetsugu et al. 1999; Yamazaki et al. 2003; Yan et al. 2003). Both the WASP and WAVE family members are linked to the actin cytoskeleton through their interaction with the Arp2/3 complex. In the case of WASP/N-WASP, these proteins have been shown to directly bind the activated form of Cdc42. This induces a conformational change that releases the WASP from auto-inhibition,

allowing it to activate the Arp2/3 complex to nucleate the formation of new actin filaments in vitro (Machesky et al. 1999; Rohatgi et al. 1999, 2000; Kim et al. 2000). The WAVE proteins also mediate actin cytoskeletal changes downstream of Rac but without directly binding to it. They, in addition to directly activating the Arp2/3 complex, also influence the activity of profilin which binds a number of actin monomers, preventing spontaneous nucleation and the addition of actin monomer to the pointed end of the filament, but not to the barbed end, and thus directly controlling actin polymerization dynamics (Pollard et al. 2000).

The major downstream effectors of RhoA that mediate GTPase's effects on the cytoskeleton are members of the Rho-kinase (also called ROK/ROCK) family (Leung et al. 1995; Matsui et al., 1996; Nakagawa et al. 1996; Leung et al. 1996).

Rho-kinases are serine/threonine kinases that play several roles in RhoA-induced actin reorganization. They control actin filament bundling by directly phosphorylating and activating MLC, or by phosphorylating and inactivating MLC phosphatase, thereby indirectly increasing MLC phosphorylation and activation (Amano et al. 1996; Kimura et al. 1996). Furthermore, Rho-kinases may promote F-actin accumulation by phosphorylating and activating LIM-K, which in turn phosphorylates and inactivates the actin depolymerization factor (ADF) cofilin (Maekawa et al. 1999; Sumi et al. 1999, 2001; Ohashi et al. 2000; Amano et al. 2001) (see **figure 5.4**).

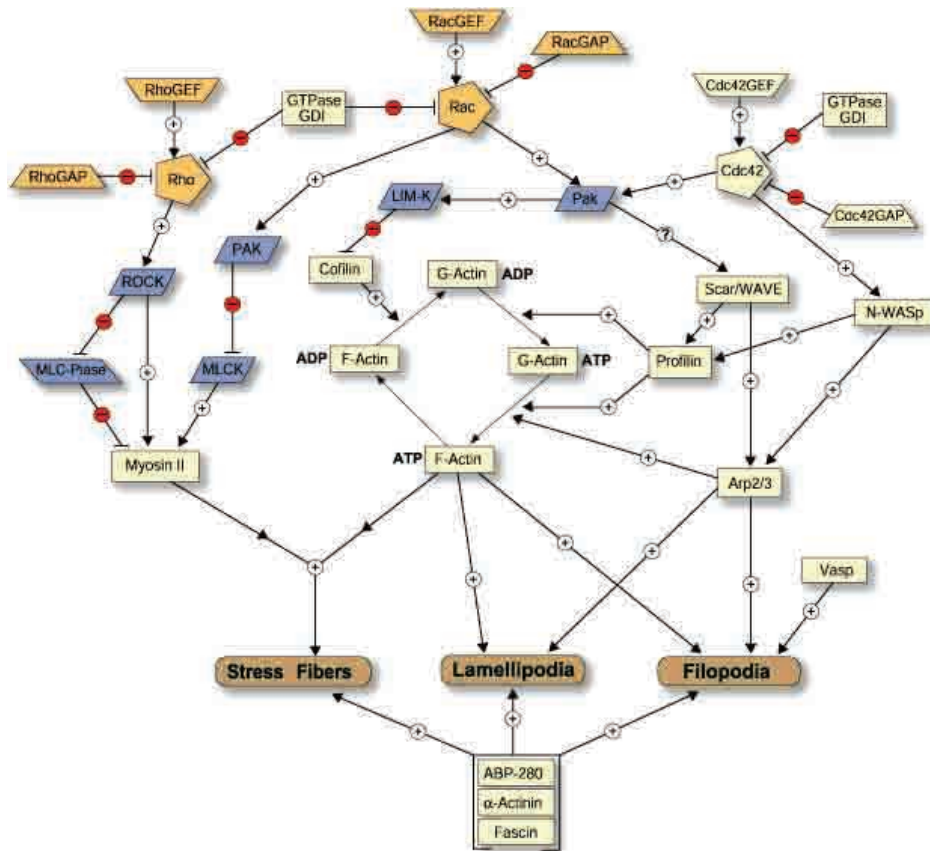


Figure 5.4. The actin cycle: signalling downstream of Rho GTPases (see text for details). Rho, Rac and Cdc42 are positively regulated by GEFs and negatively regulated by GAPs. Other GTPases can

also influence the state of phosphorylation of Rho GTPases. Activation of Rho triggers a signalling cascade mediated by Rho kinase (ROCK) which phosphorylates and activates myosin also through the inhibition of myosin light chain phosphatase (MLC-Ptase). Rac and Cdc42 mediate part of their effects through p21 activated kinase (PAK). PAK can also phosphorylate myosin light chain (MLC) but its main activity is the activation of Lin-11, Isl-1, and Mec-3 kinase (LIM-K); which in turn negatively regulate cofilin contributing to the shift of the equilibrium between G-actin and F-actin towards the filamentous form. PAK may also induce WASP family Verprolin-homologous protein (scar/WAVE) activity positively regulating profilin and activating the complex Arp2/3 and therefore actin polymerization. Activation of Cdc42 positively regulates neuronal Wiskott-Aldrich-Syndrome protein (N-WASP) which in turn activates profilin and Arp2/3 complex promoting actin polymerization.

(From: www.signaling-gateway.org/molecule/rsc/maps/actin_pathway_0.jpg)

5.2.3.3 Extracellular cues that trigger Rho family GTPases signalling cascade

Several studies have shown that synaptic activity is able to regulate dendritic arbour growth and branch dynamics. *In vivo* experiments with *Xenopus* tectal neurons showed that visual stimulation favours dendritic arbour growth and the rate of branch addition and that this effect is abolished by the treatment with blockers of *N*-methyl-D-aspartate (NMDA) and α -amino-3-hydroxy-5-methyl-4-isoxazole propionic acid (AMPA) glutamate receptors suggesting that glutamatergic synaptic transmission is required for the dendritic growth rates (Jan et al., 2003).

Visual stimulation was also reported to promote endogenous Rac activity and to decrease Rho A activity in the optic tectum. Similarly, glutamate receptor activity increases Rac and Cdc42 activity (Li et al., 2002; Sin et al., 2002). Finally, it was shown that the use of dominant negative forms of Rac and Cdc42 and of dominant active Rho A completely blocks arbor development following visual stimulation (Li et al., 2002).

The other main upstream cues that lead to the activation of Rho GTPase signalling and contribute to dendrite complexity, are extracellular signalling molecules whose activity is in some cases, also connected to neuronal activity. These cues, among others, are neurotrophins, semaphorins, slit and the ephrins. Most of the studies have been carried out in the context of axonal growth and guidance and still little is known about the mechanisms through which the above mentioned factors exert their effect on dendritic development and spine formation.

Several studies show the involvement of neurotrophins in dendritic development through Rho GTPase signalling in combination with neuronal transmission, in particular through the NMDA receptors. (Engert et al., 1999; McAllister et al., 1997; McAllister et al., 1995; Schumann, 1999).

Other studies trying to connect neurotrophins and Rho GTPases have suggested that in cortical neurons BDNF is likely to increase arbor complexity by increasing the rate of branch addition and stabilization in a very similar way to that induced by Rac over-expression (Nakayama et al., 2000) .

The already mentioned study by Yu and Malenka (Yu et al., 2003) has shown a connection between dendritic development and the soluble factor Wnt (Wingless), via β -Catenin and through Rho GTPases. Over-expression of β -Catenin increases dendritic arbor growth by a mechanism that requires the interaction with its binding partner N-Cadherin and neuronal activity. Wnt signalling starts from the interaction of the soluble ligand with its membrane receptor, Frizzled, and this leads to the dissociation of β -Catenin from N-cadherin and to the subsequent enhancement of dendritic arbor growth. Neuronal activity induces a release of soluble Wnt and this positively regulates dendritic growth.

5.2.3.4 Spine formation

(also see chapter in Eph-ephrin signalling)

Once a neuron has extended its dendritic tree and covered its target field it begins to establish connections with the axonal projections of other neurons in its environment. The major path of communication between dendrites and axons are the so aforementioned “spines”, typical of excitatory synapses. Immature dendritic protrusions, classified as filopodia, tend to be long and thin, while mature protrusions, or spines, tend to have a well-defined head and neck structure. The cytoskeleton of spines and filopodia is mainly actin based. Because of the importance of actin for spine shape and function, the Rho GTPases play a predictable crucial role in spine formation, maintenance, and physiology (Bonhoeffer and Yuste 2002; Lisman 2003). On the other hand, little is known about the external cues that influence Rho GTPase activity in the context of spine morphogenesis. In general, the effect of Rho A, Rac1 and Cdc42 on spine formation can be generalized such that: activation of Rho causes spine loss whereas activation of Rac and Cdc42 signalling promotes dendritic spine formation (RhoGTPase signalling and their effect on spine morphogenesis are summarized in **figure 5.5**).

Most of the evidence comes from the characteristic spine phenotypes produced by the overexpression of Rho GTPase mutants in neurons or by the treatment with specific inhibitors. Constitutively active Rho A decreases spine density and length in pyramidal neurons in rat and mouse hippocampal slices and cultured rat hippocampal neurons. The use of Rho A inhibitors though, has somewhat contradictory effects depending on the system used: they cause elongation of spine necks, reduce spine density, and increases filopodia density in cultured rat hippocampal neurons but they also increases the density and length of spines in mouse cortical and hippocampal pyramidal neurons in organotypic slices, although dominant negative Rho A does not affect pyramidal spine density in rat hippocampal slices neurons (Nakayama et al. 2000; Tashiro et al. 2000; Pilpel and Segal 2004). The effects of constitutively active Rho A on hippocampal spines has been shown to be mediated by the Rho effector Rho kinase (Nakayama et al. 2000). Rac1 has been shown to play a role in both, the formation and maintenance of dendritic spines. Neurons expressing constitutively active Rac1 tend to form overlapping protrusions which are composed of numerous “mini” spines. Rac activation decreases spine size and increases their density in mouse and rat cortical and hippocampal pyramidal neurons in slices and in cultured rat hippocampal neurons (Tashiro et al., 2000; Nakayama et al., 2000; Pilpel and Segal 2004). In contrast, dominant negative Rac1 causes a reduction in spine density in rat and mouse pyramidal neurons in hippocampal slices (Nakayama et al., 2000; Tashiro and Yuste 2004). Regulators of Rac in the context of dendritic spine morphogenesis include Kalirin and β -PIX. Kalirin-7 is one of the most prevalent RhoA/Rac1 GEF isoforms in the adult rat brain. It contains only the Rac1 GEF domain and it has been shown to activate Rac1 (Penzes et al. 2000, 2001b). In primary cortical neurons, ectopically expressed Kalirin-7 is targeted to spines and increases the number and size of spine-like structures. Conversely, reduced expression of Kalirin in CA1 neurons in hippocampal slices or dissociated rat hippocampal neurons results in reduced spine density (Ma et al.2003). Kalirin-7 has also been implicated in a signalling cascade whereby ephrin-B1 treatment of cultured neurons induces phosphorylation and activation of the EphB2 receptor, redistribution of the Rho-GEF Kalirin to synapses, and

activation of Rac1 and its effector PAK, leading to an increase in the number and size of dendritic protrusions with different morphologies. Interestingly, dominant negative forms of EphB receptor, catalytically inactive Kalirin, dominant negative Rac1 or inhibition of PAK interfere with ephrin-B1-induced spine development (Penzes et al. 2003).

Another important player in Rac-mediated spine formation is β -PIX. β -PIX is a Rac GEF implicated in dendritic spine morphogenesis involving G protein-coupled receptor kinase interacting protein (GIT)1. In cultured hippocampal neurons, a dominant negative GIT1 mutant results in a significant decrease in the number of synapses and normal mushroom-shaped spines, with a concomitant increase in the number of long, thin dendritic protrusions. This phenotype results from disruption of the synaptic localization of GIT1 and mislocalization of its binding partner Beta-PIX and Rac (Zhang et al. 2003). Beta-PIX and GIT1 have also been found in a complex with PAK and Shank, a post-synaptic scaffolding protein shown to interact with glutamate receptors and actin cytoskeletal proteins (Ehlers 1999; Tu et al. 1999; Boeckers et al. 2002 ; Park et al. 2003).

The role of Cdc42 in spine morphogenesis is less defined compared to RhoA and Rac1. Neither constitutively active nor dominant negative Cdc42 appear to have any significant effect on spine density or length in mouse cortical and hippocampal pyramidal cells in slices (Tashiro et al. 2000). Regulators and effectors of Cdc42 implicated in dendritic spine regulation include intersectin-1, N-WASP, and insulin receptor tyrosine kinase substrate (IRSp53). Activated EphB2 receptor physically associates with Cdc42 GEF intersectin-1 and activates its GEF activity in cooperation with neural N-WASP, a regulator of Arp2/3-mediated actin nucleation. This in turn activates Cdc42 and spine morphogenesis in dissociated mouse hippocampal neurons. Interestingly, mutants of intersectin-1, N-WASP, and Cdc42 are all capable of inhibiting spine formation in this system, leading to an increase in protrusion length and a decrease in width, and consequently a loss of mature spines and an increase in filopodia (Irie and Yamaguchi 2002).

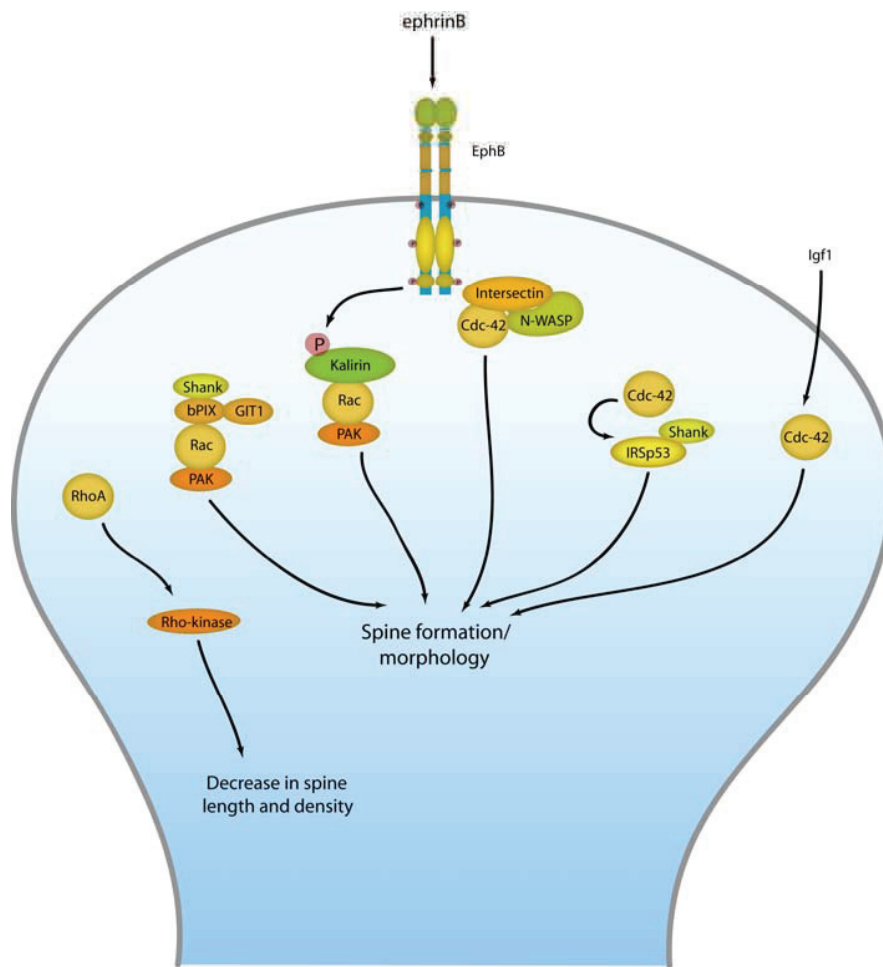


Figure 5.5. Rho GTPase signaling cascades that affect dendritic spine formation. In general, activation of Rac and Cdc42 signaling promotes dendritic spine formation, while activation of Rho/Rho-kinase causes spine loss. See text for details. (GIT1) G protein-coupled receptor-interacting protein; (IRSp53) insulin receptor substrate of 53 kDa; (Igf1) insulin-like growth factor 1 (modified from Govek and Van Aelst, 2005).

5.3 Eph receptors and their ephrin ligands

The Eph receptors constitute the largest class of receptor tyrosine kinases in the human genome. They are conserved among vertebrates, insects, nematodes and even sponges. They function in a broad variety of developmental and adult processes ranging from cell migration, to synapse plasticity. Ephs and ephrins signal in a bidirectional way, i.e. Eph receptors as well as their ligands transduce signals into the cells expressing them, thus, ephrin ligands also act as receptor-like molecules. Signalling downstream of the receptors is termed as ‘forward’ and downstream of the ligands as ‘reverse’ signalling.

5.3.1 The Eph class of receptor tyrosine kinases

The human genome encodes 13 different Eph receptors. Based on sequence similarity and ligand binding characteristics they are subdivided into 8 EphA receptors (EphA1-EphA8) and 5 EphB receptors (EphB1-EphB4, EphB6). Chicken encode an additional EphB receptor, EphB5 (Wilkinson, 2001). The genomes of the nematode *Caenorhabditis elegans* and the fruitfly *Drosophila melanogaster* encode one Eph receptor each (Vab-1 and Dek respectively) (George et al., 1998; Scully et al., 1999). Ephs are type I transmembrane receptors. Their extracellular domain consists of an N-terminal globular ligand-binding domain, followed by a cysteine rich region and two fibronectin type III repeats. The single transmembrane region is followed by a juxtamembrane region, a tyrosine kinase domain, a sterile- α -motif (SAM)-domain and a C-terminal PDZ-binding domain. Ligand binding specificity is encoded within the N-terminal globular domain (see **figure 5.6**).

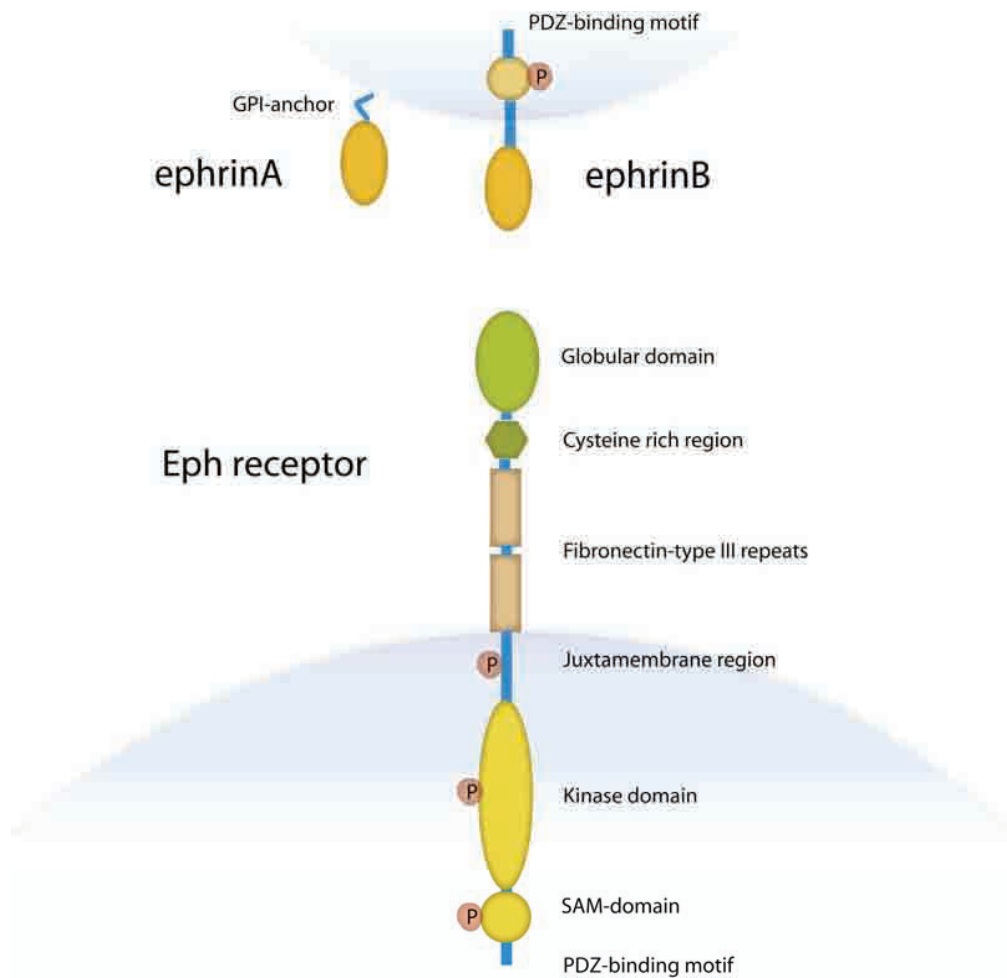


Figure 5.6. Main structural features of Eph receptors and their ephrin ligands (see text for explanation)

5.3.2 Ephrin ligands

Similarly to the Eph receptors, the vertebrate ephrin ligands are also subdivided into two classes. While all ephrins share a homologous N-terminal ephrin-domain, only the ephrinB ligands have a single transmembrane domain and a cytoplasmic domain containing 5-6 conserved tyrosine residues and a C-terminal PDZ-binding motif. EphrinA

ligands are linked to the membrane by a glycosyl-phosphatidyl-inositol (GPI)-anchor. Vertebrates have 5 ephrinA ligands (ephrinA1-ephrinA5) and 3 ephrinB ligands (ephrinB1-ephrinB3).

EphA receptors bind ephrinA ligands, whereas EphB receptors bind ephrinB ligands. Cross-binding among subclasses is not very common with the exception of EphA4 (Wilkinson, 2000). Binding specificity within a subclass is low. All EphA receptors bind to all ephrinA ligands. EphB1, EphB2, and EphB3 receptors bind equally well to both ephrinB1 and ephrinB2. There is some specificity within subclass B: EphB4 appears to only bind ephrinB2 (Wang et al., 1998; Adams et al., 1999; Gerety et al., 1999). In *C. elegans* there are 4 GPI-anchored ephrin ligands (EFN1-EFN4). The sequence of their N-terminal domains shares similarities with vertebrate A- and B-type ephrins (Chin-Sang et al., 1999). In *Drosophila*, D-ephrin is the only known ligand for Dek. The D-ephrin coding sequence predicts 3 transmembrane domains, an extracellular ephrin domain after the first transmembrane domain and a cytoplasmic domain with some sequence similarity to vertebrate B-type ephrins (Bossing and Brand, 2002) (see **figure 5.7**).

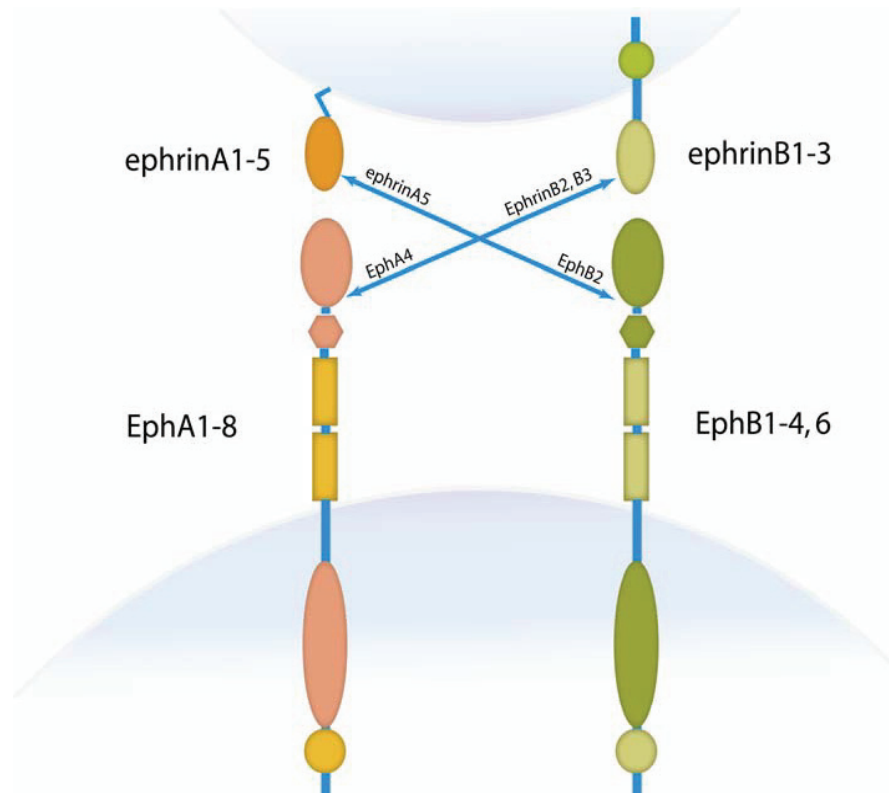


Figure 5.7. Eph receptor classes and their ligands. Eph receptors can be subdivided according to their binding specificity to their ephrin ligands. The B-subclass (in mammals EphB1-B4, EphB6) binds to ephrinB1-B3, whereas EphA receptors bind to ephrinA1-A5. Exceptions are EphA4 which can bind to both ephrinAs and ephrinB2 and -B3; and EphB2 which also interacts with ephrinA5.

5.3.3 Signaling mechanisms by Eph receptors and ephrin ligands

5.3.3.1 Mechanisms of Eph receptor forward signaling

Most RTKs activate signalling pathways that target transcription in the nucleus leading to proliferative and/or differentiation responses. By contrast, Eph receptors regulate cell migration, repulsion, and attachment to the extracellular matrix. The signalling cascades that they activate, therefore, ultimately converge on the cytoskeleton and on adhesion sites.

The first step in initiation of Eph signalling is the recognition and binding of receptors with ligands on opposing cell surfaces. Several studies lead to a model of a two step mechanism: initially a high affinity heterodimer is formed between one N-terminal globular domain of the Eph receptor and the N-terminal domain of an ephrin molecule. Recognition proceeds via an induced fit mechanism where a loop of the ligand induces the folding of a hydrophobic binding pocket on the receptor. This heterodimeric 1:1 complex then favors tetramerization to a 2:2 complex. Low affinity binding sites between tetramers may then lead to further oligomerization (Himanen et al., 2001). It has been shown that Eph-receptors require higher order oligomerized ligands for full activation when presented as soluble recombinant Fc-fusion proteins (ephrin-Fc) (Stein et al., 1998). It is thought that this oligomerization mimics the membrane anchorage of the ligand. (see **figure 5.8**)

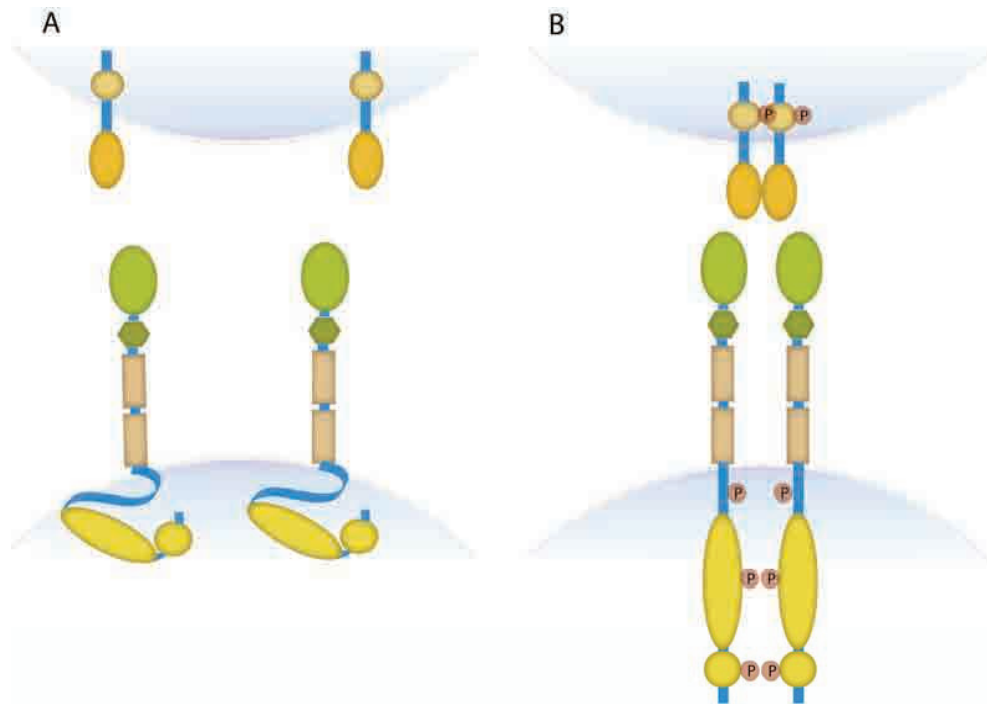


Figure 5.8. Mechanisms of Eph receptor activation. (A) In the unbound state, the cytoplasmic domain of Eph receptors is in a close and inactive conformation held by a fold in the juxtamembrane region. A tyrosine residue in the A-loop of the kinase domain keeps the enzyme inactive. (B) The binding of ligand induces a conformational change in the globular domain. Ligand-receptor interactions promote the formation of a heterotetramer followed by higher order heteromultimers (not shown). Kinase domains come close together and basal activity leads to trans-autophosphorylation. Phosphorylation of the A-loop tyrosine activates the kinase. Phosphorylation at the juxtamembrane tyrosines opens up the close conformation leading to full kinase activity.

There is no evidence that the ligand induced change in the secondary structure of the receptor is transferred outside of the globular domain. Thus, the mechanisms of kinase activation are rather similar to those of other RTKs. Ligand binding brings together two catalytically autoinhibited receptors into an orientation that favors trans-autophosphorylation on a tyrosine residue located on the so called activation-loop (A-loop) within the kinase domain. In its unphosphorylated form, the A-loop folds into the catalytic pocket of the kinase domain, thereby inhibiting its activity. Steric forces liberate the phosphorylated loop outside the pocket, leading to kinase activation. Another inhibitory interaction exists between the kinase

domain and the juxtamembrane region. Upon phosphorylation of two conserved tyrosines within this region, this interaction folds up permitting the full activation of the receptor. The activated receptors then interact with adaptor molecules that transmit signals into the cell. Adaptor molecules contain functional protein-protein interaction domains such as the src-homology-2 (SH2) and SH3 domains. SH2 domains bind to phosphorylated tyrosine motifs of the receptor thereby connecting upstream and downstream signalling events. The interaction of a variety of such adaptors with Eph receptors has been shown. The SH2 domains of the non receptor tyrosine kinases Abl and Arg bind to the phosphorylated juxtamembrane tyrosine residues. Abl and Arg are known regulators of the actin cytoskeleton and activation of EphB1 receptor leads to a decrease in Abl activity. Eph receptors also interact with the related non receptor tyrosine kinases of the Src family (SFK) (Ellis et al., 1996; Zisch et al., 1998). SFKs have been implicated in regulation of cytoskeletal dynamics and cell-substrate adhesion via integrins (Thomas and Brugge, 1997).

The Rho GEF Ephexin (Eph interacting exchange protein) provides another link between Eph receptors and Rho family GTPases. Ephexin binds to the kinase domain of EphA4 and has differential effects such that RhoA is activated and Rac as well as Cdc42 are inhibited. The net result is a shift of actin dynamics towards contraction and reduced extension. Dominant negative forms of Ephexin abolished Eph receptor dependent growth cone collapse (Wahl et al., 2000; Shamah et al., 2001).

Eph receptors are regulators of substrate adhesion via integrins. Their action can lead to enhanced or reduced adhesion. Activated EphB2 receptor in NIH3T3 fibroblasts leads to phosphorylation of the GTPase R-Ras, a known regulator of integrin mediated adhesion. Phosphorylation of R-Ras led to decreased adhesion (Zou et al., 1999). Focal adhesion kinase (FAK) is an important regulator of integrins. EphA2 receptor was shown to dephosphorylate FAK, suppressing the adhesion of prostate carcinoma cells in culture (Miao et al., 2000). Other studies reported that Eph receptor signalling can lead to enhanced adhesion by integrins. In human kidney cells EphB1 can promote integrin adhesion via the SH2-SH3 adaptor Nck (Huynh-Do et al., 2002) activating the Nck

interacting kinase (NIK) (Becker et al., 2000). In NIH3T3 and HEK293 cells activation of EphA8 receptor caused the plasma membrane recruitment of the p110 γ subunit of phosphatidylinositol 3-kinase (PI3K γ), promoting integrin mediated adhesion and cell migration (Gu and Park, 2001; Gu and Park, 2003). The signalling events described are summarized in **figure 5.9**.

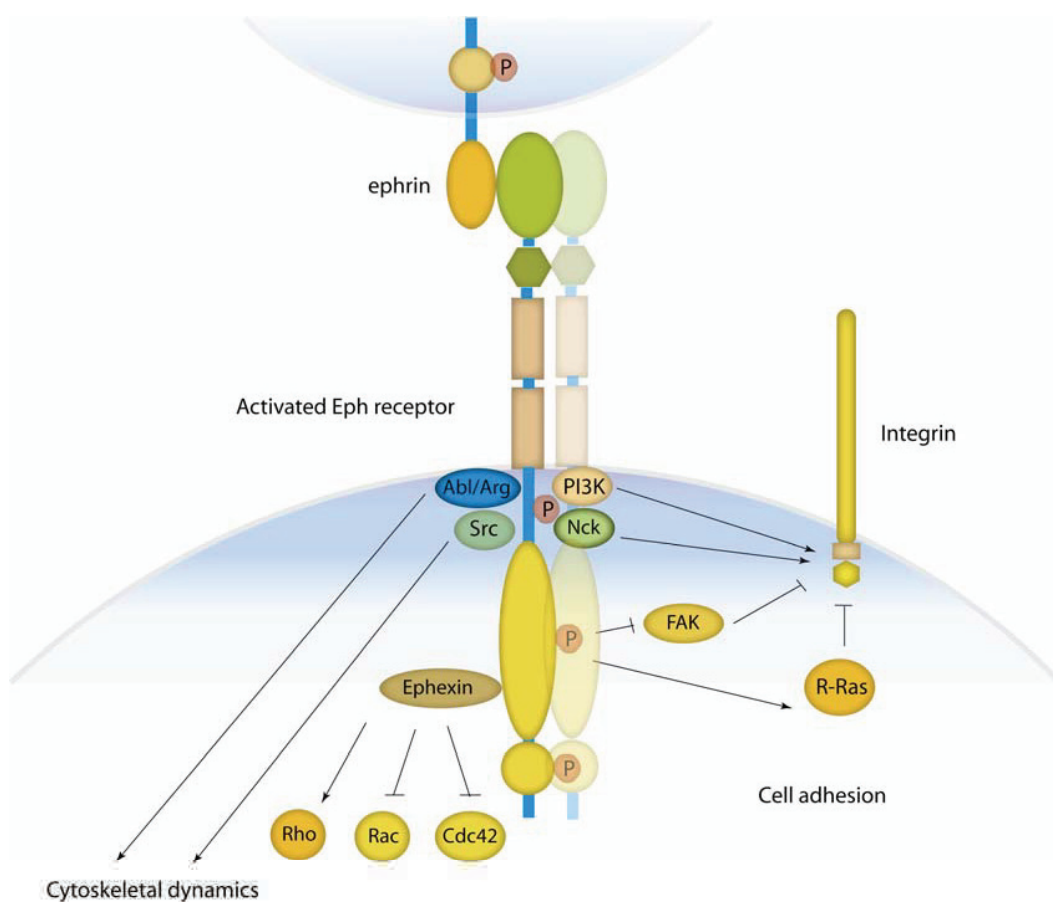


Figure 5.9. Summary of adaptor interactions described in the text. Cytoplasmic tyrosine kinases like Abl/Arg and Src act downstream of Eph receptors to regulate cytoskeletal dynamics. The GEF Ephexin shifts the balance of Rho family GTPase activity towards Rho. Signaling via PI3K, Nck, FAK and R-Ras modulates cell adhesion by integrins.

As mentioned before, Eph receptors also regulate synaptic spine morphology (see section about spine formation in the dendritic development chapter). In this case the neuronal cell surface proteoglycan syndecan-2, a cell adhesion molecule, plays an important role in the process of spine maturation (Ethell and Yamaguchi, 1999). EphB2 activation leads to syndecan-2 clustering in cultured hippocampal neurons resulting in the formation of new spines. This effect depends on the PDZ-domain protein syntenin, a known interactor of syndecan-2 and EphB2, as well as tyrosine phosphorylation of syndecan-2 by EphB2 (Ethell et al., 2001). As mentioned before, filamentous actin is an important structural feature of spines.

Stimulation of neurons with soluble ephrinB1-Fc activates the RhoGEF kalirin. A pathway involving the Rho family GTPase Rac1 and its downstream effector p21 activated kinase (PAK) and links EphB receptors to actin dynamics in spines (Penzes et al., 2003). EphB2 also interacts with the RhoGEF intersectin, an activator of Cdc42, providing another link between EphB receptors and actin assembly in spines (Irie and Yamaguchi, 2002). EphB2 receptor can directly modulate the activity of NMDA receptors. In young immature neurons activated EphB2 caused the co-clustering of NMDARs. EphB2 activates the cytoplasmic tyrosine kinase Src, which can phosphorylate cytoplasmic tyrosine residues in NMDAR. Phosphorylation enhances the ability of NMDAR to flux calcium ions, an important step in synaptic plasticity (Dalva et al., 2000; Takasu et al., 2002).

5.3.3.2 Mechanisms of ephrin ligand reverse signalling

Much less is known about the signalling mechanisms that act downstream of ephrinB ligands. The conservation of the five tyrosine residues in all ephrinBs suggests a role in downstream signalling similar to that of RTKs (see **figure 5.10**).

EphrinB immunoprecipitates from embryonic nervous tissue are tyrosine phosphorylated (Brückner et al., 1997). Phosphorylation occurs mainly at tyrosine residues -23, -18 and -4 (C-terminal residue counted as -1) (Kalo et al., 2001). Stimulation of cells heterologously expressing ephrinB ligands with soluble Fc fusions of EphB receptors (EphB-Fc) results in their subsequent phosphorylation on tyrosines (Holland et al., 1996; Brückner et al., 1997). Ephrin phosphorylation was also induced in these cells by contact with EphB expressing cells (Holland et al., 1996). Thus, trans-interactions of ephrinBs with their cognate receptors, activates signalling pathways, involving tyrosine kinases, in the ligand expressing cells. Concomitant overexpression of ephrinB with Src leads to ephrinB phosphorylation (Holland et al., 1996). Tyrosine phosphorylation of ephrinBs can also be achieved in *cis* by activation of platelet derived growth factor (PDGF)-receptors or fibroblast growth factor (FGF)-receptors if they are expressed in the same cells (Brückner et al., 1997; Chong et al., 2000). Therefore it is likely that ephrinBs can serve as components of the signalling pathways downstream of these receptors. So far one adaptor molecule has been identified to bind to ephrinB ligands in a phosphotyrosine dependent way: The SH2- and SH3 domain containing

Nck homologue Grb4 (Nck β). Prolonged stimulation of cells heterologously expressing ephrinB molecules with EphB-Fc results in a reduction of F-actin stress fibers and the disassembly of focal adhesions, leading to the detachment of the cells from the substratum. This effect is accompanied by FAK phosphorylation and delivery of the focal adhesion protein paxillin from the plasma membrane, suggesting a the regulated disassembly of focal adhesion sites. The rearrangements in the actin cytoskeleton are abolished by co-overexpression of a dominant negative form of Grb4. Grb4 binds to a variety of other signalling molecules including Abl interacting protein-1 (Abi-1), axin, a scaffold protein in the Wnt signalling pathway and the c-Cbl associated protein CAP (Cowan and Henkemeyer, 2001). EphrinB ligands interact with several PDZ domain proteins (Torres et al., 1998; Brückne et al., 1999; Lin et al., 1999; Lu et al., 2001). Some of them like GRIP1, GRIP2 and syntenin are adaptor proteins containing only PDZ-domains. Others are linked to functional domains like the protein interacting with C-kinase (PICK1) or the tyrosine phosphatase PTP-BL. Interestingly the PDZ binding motif in ephrinBs (YKV) contains one tyrosine phosphorylation site. *In vitro* peptide binding

studies revealed that phosphorylation might influence PDZ binding (Lin et al., 1999). Not so much is known about ephrinB-PDZ interaction. Both, B- and A-type ephrins localize to lipid rafts. Rafts are small subdomains in cell membranes rich in cholesterol and sphingolipids. Rafts serve as signalling platforms harboring a variety of membrane anchored signalling molecules (Simons and Toomre, 2000). EphrinB ligands recruit the PDZ domain containing proteins GRIP1 and -2 to lipid rafts (Brückner et al., 1999). The GPI anchor targets ephrinA ligands to rafts. EphrinA molecules engaged with their cognate EphA receptor activate the Src family kinase (SFK) Fyn, which is also targeted to rafts via its myristoyl moiety. Associations via rafts are thought to provide a mechanism as to how ephrinA ligands are able to transduce signals despite the fact that they lack a cytoplasmic domain. EphrinA reverse signalling regulates integrin mediated adhesion (Davy et al., 1999; Davy and Robbins, 2000; Huai and Drescher, 2001). These data together with recent findings in our lab (Palmer A. and Zimmer M.) lead to the proposal of a 'switch model' for ephrinB reverse signaling. EphrinB engagement with its EphB receptors induces the rapid co-clustering of ephrinB and SFKs, causing SFK activation and ephrinB phosphorylation. Both active SFKs and phosphorylated ephrinB activate signaling pathways, either independently or in concert with each other, involving phosphotyrosine/SH2 interactions. With delayed kinetics, ephrinB clusters recruit PTP-BL, which dephosphorylates

both Src and ephrinB, effectively turning off signaling by ephrinB and Src via phosphotyrosine. The recruitment of PTP-BL to ephrinB may not terminate ephrinB signaling completely, but rather shifts signaling from phosphotyrosine-dependent to PDZ-domain-dependent signaling.

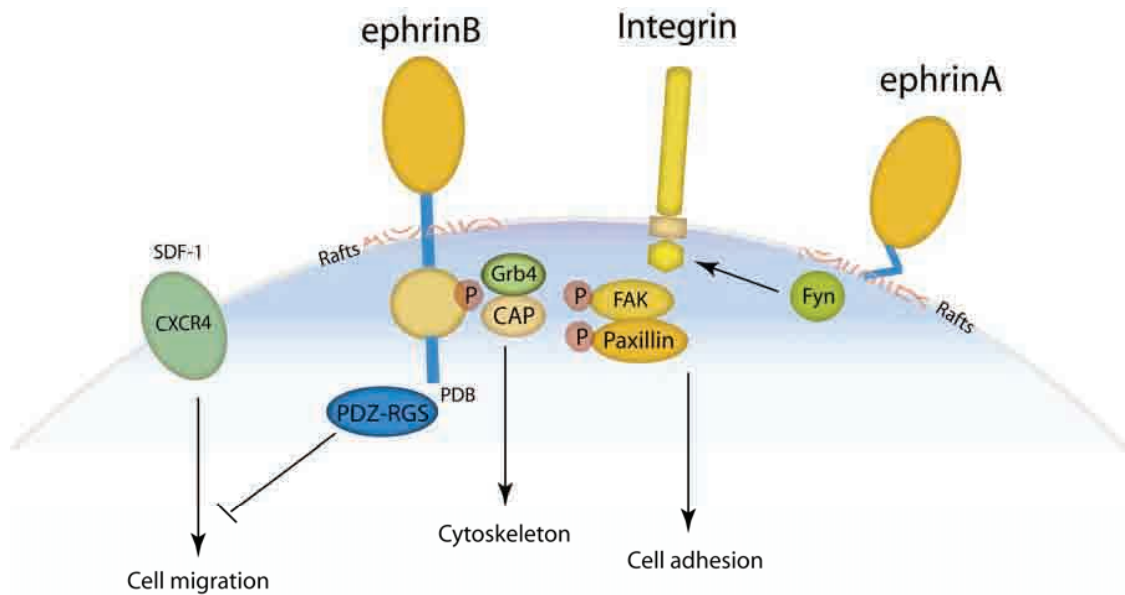


Figure 5.10. Ephrin reverse signaling. EphrinB ligands signal via PDZ-RGS to inhibit SDF-1/CXCR4 mediated cell migration. Upon receptor binding ephrinB ligands become tyrosine phosphorylated on their cytoplasmic domain. This provides docking sites for the SH2 adaptor Grb4. Grb4 signals via CAP to the cytoskeleton. The focal adhesion proteins FAK and Paxillin become tyrosine phosphorylated downstream of ephrinB ligands. Integrin adhesion can be modulated by both ephrinB and ephrinA reverse signaling. EphA receptor binding to ephrinA ligands leads to activation of Fyn kinase. The mechanism of Fyn activation may rely on interactions within rafts.

5.3.4 Effects of Eph-ephrin signaling

As previously mentioned, Eph-ephrin signaling is at the basis of several crucial developmental and adult processes, axon pathfinding and topographic mapping, synapse morphology and synapse plasticity, but also cell migration, segmental patterning, angiogenesis and tumorigenesis. The influence of Eph-ephrin activation on cell behaviour differs according to the cell type but can generally be attributed to repulsion of cells or

cellular processes, such neuronal growth cones. In a few cases Eph-ephrin activation leads to increased adhesion/attraction. In molecular terms many of the signalling pathways downstream of Eph and ephrins converge to regulate the cytoskeleton.

Eph-ephrin mediated cellular effects can be classified in three different categories: those that require forward signalling, those that require reverse signalling and those that require both. Some well studied examples of Eph-ephrin signalling in the development of the nervous system will be given below.

5.3.4.1 Forward and reverse signaling during axon guidance

Developing neurons must extend their axonal projections in order to reach their specific innervation territories. Neurons of many sensory organs, like the visual system, project in a topographic manner. For example neighbouring neurons within the vertebrate retina (Retinal ganglion cells, RGCs) project to neighbouring regions in the mammalian superior colliculus (SC) or the avian tectum. Their relative positions in the retina with respect to the temporal-nasal axis determine their target areas in the tectum/SC with respect to the anterior-posterior axis. Ephs/ephrins were first described as molecules involved in retinotopic map formation during development (O'Leary and Wilkinson, 1999). EphrinA ligands are expressed in an anterior (low) to posterior (high) gradient in the tectum/SC. EphA receptors are expressed in a nasal (low) to temporal (high) gradient in the retina (see **figure 5.11**).

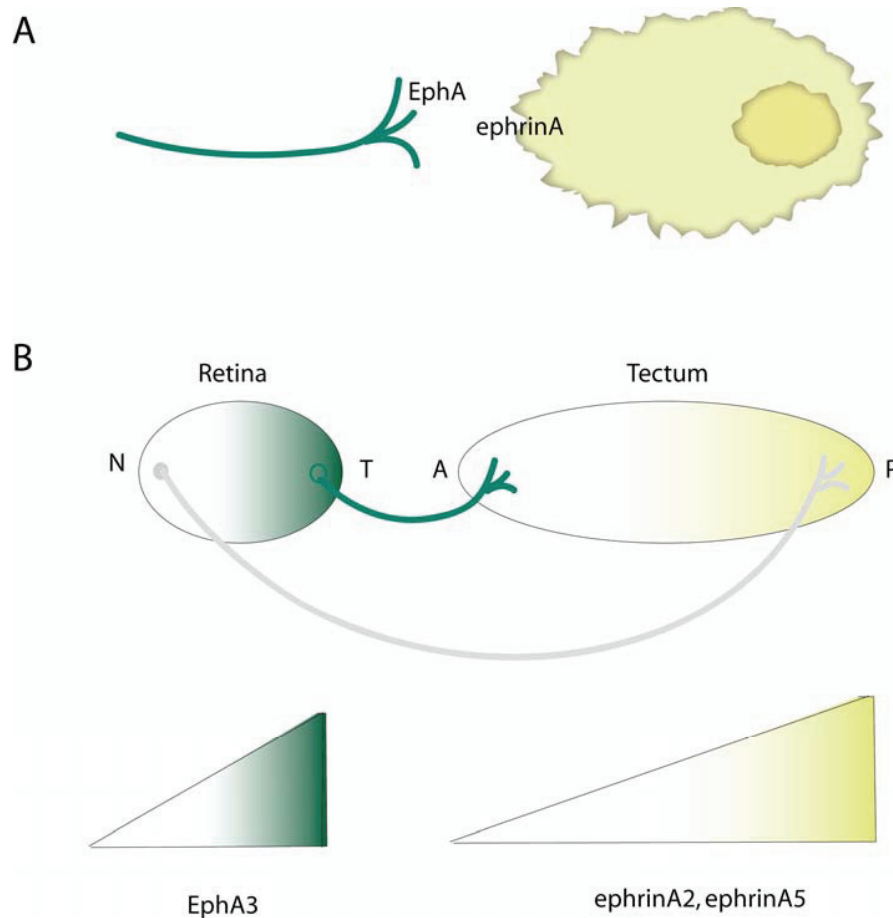


Figure 5.11. Simplified model of retinotopic mapping by EphA receptors and ephrinA ligands. (A) EphA receptors are expressed on growth cones of retinal ganglion cell (RGC) axons. EphrinA ligands are expressed on tectal or superior collicular cells. They are repellents that transmit growth inhibitory signals into the EphA receptor expressing cell. (B) EphA3 is expressed in a nasal (N) to temporal (T) gradient in the retina. EphrinA ligands are expressed in an anterior (A) to posterior (P) gradient in the tectum. RGCs located to nasal positions in the retina express lower levels of EphA3. High levels of ephrinA ligands are required to stop their growth. The result is that their axons project into relative posterior regions in the tectum. Conversely, temporally located RGCs expressing high levels of EphA3 receptor stop growing already in response to low levels of ephrinA ligands in the anterior tectum.

EphrinA ligands represent repellents for axons expressing high amounts of EphA receptors. In a simplified model axons from temporal neurons expressing high EphA receptor, respond already to low levels of ephrinA ligand in the anterior tectum. Conversely, axons from nasal neurons expressing low levels of EphA receptors require

high levels of ephrinA ligand to respond, thus they can extend to more posterior positions within the tectum/SC. (Wilkinson,

2000; McLaughlin et al., 2003). Not only ephrins but also the Eph receptors can represent guidance cues for axons. EphB2^{-/-} mice have a defect in the posterior part of the anterior commissure (ACp). In mammals, axons originating from the temporal sides of the cortex normally fasciculate and cross the midline in the dorsal forebrain to find their targets on the contra-lateral sides of the cortex. In EphB2^{-/-} mice these axons fail in crossing the midline and instead misproject into the ventral forebrain. Interestingly, this phenotype is rescued in genetically engineered mice expressing a chimeric EphB2 receptor which has its cytoplasmic domain replaced by lacZ (EphB2-lacZ). Thus, the N-terminal domain of EphB2 is sufficient for correct guidance. EphB2 is not expressed by ACp axons but in the tissue of the ventral forebrain. Conversely, ephrinB ligands are expressed on the axons (Henkemeyer et al., 1996; Orioli et al., 1996). These data suggested that ACp axons sense a repellent represented by the extracellular domain of EphB2 in the ventral forebrain and ephrinB ligands act as receptor-like molecules transducing signals *in reverse* via their cytoplasmic domains. Eph/ephrins are crucial for the formation of many other axonal projections. In some cases reverse signalling, and in other cases classical Eph receptor forward signalling is required (Palmer and Klein, 2003).

5.3.4.2 Eph/ephrins and synaptic plasticity

Several Eph receptors and ephrin ligands have been shown to be expressed at neuronal synapses (Gerlai, 2001; Murai and Pasquale, 2002). In many CNS synapses the postsynaptic sites are formed by spines. The morphology of spines is thought to be important for synaptic function (Hering and Sheng, 2001; Bonhoeffer and Yuste, 2002). Eph receptor signalling has been shown to be involved in synaptic spine formation and morphology (see above).

Activity dependent synaptic plasticity often requires N-methyl-D-aspartate (NMDA)-type glutamate receptors. NMDAR dependent Ca^{2+} influx and associated signalling pathways orchestrate synapse formation and plasticity (Helmchen, 2002). In young hippocampal neuron cultures EphB2 receptor activation leads to interaction with and clustering of NMDAR. EphB receptor signalling can enhance NMDAR dependent Ca^{2+} influx leading to increased CREB (cAMP Response Element Binding Protein) dependent transcription, a process important for

synapse plasticity, learning and memory. In the same system EphB receptor stimulation elicits the formation of new synapses. These findings suggest that ephrinB ligands in presynaptic membranes induce the maturation of glutamatergic synapses by NMDAR aggregation and regulating NMDAR function (Dalva et al., 2000; Takasu et al., 2002). The EphB2-NMDAR interaction has been confirmed to occur in adult mice and targeted inactivation of the mouse EphB2 gene in the hippocampus interfered with spatial learning and long-term potentiation of synapses of the Schaffer collateral pathway. Interestingly, expression patterns and genetic studies suggested that ephrinB ligand reverse signalling is important for these processes (Grunwald et al., 2001). Recent data support a model where ephrinB ligands signal in postsynaptic membranes via the PDZ domain protein GRIP to glutamate receptors of the AMPA type, regulating their surface distribution at synapses (Grunwald et al., 2003). NMDAR independent LTP occurs at hippocampal Mossy fiber synapses. Electrophysiological studies suggested that postsynaptic PDZ interactions link EphB receptor forward signalling to non-NMDA type glutamate receptor functions. Presynaptic ephrinB reverse signalling in this case may regulate long lasting presynaptic changes (Contractor et al., 2002).

5.4 cDNA Microarrays

The cDNA Microarray technology, with all its variants, was developed a few years ago and it immediately showed a high experimental potential as it allows to take gene expression snapshots of a system under specific conditions. The Microarray technique is a mostly automated procedure that uses robotics and bioinformatics, and allows to simultaneously detect the gene expression profile of thousand of genes. The version used in this study consisted of a glass support on which up to 15'000 genes were arranged in an organized order (array). The source of the genes spotted can vary according to the system used (in our case a mouse cDNAs developmental library). The spotted glass support is the constant in a microarray experiment. Using the principle of base pairing, the slide is hybridized to complementary sequences coming from a reference and a test, the difference between the two being the experimental condition to be tested. Total mRNA is extracted from the reference and the test, then reverse transcribed using oligonucleotide labelled with two different fluorophors. The freshly synthesized fluorescent cDNAs are then pooled and hybridized to the microarray. After the hybridization, each spot on the slide will contain a certain ratio of the two fluorescent signals directly proportional to the abundances of that specific gene in the test conditions and in the reference. If, for example, the fluorophor used for labelling the test cDNA prevails, the original amount of mRNA for the specific microarray spot was more abundant in the test than in the reference, that is to say, compared to the reference, once a condition X is applied to the system, the gene is induced. The output of the resulting fluorescence ratio between test and reference is then measured by a fluorescence scanner. The ratios for each hybridization spot are then automatically processed by a computer which generates a list of expression ratios for all the genes on the chip (see **figure 5.12**) (Ekins and Chu, 1999).

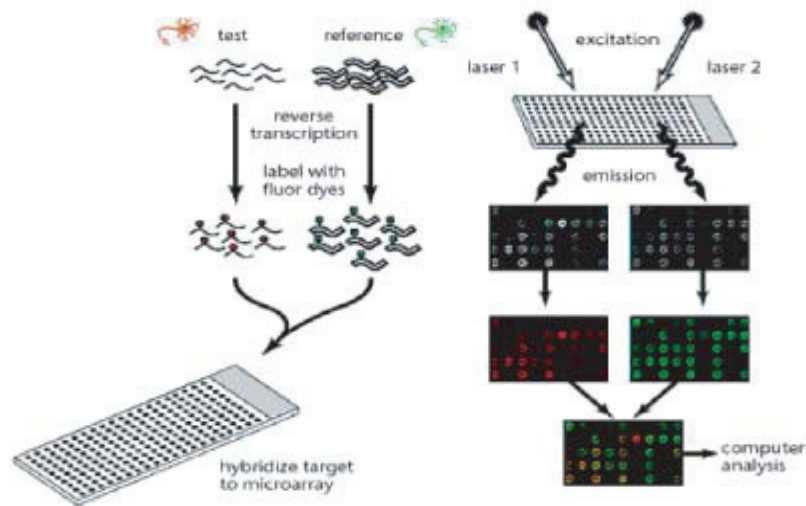


Figure 5.12. Schematic drawing illustrating the Microarray technique. Total mRNA from the experimental test and the reference are reverse transcribed incorporating different fluorescently-tagged nucleotides. The fluorescent probes are then hybridized to the microarray chips containing an array of different genes. Fluorescent light is then shone on the chip and emission fluorescence for each spot is measured by a fluorescence scanner. Computer analysis follows to determine the ratios between the two different fluorescent dyes in order to assess if the signal relative to a precise spot is more abundant in the test or in the reference condition. (Modified from NCVS: <http://www.ncvs.org/ncvs/groups/cmb/mrna.html>)

The experimental information about Eph-ephrin signalling pathway helps to explain the basic cellular events that bring about Eph-ephrin biological function and the resulting macroscopic developmental processes driven by them. As mentioned before, most of the crucial Eph-ephrin responses, repulsive or attractive, from axonal guidance to changes in cell motility, are mediated by changes in cytoskeleton dynamics leading to a local rearrangement of the cytoskeleton and of cell shape. The most widely studied cellular responses mediated by Eph-ephrin signalling are local cues, involving the two

juxtaposing surfaces during cell to cell interaction and then leading to nearby local rearrangements i.e. via the influence Rho GTPases have on actin dynamics. Little is still known about the extent to which Eph-ephrin signalling also reaches the nucleus and induces the activation or the repression of specific genes that might be involved in triggering later events and therefore later responses, on a broader cellular level and not so much is known about the extracellular cues directing dendritic growth, development and complexity and about the eventual nuclear events downstream. We have shown that δ -Catenin, a nervous system specific, developmental protein is up-regulated upon activation of Eph-ephrin signaling in a microarray screening (see below). Published information, structural features and patterns of expression suggested a role of δ -Catenin in dendritic morphogenesis downstream of Eph-ephrin signalling.

5.5 New candidate molecules for dendritic development: δ -Catenin

The gene for δ -Catenin was first cloned from a human fetal brain library using oligonucleotides deduced from a plakophilin 1 related expressed sequence tag (EST) (Paffenholz and Franke, 1997) and named neural plakophilin-related arm-repeat protein (NPRAP) /Neurojungin. Independently, the product of the same gene was discovered in a yeast two-hybrid assay as an interactor with the loop region of presenilin 1 (PS1) (Zhou et al., 1997). PS1 harbors numerous autosomal dominant mutations that cause an early onset of familial Alzheimer disease (Cruts and Van Broeckhoven, 1998). It functions early in development during somitogenesis (Wong et al., 1997) and formation of the neocortex (Shen et al., 1997). Like the mammalian gene β -Catenin and its *Drosophila* orthologue Armadillo, δ -Catenin is a member of the Armadillo repeat family, characterized by a 42-amino acid imperfect repeat unit (Arm) involved in protein-protein interactions. Among members of the Arm repeat family, the number of repeated units varies, as well as most of the -NH₂ and COOH- terminal sequences flanking the repeats.

δ -Catenin belongs to a subfamily with 10 Arm repeats whereas β -Catenin has 12 repeats (see **figure 5.13**). More specifically, the subfamily to which δ -Catenin belongs is termed p120ctn subfamily, and also includes other proteins containing 10 Arm repeats (see **figure 5.13**). p120 is the founding member of the subfamily (Peifer et al., 1994), other members of the subfamily are p0071 and the plakophilins, both components of the desmosome (Kapprell et al., 1988; Hatzfeld and Nachtsheim 1996), and ARVCF, a protein with unknown function (Sirotkin et al., 1997). In the subfamily, δ -Catenin has greatest similarity with the Arm repeats of p0071 (69.3% identity), and is somewhat less related to p120ctn (48% identity).

5.5.1 Molecular structure

The gene for human δ -Catenin encodes a 1,224-amino acid product with a predicted molecular weight of 132,544 Dalton and a pI of 7.94 (Lu et al., 1999). Mouse δ -Catenin encodes a 1,247-amino acid protein with a 25-amino acid insert at position 879 in the 8th Arm repeat. Mouse δ -Catenin is highly related with 95% identity and 98% similarity to the human protein (Paffenholz and Franke, 1997).

Apart from the 10 Arm repeats that occupy most of the central part of the molecule (amino acids 551 to 971) a significant portion of the molecular mass still lies NH₂- and COOH- terminal to those repeats and it displays several interesting structural features (see **figure 5.13**):

- Three potential SH3 binding motif with the sequence XPXXPP within a region encompassing amino acids 32 and 440
- A proline rich motif (aa 216-226), absent in p120ctn
- Two Abl tyrosine phosphorylation consensus sites (Y289 and Y429).
- Amino acids 811-817 represent a lysine rich motif that could represent a potential nuclear localization signal (NLS)
- A poly-proline tract, also not present in p120ctn
- Numerous (17) potential phospho-tyrosines between aa 975 and 1230

- A DSWV sequence at the very carboxyl terminus that binds to PDZ motif containing proteins (Ide et al., 1999)

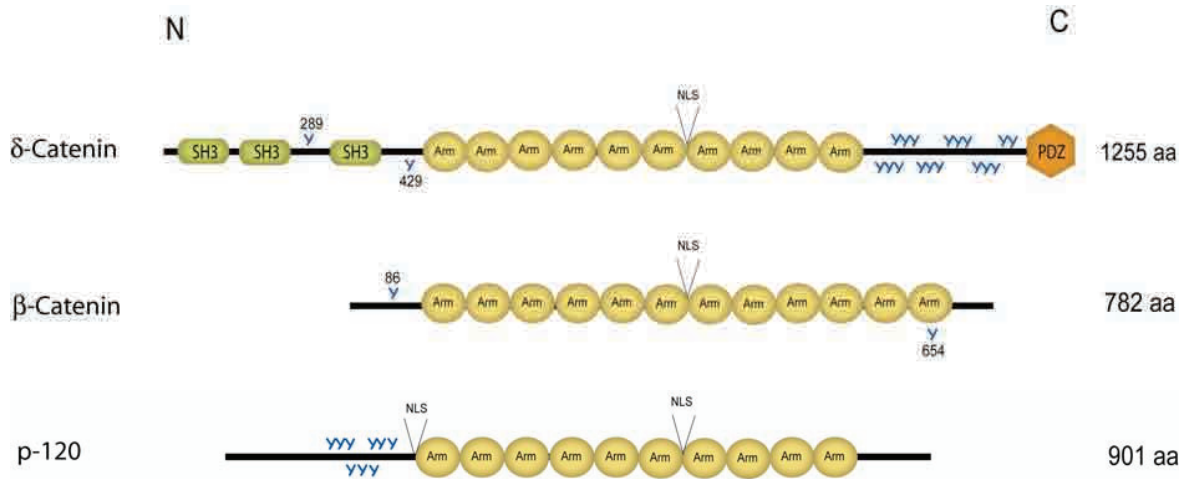


Figure 5.13. δ -Catenin structure in comparison with related proteins β -Catenin and p-120. δ -Catenin is a 1,255 amino acid protein. A significant portion of the molecule is constituted by ten Armadillo (Arm) repeats in the central part (yellow circles). Besides, other domains of interest are: 3 Src homology 3 binding motifs (SH3, green boxes), a nuclear localization signal (NLS) and a PDZ binding motif (PDZ, red box) at the very C-terminus. Additionally, two potential Abl tyrosine phosphorylation consensus sites are present at positions 289 and 429 and a potential phospho-tyrosine rich area (17 residues) stretches from position 975 to 1230. β -Catenin, a 782 aa protein, contains 12 Arm repeats, a NLS included in the sixth Arm repeat and two phosphotyrosines at positions 86 and 654. p-120 contains 10 Arm repeats and two NLS. The COOH terminus of the molecule includes a long stretch of potentially phosphorylatable tyrosines. Numerous splice variants exist.

5.5.2 Expression pattern

δ -Catenin is mostly a nervous system specific protein even though it has been recently found to be present in pancreatic tissue and the outer limiting zone of the retina. It is also expressed in glial cells and ependymal stem cells as well as in the P19 embryonic carcinoma stem cells and Pheochromocytoma PC12 cells. (Kim et al., 2002)

δ -Catenin appears very early in the development of the nervous system at about the time of neurulation; δ -Catenin mRNA is detectable in the mouse embryo by embryonic day 8 (E8), its level increases through post natal day 7 (P7) but it appears to decrease in the adult brain.

More specifically, at E10 δ -Catenin is already detectable along the neuraxis from the telencephalon to the rhombencephalon but not in the developing spinal cord. By E12 it is strongly expressed in the telencephalic vesicle with slightly lower levels in the diencephalon and mesencephalon. Expression is also detectable in the rhombencephalic lip which includes the myelencephalon (future pons) and metencephalon (future cerebellum), the dorsal root ganglia and the developing spinal cord (Ho et al., 2000). (See **figure 5.14**)

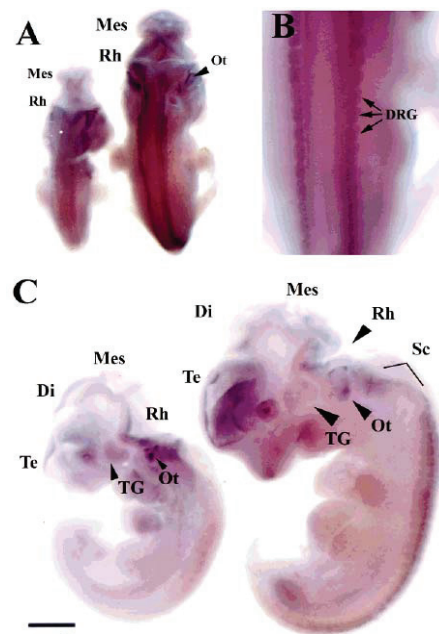


Figure 5.14. Whole mount in situ hybridization with an anti-sense δ -catenin probe in embryonic days E10 and E12 embryos. Dorsal (A, B) and sagittal (C) views of E10 (left; A and C) and E12 (right; A and C) mice are shown. At E11 (A and C), mRNA expression is detectable in the mesencephalon (Mes) and rhombencephalon (Rh) but not in the developing spinal cord. By E12, mRNA expression is intense in the telencephalon, mesencephalon,

rhombencephalon and the developing spinal cord (Sc; A). The sagittal view of the E12 embryo (right; C) illustrates the intense labeling of the telencephalic vesicle (Te). For abbreviations, see list. Scale bar 0.6 mm (from Ho et al., 2000).

At E11 the undifferentiated ventricular neuroepithelium of the cortex is the region that shows the strongest δ -Catenin expression (other regions that show high expression of δ -Catenin between E11 and E18 are the hippocampus, the pons, the ventral portion of the rostral medulla and the external granular level of the cerebellum).

An interesting event happens in the neuroepithelium as embryonic development progresses further. Between E11 and E18 a gradual decline in proliferative activity leads to a decrease in the thickness of the neuroepithelium and to a parallel enlargement of the postmytotic marginal zone to form the cortical plate (Bayer and Altman, 1991; Berry and Rogers, 1965; Caviness et al., 1982; Leavitt and Rakic, 1982). At E15 δ -Catenin expression is still ubiquitous both in proliferative and postmytotic regions and both the neuroepithelium and the emerging cortical plate express high levels of the protein. However, in the intermediate zone, consisting of migrating neurons and elongating axonal processes δ -Catenin is less expressed. By E18 when the majority of the neurons have differentiated and axonogenesis and elaboration of dendrites is under way, δ -Catenin shows a peculiar and defined laminar expression pattern corresponding exactly to the spatial segregation of proliferating, migrating and arborizing neurons. The thinning neuroepithelium still shows a strong expression of δ -Catenin, whereas the intermediate zone, through which cells are migrating, now appears almost devoid of δ -Catenin. The thickening cortical plate though, again shows a steadily increasing δ -Catenin expression. At the cellular level, δ -Catenin's distribution reflects the changes that migrating and differentiating neurons undergo. In the dividing cells forming the neuroepithelium, δ -Catenin shows a honeycomb distribution pattern typical of adherens junction molecules. This is consistent with the fact that cells forming the neuroepithelium are tightly packed and have dense adherens junction complexes. The thickening cortical plate on the other hand shows a completely different δ -Catenin pattern: in layer I the molecule is specifically distributed to the dendrites of differentiating pyramidal neurons and not in the cell bodies. The intermediate zone and its migrating cells do not express δ -Catenin.

The molecule undergoes a dynamic change in its cellular distribution and expression levels, from the cell junction where it contributes to the structure and cellular adhesion of the neuroepithelium (as well as other areas of the CNS where cells are still undifferentiated), to the differentiating dendrites of postmitotic neurons, most likely playing a role in the correct development of dendritic arbors. Migrating neurons in the intermediate zone require less adhesive properties, and that stop expressing the molecule (Ho et al., 2000) (see **figure 5.15**).

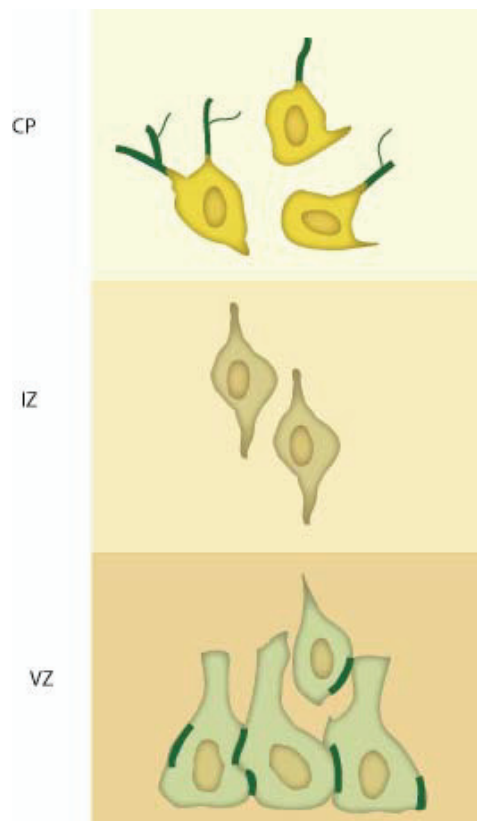


Figure 5.15. Differential expression of δ -Catenin in the mouse cerebral cortex during development. δ -Catenin expression is indicated in dark green. By embryonic stage 15, the cerebral wall is compartmentalized into a ventricular zone (VZ), intermediate zone (IZ), and cortical plate (CP). By this developmental stage, an otherwise uniform δ -Catenin expression pattern undergoes a dramatic change and shifts from a cell junction distribution in proliferating cells in the VZ to the arborizing dendrites of differentiating neurons in the CP. Migrating neurons in the intermediate zone (IZ) cease to express δ -Catenin. Growing axons do not express δ -Catenin either.

Only a few areas of the nervous system still show some δ -Catenin expression in the adult. Among them the cerebellum where δ -Catenin appears to specifically distribute to dendrites (Ho et al., 2000). (See **figure 5.16**)

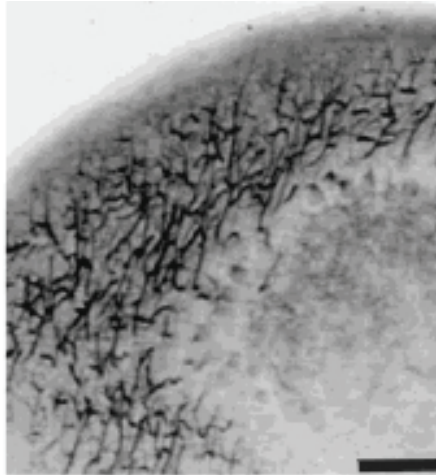


Figure 5.16. Microphotograph of δ -catenin immunolabeling of coronal sections of adult cerebellum. Magnification image of adult mouse cerebellum. δ -Catenin labeling is restricted to dendrites. Unlabeled neuronal somata appear as halos. Scale bar = 100 μ (from Ho et al., 2000)

5.5.3 The biological functions of δ -Catenin

5.5.3.1 δ -Catenin in cell junctions

Adherens junctions, typical of epithelia, are tight junction points between neighboring cells, responsible for the proper organization of tissues and crucial for the mobility properties of their cells. (See **figure 5.17**). The adherens junction complex between two neighboring cells is composed of three compartments: the intracellular compartments of

the first and the second and the common extracellular space in-between. Important members of the adherens junction complex are Cadherins, which are single membrane-spanning glycoproteins that directly anchor the cells via Ca^{2+} -dependent homophilic interactions of their extracellular domains and intracellularly connect with the cytoplasmic complexes involved in the junction. The classical Cadherins, which include E-, N-, and P-cadherin (Marrs and Nelson, 1996), have a highly conserved cytoplasmic domain to which a set of associated proteins bind (Nagafuchi and Takeichi, 1988; Ozawa et al., 1989). Together they form a cytoplasmic plaque complex which links cadherins to the actin cytoskeleton (Takeichi, 1991, 1995; Yap et al., 1997), therefore adhesive activity of the junctions derives from both the cadherin ectodomain which has a weak adhesive activity of its own (Brieher et al., 1996) and the cytoplasmic complexes which significantly strengthen the homophilic interaction.

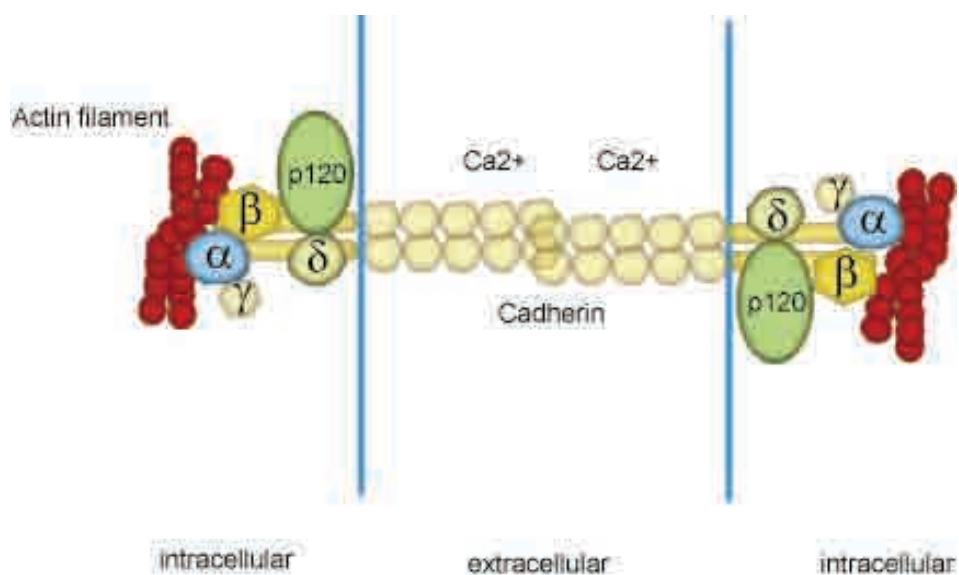


Figure 5.17. Scheme of an adherens junction.

Cadherins from adjacent cells maintain homophilic Ca^{2+} -dependent interactions through their extracellular domains. Their intracellular domain forms a cytoplasmic plaque with the catenins α , β , γ , δ and p120 catenin. The latter two bind a juxtamembrane portion of Cadherins whereas

the other catenins interact with the COOH- terminus of the molecule. The cytoplasmic plaque serves to anchor cadherins to the cytoskeleton by directly binding to actin filaments.

The most important members of the cytoplasmic plaque complex are the Catenins. They bind to Cadherins via their highly conserved cytoplasmic domain; β -Catenin binds to Cadherins, α -Catenin (which also directly interacts with actin) in turn binds to β -Catenin and this secures the Cadherins-Catenin complex to actin filaments (Aberle et al., 1994; Hoschuetzky et al., 1994; Funayama et al., 1995; Jou et al., 1995; Rimm et al., 1995). Other members of the Catenin family which bind to Cadherins are: γ -Catenin/Plakoglobin (closely related to β -Catenin), p120ctn and δ -Catenin (Lu et al., 1999). P120ctn and δ -Catenin, though, bind to a juxtamembrane region of Cadherins in contrast with all the other catenins that bind to a more distal region of the cytoplasmic tail of the Cadherins (Ozawa and Kemler, 1998; Yap et al., 1998). As mentioned before, δ -Catenin is strongly expressed in the highly proliferative neuroepithelium of the cortical ventricular zone in the developing mouse brain from E10 to E18. In early stages during neurogenesis the intracellular distribution of δ -Catenin is typical of cell junction proteins, that is, prominent along the lateral surface and the apical end of neuroepithelial cells. Here, δ -Catenin was shown to co localize with β -Catenin and N-Cadherin. In cell lines δ -Catenin was shown to interact with E-Cadherin. Like its close relative p120, δ -Catenin binds to a 41 aa juxtamembrane region of Cadherins, which contains a DEGGGE sequence conserved among mouse E-Cadherin, OB-Cadherin, N-Cadherin, *Xenopus* C-Cadherin and *Drosophila* E-Cadherin (Lu et al., 1999). The strength and the number of cell junctions are crucial in regulating important developmental processes like cell motility and migration, and therefore it is conceivable that the interactions between the various players of the plaque complex should also be finely regulated: a shift in Cadherin subtypes or a change in the composition of the protein pool in the cell junction complex, can cause, for instance, a weakening or a strengthening of cell-cell interaction, influencing the motility of the cells. For example, during neurulation, some ectodermal cells change cadherin expression from E- to N-cadherin; this shift allows neural precursor cells to segregate from other cells derived from the ectoderm. Subsequently, neural crest

cells, which down-regulate N-Cadherin expression, migrate from the dorsal ectoderm to specific locations in different germ layers (Hatta et al., 1987)

It has been shown that in the case of E-Cadherin, the juxtamembrane region negatively regulates adhesion by preventing lateral dimerization of the extracellular domain (Ozawa and Kemler, 1998), therefore molecules which bind to this site, such as δ -Catenin may be important regulators of cell adhesion.

Transient expression of δ -Catenin in MDCK epithelial cells further enhances the typical cell scattering response upon stimulation with hepatocyte growth factor (HGF). Interestingly, during this process δ -Catenin changes its intracellular distribution from the cell junctions to the cytoplasm (Lu et al. 1999).

In the tightly packed epithelial cell layer of the cortical ventricular zone, the down regulation of δ -Catenin may weaken cell to cell contacts, loosening the adherens junctions and thereby allowing cells to migrate to form the cortical plate. Then, upon reaching the proper position, neurons could potentially re-express δ -Catenin to establish new cellular contacts and secure new tissue contexts to the differentiating neurons.

5.5.3.2 δ -Catenin in dendrites and synapses

At later embryonic stages, and in post natal and adult brain, δ -Catenin shifts to a typical dendritic distribution as neurons differentiate and extend their dendritic arbor where it could be involved in the correct development of dendritic processes.

Recent findings show that increased cellular levels of other members of the Cadherin/Catenin complex, namely N-cadherin, α -N-Catenin and β -Catenin all enhance dendritic arborization in rat hippocampal neurons, in the latter case independently of the Wnt/ β -Catenin signaling pathway. Conversely, sequestering of β -Catenin decreases dendritic arborization (Yu and Malenka, 2003).

δ -Catenin over-expression in cultured hippocampal neurons alters cell morphology, causing a massive overgrowth mostly affecting primary dendrites and branching in general. In addition, overexpression induced filopodia-like processes devoid of

microtubules but highly enriched in actin filaments. This will be later on defined as δ -Catenin “complexing” phenotype (Kim et al., 2002; Martinez et al., 2003).

Interestingly NIH3T3 cells that transiently express δ -Catenin assume a typical “dendritic” phenotype, with extensive formation of heavily branched dendrite-like structures and numerous filopodia (Kim et al., 2002).

A similar effect is observed in PC12 cells in a typical assay involving their differentiation upon stimulation with NGF. PC12 cells, normally round, undergo major morphological changes upon stimulation with NGF forming a complex network of dendrite-like processes. Transient expression of δ -Catenin further accentuates these stimulatory effects (Lu et al., 2002). In all cases, a massive generation of actin filaments was observed to be responsible for the morphological alterations.

Another interesting and most likely related role that the Cadherin/Catenin complex may play is in the formation, regulation and maintenance of contacts between pre- and postsynaptic membranes at synaptic junctions which, after all, represent a highly specialized type of cellular junction. Homophilic cadherin interactions between pre- and post-synaptic cells, reinforced by the Catenin complex and the underlying actin cytoskeleton may play a role in the stabilization of synaptic junctions. It has been shown that Cadherins and Catenins may play important roles in synapse formation: α -Catenin and β -Catenin co-localize with synaptophysin, a presynaptic marker (Uchida et al. 1996; Jones et al., 2002). N-Cadherin and β -Catenin are present in axons and dendrites before synapse formation and then cluster at developing synapses in hippocampal neurons (Benson and Tanaka, 1998; Yu and Malenka, 2003). δ -Catenin, like Cadherins and other Catenins, is enriched in synaptosomes but it has been found to localize mainly to the post synaptic compartment of the synapse.

The postsynaptic density consists of a conglomeration of membrane bound scaffolding proteins, receptors and cytoskeletal elements that play a crucial role in the maintenance of synaptic structure, in synaptic transmission and synaptic plasticity and δ -Catenin interacts with several post synaptic density components like PSD-95 (post synaptic density-95), mGluR1 α - (type I metabotropic glutamate receptor) and NR2A (ionotropic NMDA receptor) (Jones et al., 2002), S-SCAM (synaptic scaffolding molecule) via its PDZ binding domain (Ide et al., 1999), suggesting an important role for the molecule.

5.5.3.3 δ -Catenin and actin cytoskeleton dynamics

Actin mediated changes in cell shape, are essential for a wide range of cellular activities, from cell motility to dendritogenesis to axon guidance.

The actin binding properties of some Catenins together with their strategic proximity to the cellular membrane and its molecular machinery confer to these molecules important roles in the regulation of cytoskeletal dynamics in response to extracellular stimuli. All known phenotypes of δ -Catenin, from the effect on cell junctions in MCDK cells to the effect in dendritic organization in hippocampal neurons are very likely to be exerted via a δ -Catenin mediated change in cytoskeletal processes.

δ -Catenin has been shown to physically interact with actin in cell lines and cultured hippocampal neurons where they co-localize in growth cones (Lu et al., 2002).

δ -Catenin also interacts with cortactin. Cortactin is a linker protein in the actin cytoskeleton: as it cross-links actin filaments in a tyrosine phosphorylation dependent manner (Weed and Parson 1993, Huang et al., 1997). δ -Catenin and cortactin form a complex in which a COOH region just downstream of the last Arm repeat of δ -Catenin appears to be crucial (Martinez et al., 2003). In rat hippocampal neurons and in PC12 the complex is responsible for primary process extension and its absence (by deleting δ -Catenin and Cortactin interaction domains) has negative effects on the ability of the cells to generate processes and branches. The δ -Catenin and cortactin complex recruits the Arp 2/3 complex through which the actin dependent-outgrowth process is most likely driven. The Arp 2/3 complex comprises 7 polypeptides and regulates both the formation and structure of actin networks directly. By increasing the nucleation rate, the Arp2/3 complex generates the large number of new filaments needed for actin network formation and helps create the branched network by cross-linking the slow growing pointed end of one filament to the side of another (May, 2001; Weaver et al., 2001). The Arp 2/3 complex-mediated cross-links are relatively unstable and cortactin and δ -Catenin may

stabilize the Arp 2/3 complex-mediated branches. This may serve to localize protrusions to sites of neuronal activity in light of the interaction of both δ -Catenin and Cortactin with postsynaptic scaffolding proteins. The interaction between δ -Catenin, Cortactin and in turn Arp 2/3 is regulated by the state of phosphorylation of δ -Catenin and Cortactin. The application H₂O₂ and orthovanadate triggers δ -Catenin phosphorylation, via a non identified Src kinase family member and causes the dissociation of the complex and the inhibition of processes outgrowth (Martinez et al., 2003).

Process elongation and process branching are most likely regulated in a different fashion, the modulation of neurite complexity being a result of the balance between the two. As mentioned before, Rho A has been shown to be important in dendritic branching. Its inhibition, in particular, promotes dendritic branching whereas its over-expression or the expression of dominant active versions has strong inhibitory effects. The generation of new primary processes and their elongations are, on the other hand, mostly unaffected (Nakayama et al., 2000 and Neumann et al., 2002). δ -Catenin appears to be connected with both process elongation and process branching as its over-expression enhances (or mimics) the effects of Rho A mutants (or Rho A inhibitors) through a possible δ -Catenin Rho A inhibitory activity. This still unidentified mechanism may be similar to that of its close relative p120ctn (Anastasiadis et al., 2000 and Noren et al., 2000). On the other hand, δ -Catenin mutants unable to form a complex with cortactin show a decrease in the number of primary dendrites and a defect in their elongation whereas the Rho A-dependent branching activity is partially retained (Martinez et al., 2003) (See **figure 5.18**)

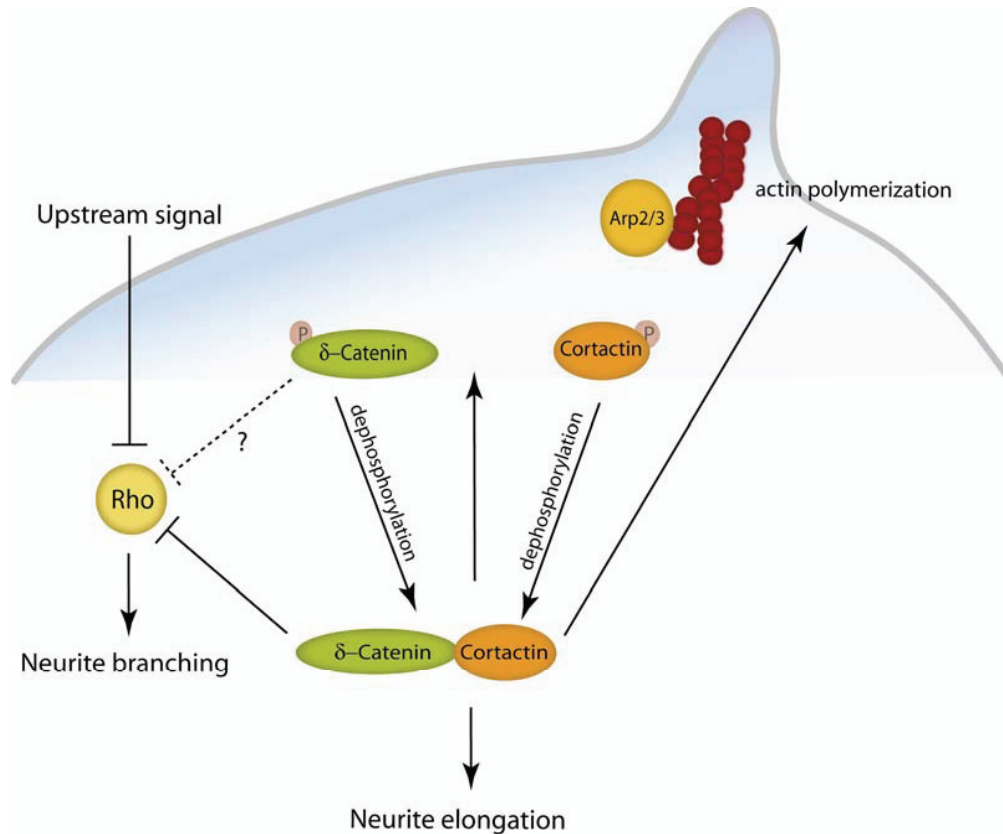


Figure 5.18. δ -Catenin and primary process extension versus branching. Two different pathways regulate the effects of δ -Catenin on process elaboration. Unphosphorylated δ -Catenin forms a complex with unphosphorylated Cortactin; the complex then recruits Arp2/3 to promote new generation of actin filaments. Not yet identified extracellular signals can lead to phosphorylation of the δ -Catenin–Cortactin complex causing the disruption of their interaction and the complex with Arp2/3 arresting dendrite elongation. Rho inhibition can be amplified by phosphorylated δ -Catenin, which leads to branching (modified from Martinez et al., 2003).

δ -Catenin has also been shown to bind the cytoplasmic non receptor tyrosine kinase c-Abl (the cellular homologue of Abelson murine leukemia virus) (Lu et al., 2002). The presence of nuclear and cytoplasmic pools of Abl and its actin-binding capability indicates a role of the molecule in the regulation of cell cycle, cytoskeletal organization (Van Etten, 1999) and in neuronal morphogenesis (Koleske et al., 1998 and Zuckerberg et al., 2000). Abl interacts with several different protein families, including catenin/cadherin cell adhesion complexes, Trio family GEF exchange factors (GEFs) and

Ena/VASP (vasodilator-stimulated phosphor-protein) family actin regulatory proteins (Lanier and Gertler, 2000).

δ -Catenin has strong consensus sites for Abl binding and Abl-induced tyrosine phosphorylation in the N terminal part of the molecule. The two proteins form a stable complex in neurons and they co localize with F-actin filaments in the growth cone. Furthermore MDCK cells irradiated with UV light (which was shown to activate c-Abl kinase activity) shows a strong δ -Catenin phosphorylation. The use of specific c-Abl kinase inhibitors enhances the effects of δ -Catenin in PC12 differentiation upon treatment with NGF (Lu et al., 2002). The alteration of MDCK cell shape in response to HGF (Lu et al., 1999) is also more pronounced in the presence of c-Abl kinase inhibitors. Both events are mediated by a reorganization of the actin cytoskeleton, consistently with the hypothesis that the unphosphorylated δ -Catenin is the one responsible for actin polymerization promoting/regulating activity.

6. RESULTS

6.1 Identification of novel Eph-ephrin downstream effectors using a Microarray screening: δ -Catenin

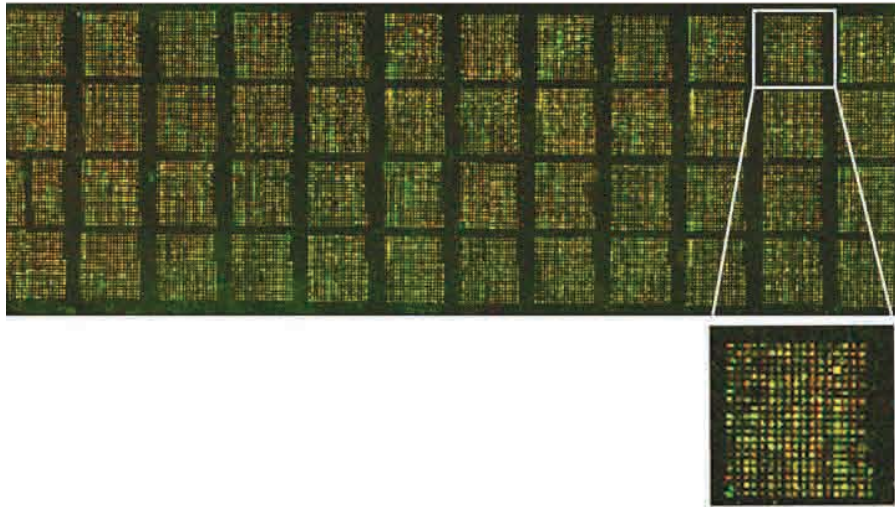
The dynamics of Eph-ephrin signaling have been extensively studied together with the cellular effects they bring about and the developmental processes they govern. In order to assess the extent to which Eph-ephrin signaling reaches the nucleus and affects gene expression and in order to identify new genes whose activation or repression can participate in mediating Eph-ephrin response, a microarray screening was carried out on mouse cortical neurons cultures. High density glass slides containing the National Institute of Aging (NIA) 15,000 mouse embryonic clone set (Tanaka et al., 1997) were produced in house, in collaboration between T. Iwata and G. Panté, using the facilities available at EMBL (Heidelberg). All clones were first amplified by PCR using a common set of primers flanking the insert. All PCR products, free of plasmid sequences, were then checked on agarose gel. To improve the quality of the cDNAs to be printed later on the glass support, only products showing a clear band were selected while those that showed double, multiple or no bands were discarded. Before glass spotting, some PCR products were randomly selected and further checked at the sequence level in order to confirm the identity assigned in the NIA sequence database to the specific clone so that possible errors in handling the clone collection could be ruled out. The glass slides containing the cDNA collection were hybridized to fluorescent probes obtained by reverse transcription of cellular mRNA from control and differentially stimulated test neuronal cultures (see **figure 6.1**).

Two screenings were performed, the first using 3DIV E15 mouse cortical neurons stimulated for 1 hour with either Fc as a control, or ephrinB2-Fc as test; the second screening was performed using 1DIV E15 mouse cortical neurons stimulated with Fc, as a control and with either ephrinB2-Fc or Eph-B1-Fc for 4 hours as test. The difference between the two screenings was the age of the neuronal cultures used, older and morphologically more differentiated neurons in the first case and younger, less differentiated neurons in the second; with the aim of evaluating changes in gene activation according to the developmental stage. EphrinB2 and EphB1 were arbitrarily chosen to stimulate the cortical neuron cultures because cortical neurons

are a heterogeneous neuronal population and different neuronal subtypes express various forms of Eph and ephrins. The second screening was carried out by T. Iwata.

The processed microarray data consist of raw lists of gene names (each corresponding to one of the 15,247 spots on the slide) together with statistic parameters that indicate, among other things, the intensity of each spot (which correlates with the abundance of the transcript in the original culture) and the ratio of the two fluorescence values (which is correlated with the relative abundance of one transcript versus the other). (See **figure 6.1.B**).

A



B

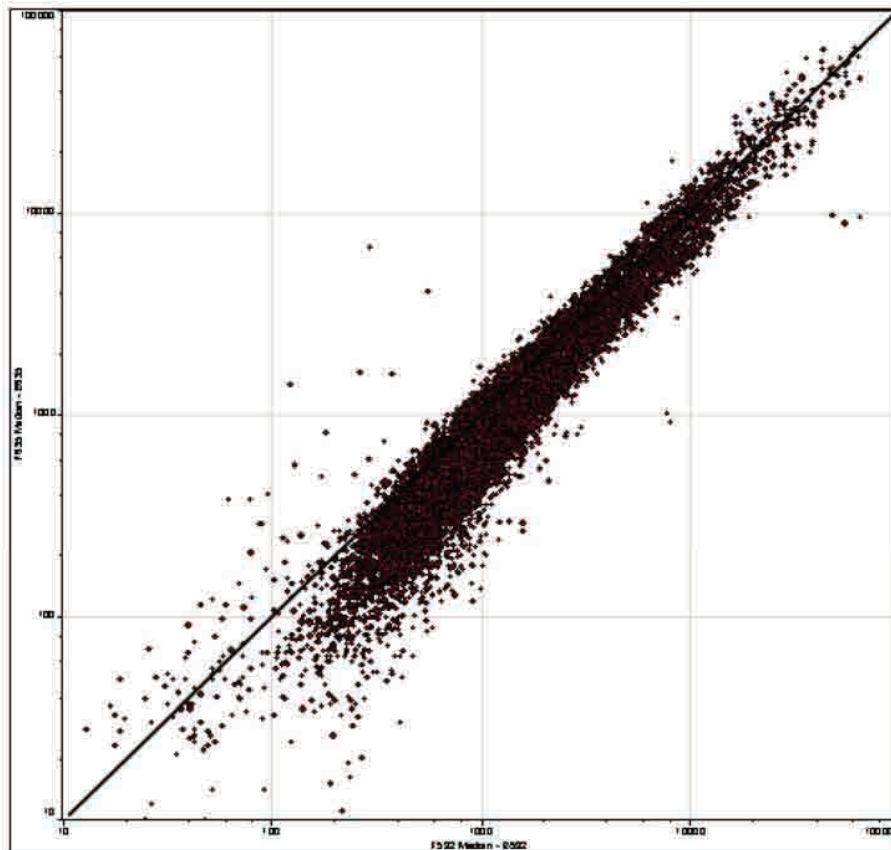


Figure 6.1. Processing a Microarray slide. A. Example of Microarray slide; 15,247 spots, each representing a single c-DNA, are arranged in 48 sub-arrays. After hybridization spots appear in

green, red and yellow. **B.** Example of “Scatter Plot”. Computer analysis calculates a set of statistic parameters important for the interpretation of the hybridization data. For each spot the median value of the red fluorescence channel (y) is plotted against the median value of the green fluorescence (x) in a logarithmic scale. The regression line indicates the 1/1 fluorescence ratio. Green fluorescence represents the control condition whereas red fluorescence represents the test. Spots along the regression line show no major difference between the control and the test conditions and appear yellow. Spots to the left of the regression line are up-regulated in the test condition and appear red. Spots to the right of the regression line are down-regulated in the test condition and appear green.

Microarray raw lists are further processed to extract, according to specific sorting criteria, shortlists of genes of interest. Raw data from screening 1 and 2 were first sorted according to spot intensity, in order to exclude all the rare cellular products and then according to a threshold of +1.99 or -3.79 folds of gene induction or repression, respectively, between the control and the test, in order to select the activities whose changes in expression levels were most striking upon stimulation with ephrin-Fc or Eph-Fc. A higher threshold for down-regulated genes was chosen due to the fact that the number of repressed genes appeared to be far higher and to vary much more in expression levels than the up-regulated genes.

In the case of screening 2, the short-listed genes were further classified in three categories: genes induced or repressed by the stimulation with ephrinB2-Fc, genes induced or repressed by the stimulation with EphB1-Fc and genes induced or repressed by the stimulation with both ephrinB2-Fc and EphB1-Fc.

Table 6.1 shows the shortlists of candidate genes from screening 1 (**A**) and from screening 2 (**B**), with clone number, number of folds of induction/repression in the microarray experiment and ID (if known). As mentioned before, the NIA 15K mouse embryonic clone set consists of 15,247 cDNAs. In fact, a major number of ESTs correspond to specific gene sequences with known ID whereas a portion of those sequences, namely 50% are novel genes with unidentified function. Thus, this gene collection was also chosen in order to uncover the role of novel molecules in Eph-ephrin signaling. Once sorted according to spot intensity and folds of induction/repression, the shortlist was further screened according to other parameters in order to obtain a number of candidate genes. These criteria comprise published data including expression patterns, structural features etc. The sequences of all hits with no annotated ID were extensively

compared to sequences in public and private databases (Genbank, Celera); some gave unclear hits, as their sequence matched several different gene sequences. In other cases the clone sequence was too short, most likely corresponding to non coding regions of the original transcript. Overall, even though potentially more promising, the genes with no ID were not studied further. Another important selection criterion was the validation, in the same cortical neuron cultures and the same stimulation conditions, of microarray induction/repression data by another experimental method, such as Northern Blot or RT-PCR, to assess gene expression changes in mRNA levels or Western Blot, for protein levels. RT-PCR was carried out in a semi quantitative way using the Light Cycler technology. RT-PCR is a two step method: RNA is first extracted then reverse-transcribed to cDNA. Specific PCR primers are then used in a standard amplification reaction. RT-PCR can be useful to visualize the levels of a transcript in a given condition as the intensity of the PCR band on agarose gel will be proportional to the abundance of the original mRNA in the system. Semi-quantitative RT-PCR compares the abundance of a transcript in two different conditions, control and test. The ratio between the abundance of the transcript in the test versus the control measures the relative increase or decrease of the specific mRNA when the stimulus is applied. The Light Cycler technology is based on the incorporation of a double strand specific fluorescent dye during the PCR reaction. The increase of fluorescence, which is detected live by an automated system, is a direct effect of the increase of double stranded DNA in the PCR reaction. Fluorescence intensities from control and test are calculated and compared and relative increases or decreases of the concentration of a transcript can be extrapolated. The advantage of the method lies in the fact that the fluorescence measurement takes place during the reaction and before saturation of the PCR, when both control and test products would have the same final fluorescence intensity (also see **figure 6.2**).

For clones with no ID *in situ* hybridization was also carried out in order to establish the patterns of gene expression in mouse embryos of the same developmental stage from which the original neuronal cultures used for the microarray experiments were prepared. Screening 1 yielded 28 regulated genes, 9 of them with non identified ID (**table 6.1.A**). All sequences were checked in RT-PCR analysis; most of them showed mRNA expression levels compatible with the microarray data (this also supports the suitability

of the Microarray approach). For a small percentage of clones RT-PCR data were in contrast with the Microarray and were discarded. In some cases, when RT-PCR was not applicable (i.e. difficulties in the selection of PCR primer sets), Western Blot was then used to analyze protein levels if a commercial antibody was available (L10, L23). Three clones with no ID (L1, L2, L3) were also used as probes in *in situ* hybridization experiments and all three showed an interesting embryonic nervous system specific staining (data not shown). Some clones, even if nicely induced or repressed, were discarded on the basis of literature background (for example as in the case of L15 or L17). The remaining clones with no ID annotation and genes which could not be validated with a second method were also discarded. A list of 6 genes was finally obtained (**Table 6.1**, green).

Short-listed genes from screening number two were processed and further sorted in the same way (see **table 6.1.B**). δ -Catenin was found to be the gene with the highest up-regulation fold in the category of genes induced by the activation of both Eph-forward and ephrin-reverse signaling. Because of problems in designing specific LightCycler primers for δ -Catenin (primer sets must be carefully selected in order to avoid secondary, double stranded structures, like hairpins, that may influence the measurement of fluorescence), and given the availability a good commercial antibody, Western Blot was chosen as main validation method of the Microarray data, with the limitation that only changes in protein levels would be studied.

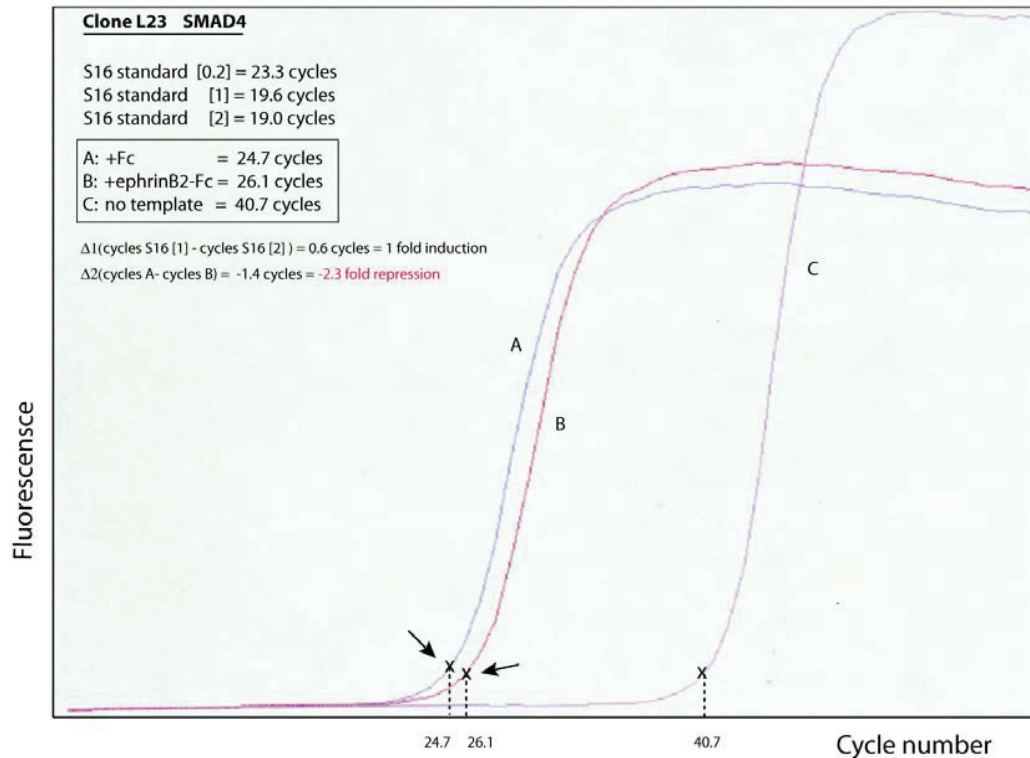


Figure 6.2. Example of Microarray validation by RT-PCR using the LightCycler technology. SMAD4 is a tumor suppressor in the TGF-beta signaling pathway and was found to be 5.7 folds repressed in Microarray experiments upon stimulation with ephrinB2-Fc (see table 1A, clone L23). Real time PCR was carried out to validate the data using the same cortical neuron culture as a system. Neurons were stimulated with either Fc or ephrinB2-Fc using the same procedure described for the Microarray. Total RNA was extracted, reverse transcribed and then used as a template for RT-PCR with the LightCycler technology. SMAD4 specific oligos were used in test reactions whereas primers for ribosomal S16 protein, an abundant transcript in the cell, were used in serial standards where template concentration is used in 2, 1 or 0.25 dilution ratios. The PCR reaction process is monitored by fluorescence detection, enabling measurement at the beginning of the detectable exponential phase or at the “crossing point” (x), which is considered the most reliable point of quantification. Crossing points are expressed as “number of cycles” and in general, a late crossing point correlates with low transcript abundance whereas an early crossing point indicates a high copy number of the original transcript and a higher abundance. In the case of clone L23, the signal from the ephrinB2-Fc stimulated condition appeared 1.4 cycles later than the signal from Fc control; this, extrapolating from the standard curve, indicated that L23 (SMAD4) was -2.3 fold repressed downstream of the activation of Eph-forward signaling, thus confirming and validating the Microarray data. The “no template” signal is most likely due to background fluorescence generated by primer dimers; due to its late appearance, it does not influence the experiment.

Figure 6.3 shows δ -Catenin protein level analysis in Western Blot. 3DIV, E15 mouse cortical neuron cultures were stimulated for 1 hour with ephrinB2-Fc, EphB1-Fc and Fc as a control. Both ephrin and Eph stimulation markedly increase δ -Catenin protein levels. The effect is detectable for up to 4 hours after stimulation. Even if the trend was very similar, less striking differences between control and Eph or ephrin-treated were detected in duplicate experiments, rather than the “black and white” pattern shown in **figure 6.3 A**, perhaps due to the fact that neurons in culture express a variable basal level of δ -Catenin even before stimulation, the protein being necessary in the homeostasis of the neurons. **Figure 6.3 B** shows an example: Fc stimulation for 1 hour and the corresponding lane for the 4 hours timepoint show a slight variability.

Western blots against two other Arm repeat family members, p120ctn and β -Catenin, showed no changes in protein levels upon stimulation with clustered ephrin or Eph receptor, this suggests that the effect observed in the case of δ -Catenin is indeed specific (data not shown).

Due to its relatively novel history and possible high experimental potential, its nervous system and development specific pattern of expression, its dendritic and synaptic distribution and of course the striking changes in gene expression and protein levels upon stimulation with both Eph and ephrins, and, last but not least, the immediate availability of several biochemical and genetic tools, δ -Catenin was preferred and selected as the candidate gene for further characterization and study.

A

CLONE #	ARRAY	RT PCR	WB	<i>in situ</i>	ID
L8	2.6				NO ID
L9	2.5				<i>polyglutamine containing pt</i>
L2	2.3	20		x	<i>Gene product [drosophila melanogaster] 1175 aa</i>
L10	2.3		OK		<i>Calsyntenin1</i>
L11	2.3				NO ID
L16	2.3				NO ID
L12	2.2	NV			<i>insulin-like growth factor II / cation-independent mannose</i>
L3	2.2	+++		x	<i>Transmembrane protein [Mus musculus] 738 aa</i>
L13	2.2	NV			NO ID
L14	2.2				<i>Perlecan</i>
L15	2.2				<i>Tubulin beta 2</i>
L17	2.2				<i>40 S Ribosomal protein</i>
L18	2.2				NO ID
L19	2.2	NV			NO ID
L20	2.2				NO ID
L5	2.1	1.8			NO ID
L28	2.1	2			<i>Riken cDNA</i>
L7	2	1.7			NO ID
L27	2	2.3			NO ID
L1	1.9	7.5		x	<i>Unknown [Mus musculus] 175 aa</i>
L4	1.9	1.9			<i>TFIID</i>
L6	1.9	1.9			<i>14-3-3 gamma</i>
L26	1.9	1.5			<i>Nfx 1</i>
L25	-3.7	-2.2			<i>Riken cDNA (SH3 domain)</i>
L23	-5.7	-2	OK		<i>Smad4</i>
L22	-5.8	NV			<i>mu-protocadherin</i>
L24	-6.5	-1.4			<i>Tangerin</i>
L21	-7.1				<i>Grasp5</i>

B

CLONE #	ARRAY Forward	ARRAY Reverse	WB	REVERSE SPECIFIC GENES
T1	1,2	2,9		NO ID
T2	1,5	2,7		<i>Synaptobrevin</i>
T3	1,4	2,6		<i>Ser/Thr kinase</i>
T4	1,6	2,6		NO ID
T5	-1,9	-5,8		<i>Riken Clone No ID</i>

CLONE #	ARRAY Forward	ARRAY Reverse	WB	FORWARD SPECIFIC GENES
T6	2,0	1,3		<i>Riken Clone No ID</i>
T7	2,0	1,3		<i>Lipin-3</i>
T8	2,0	1,8		No ID
T9	1,9	1,4		<i>Protein Kinase C, eta</i>
T10	-4,2	-1,8		<i>UBX domain containing protein</i>

CLONE #	ARRAY Forward	ARRAY Reverse	WB	FORWARD AND REVERSE SPECIFIC GENES
T11	4,3	4,7		NO ID
T12	3,8	4,1	OK	<i>Delta Catenin</i>
T13	2,3	3,0		NO ID
T14	2,9	2,6		NO ID
T15	-2,8	-4,3		NO ID

Table 6.1. Microarray shortlists. A: Microarray short list of up- and down-regulated genes from screen 1 (performed with E15 mouse cortical neurons 3 days *in vitro* stimulated with Fc

or ephrinB2-Fc for 1 hour). The table is completed with microarray validation methods and corresponding data and the gene ID, if known. Some of the array short listed genes were validated by checking mRNA levels after stimulation (RT-PCR), some by checking protein levels using Western blot. For some of them, particularly the genes with no database ID, in situ hybridization was carried out in E15 embryos in order to gather information about their expression patterns. In green are the genes whose microarray folds of induction/repression were confirmed by another method and that were interesting due to published data or structural features. In white are genes that were excluded from further analysis either because a second method gave contradictory information as compared to the microarray data or because they had no clear ID and at the same time the cDNA clones were too short (below 400 kb) to be studied further (NV=not validated). **B:** Table of genes short listed in screen 2. The selection criteria were as in the previous screen. Screen 2 was performed using E15 mouse cortical neurons 1DIV stimulated with Fc, ephrinB2-Fc or EphB1-Fc for 4 hours. “*ARRAY Forward*” indicates folds of induction upon stimulation with ephrin-B2-Fc and “*ARRAY Reverse*” indicates folds of induction upon stimulation with Eph-B1-Fc. The genes in the screen were divided in three categories: genes that were markedly up-regulated or down-regulated downstream of respectively: i. reverse signaling; ii. forward signaling; iii. both forward and reverse signaling. Each subgroup in table 1B includes the top five genes with the highest changes in gene expression for each of the three categories. δ -Catenin expression was found to be up-regulated downstream of both Eph and ephrin signaling.

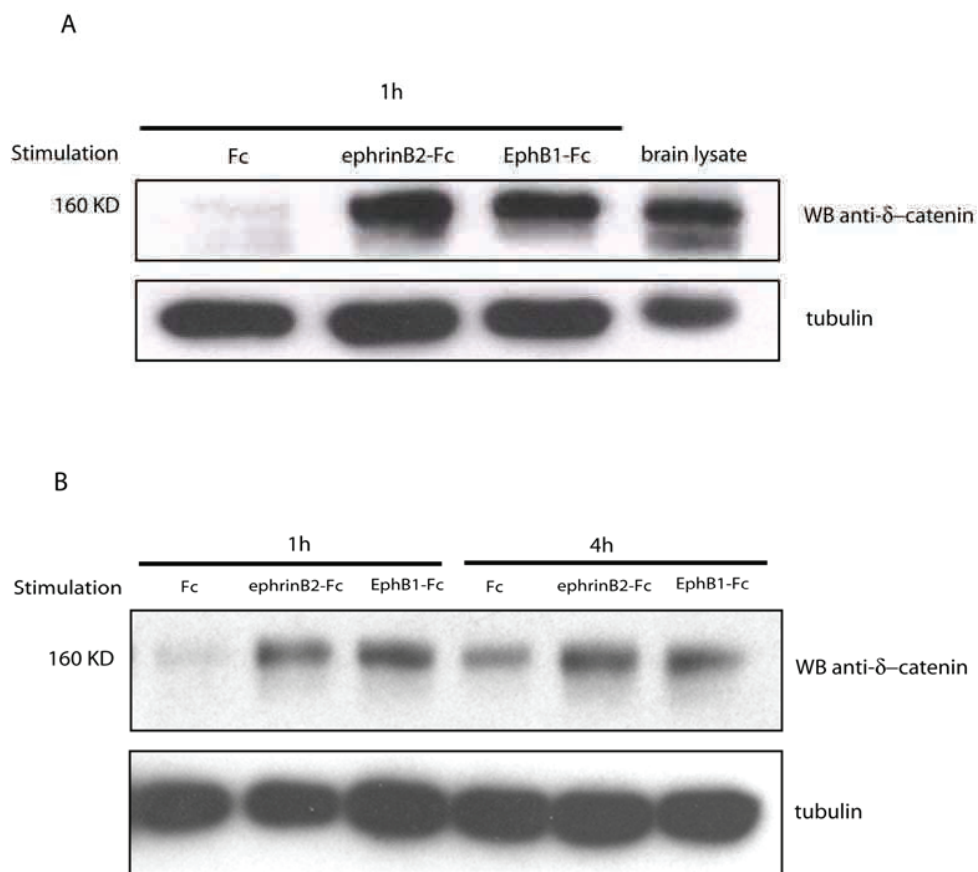


Figure 6.3. Microarray validation: δ -Catenin protein levels increase upon stimulation with both ephrin and Eph receptor. Western Blot was carried out using mouse E15 3DIV cortical neuron culture lysates and an anti δ -Catenin antibody. **A:** cultures were stimulated for 1 hour with Fc as a control, ephrinB2-Fc or EphB1-Fc. Western Blot anti tubulin was used as a loading control. Brain lysate used as a positive control for δ -Catenin protein. **B:** duplicate experiment. The increase in protein levels is sustained for 4 hours of stimulation.

6.2 δ -Catenin and Eph-ephrin signaling

The microarray data suggested that the up-regulation of δ -Catenin in neurons was a novel nuclear effect following the activation of Eph-ephrin signaling. The following experiments were aimed at addressing the questions about the nature of the effects that the induction of δ -Catenin brings about in the cell, and whether δ -Catenin could also play a direct role as a member of Eph-ephrin signaling cascade.

6.2.1 δ -Catenin is phosphorylated by Eph-forward signaling but not by ephrin-reverse

It has been shown that δ -Catenin can be phosphorylated by the cytoplasmic non-receptor tyrosine kinase c-Abl at two conserved NH2-terminal tyrosines (Lu et al., 2002). Moreover, δ -Catenin displays a long stretch of potentially phosphorylatable tyrosines in the COOH-terminus. Other members of the Arm repeat family, such as β -Catenin, have also been shown to be substrates for various kinase activities. In addition, the closest relative of δ -Catenin, p120, is also a potent Src kinase substrate. Therefore, a first experiment was to check if δ -Catenin was involved in the relay of phosphorylation following the activation of Eph-ephrin signaling. 3DIV cultures of mouse E15 cortical neurons were stimulated according to the same protocol used for the microarray experiments and their validation. Western blots using an anti phospho-tyrosine antibody showed that a band corresponding to the molecular size of δ -Catenin displayed a clear phosphorylation signal upon stimulation with ephrinB2-Fc but not with EphB1-Fc. Different stimulation time points were taken, ranging from 30 minutes to 24 hours. The phosphorylation peak was reached after 1hour and phosphorylation was sustained for at least 24h although with decreased intensity (see **figure 6.4 A**) In order to confirm the δ -Catenin phosphorylation after Eph receptor stimulation in neurons, HeLa cells were transiently co-transfected with an EGFP tagged version of δ -Catenin and wild type

EphA4 or a kinase-dead (KD) version of the receptor, that lacks kinase activity. δ -Catenin was immuno-precipitated and then probed for phospho-tyrosines. The phosphorylation signal could only be detected if δ -Catenin was co-expressed with the active form of EphA4 but not if co-expressed with the KD mutant (See **figure 6.4 B**). The product of the EphA4 construct is constitutively active and not regulated by ephrin binding; therefore no stimulation was required.

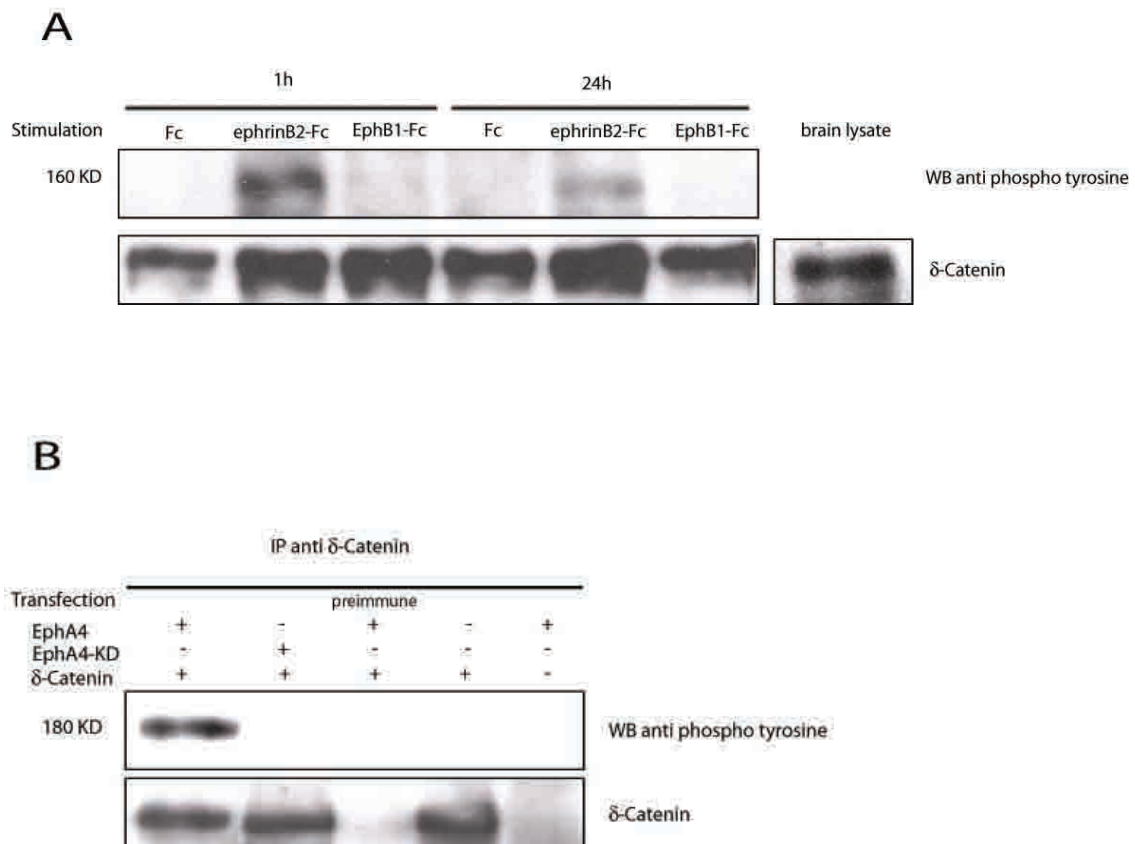


Figure 6.4. δ -Catenin phosphorylation upon activation of Eph-signaling in neurons and cell lines. **A:** δ -Catenin phosphorylation time-course in 3DIV mouse E15 cortical neuron cultures. A product of the molecular size correspondent to δ -Catenin is phosphorylated in response to ephrinB2-Fc stimulation but not to EphB1-Fc stimulation. The phosphorylation is sustained for up to 24 hours. **B:** δ -Catenin Phosphorylation in HeLa cells transiently expressing δ -Catenin and EphA4. δ -Catenin was immuno-precipitated via its EGFP tag then probed for tyrosine phosphorylation. δ -Catenin is phosphorylated by EphA4 but not by a kinase-dead (KD) version

of the receptor. If transfected alone, δ -Catenin is present in the cells in an unphosphorylated form. Rabbit pre-immune serum was used as a control and incubated with lysate from cells expressing EphA4 and δ -Catenin.

In order to define the structural domains of δ -Catenin involved in the phosphorylation induced by the activation of Eph receptor, two deletion mutants of δ -Catenin were used: one deletion covers the first 250 NH₂-terminal amino acids (Δ N250), the other lacks the final COOH-terminal 207 amino acids (Δ C207). The Δ N250 deletion covers a large portion of the NH₂-terminus of the molecule, including one of the two tyrosine residues phosphorylated by c-Abl (Lu et al., 2002). Δ C207 lacks the PDZ-binding motif and almost all of the 17 potential tyrosine phosphorylation sites of the COOH-terminus.

The two deletion mutants, both EGFP-tagged, were transiently transfected with active EphA4 in HeLa cells. The cells were also stimulated with ephrinB3-Fc because ephrinB3 as well as ephrinA1 are the two major ligands for EphA4. This stimulation was done to assess whether receptor clustering had an effect in phosphorylation levels. Immuno-precipitated Δ N250 probed for phospho-tyrosines showed a strong phosphorylation band which was as intense as in the case of full length δ -Catenin. The phosphorylation band of Δ C207, on the other hand, appeared to be weaker than in that of full length δ -Catenin and of Δ N250, suggesting that the tyrosine residues phosphorylated by EphA4 lie mostly at the COOH-terminal of the molecule. Receptor clustering appeared to play no role (see **figure 6.5**). The poor expression of the Δ C207 construct though, complicates the interpretation of this result.

The phosphorylation of δ -Catenin by Eph receptors suggests that the role of the molecule in Eph-ephrin signaling does not merely involve the induction of δ -Catenin expression but a more complex interaction that involves biochemical modifications of the molecule and that suggests a possible active role of δ -Catenin in the signaling cascade. Strikingly, the phosphorylation of δ -Catenin is specific for Eph-forward signaling as it was not observed downstream of ephrin activation. This suggests a differential involvement of δ -Catenin in the two cellular responses.

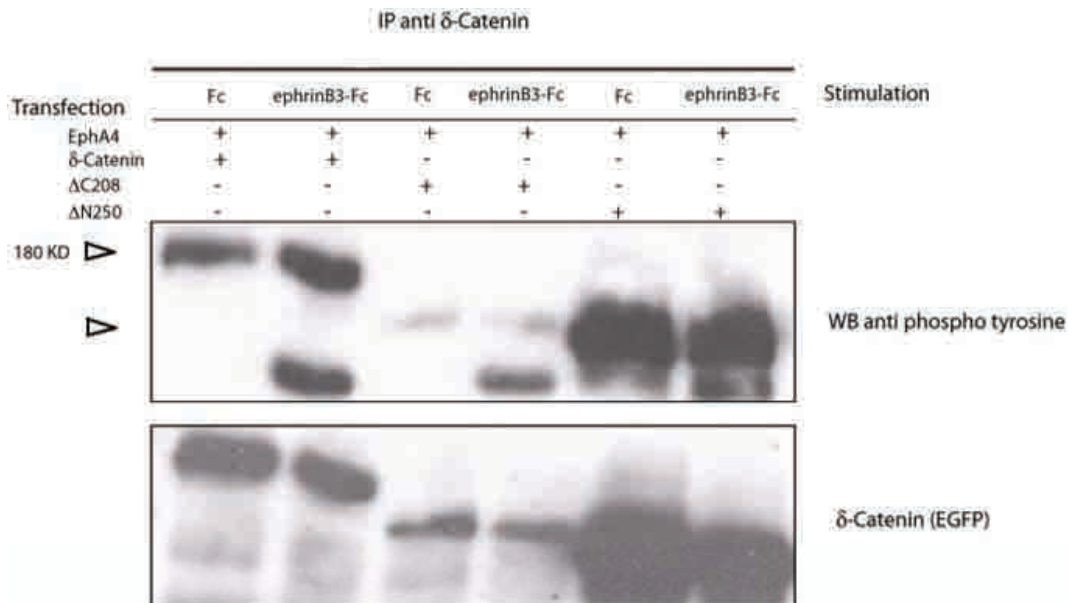


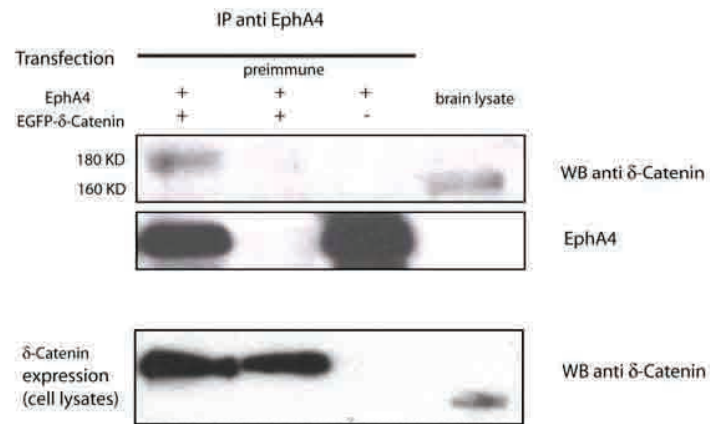
Figure 6.5. Phosphorylation of δ -Catenin and deletion mutant Δ N250 but not of Δ C208 in HeLa cells. Immuno-precipitated δ -Catenin and deletion mutant Δ N250 show a stronger phosphorylation band, when co-transfected with EphA4, than deletion mutant Δ C208; suggesting that the C terminus of δ -Catenin is likely to be the target of Eph receptor mediated phosphorylation. Arrows indicate δ -Catenin full length and the deletion mutants Δ N250 and Δ C208 (lower molecular weight). δ -Catenin and the deletion mutants were immuno-precipitated using the EGFP-tag (stripped membrane stained with anti EGFP is shown in lower panel). The cells were stimulated with ephrinB3-Fc in order to assess the role of receptor clustering in δ -Catenin phosphorylation levels as EphA4 is constitutively activated if expressed in HeLa cells. The presence of phospho bands of lower molecular weight (upper panel) in correspondence with ephrinB3-Fc treatment is currently not yet explained; one explanation could be the co-immunoprecipitation of an unidentified protein.

6.2.2 δ -Catenin and EphA4 interact physically

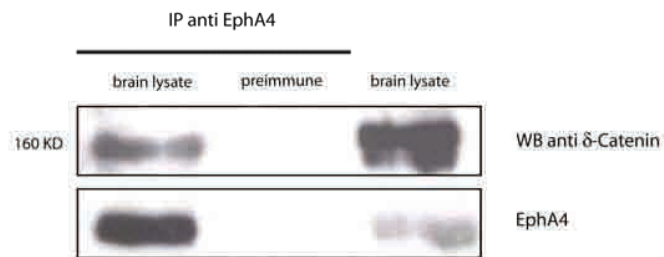
Several factors bind the activated Eph receptor, mostly adaptor molecules containing protein-protein interaction SH2- and SH3-domains, and other factors that, once phosphorylated by the receptor, help transduce the signal into the cell. δ -Catenin contains SH3-binding motifs and protein interaction moieties that suggest a role as a signaling/adaptor molecule in signal transduction cascades. The phosphorylation of δ -Catenin following the activation of Eph-ephrin signaling raised new questions about the nature of the interaction between δ -Catenin and Eph receptor. Specifically, if the two molecules interact directly, possibly through their several protein-protein interaction moieties, or if the phosphorylation of δ -Catenin is an indirect effect mediated by another protein downstream of the activated Eph receptor. Biochemical evidence for a physical interaction surfaced as EphA4 and δ -Catenin co-immunoprecipitated from HeLa cells when transiently co-transfected (**figure 6.6 A**). The result was confirmed by co-immunoprecipitation of endogenous EphA4 and δ -Catenin from mouse E17 brain lysates (**figure 6.6.B**)

In order to establish if the interaction between EphA4 and δ -Catenin requires the kinase activity of the receptor, HeLa cells were transiently co-transfected with KD-EphA4. The mutant retained the ability to interact with δ -Catenin and co-immunoprecipitated, similarly to another receptor mutant 2E-EphA4. The 2E mutant has the two conserved juxtamembrane phospho-tyrosines mutated into glutamic acid; the mutation removes the receptor autoinhibition loop and changes its conformation to constitutively active. The two phospho-tyrosines are crucial in Eph-mediated signaling as they are docking sites for several factors involved in the cascade. The 2E mutant also retained the ability to co-immunoprecipitate δ -Catenin (**figure 6.6.C**) suggesting that, at least in transiently transfected cell lines, the interaction between δ -Catenin and EphA4 is not regulated by Eph receptor kinase activity and does not require the two juxtamembrane phosphotyrosines.

A



B



C

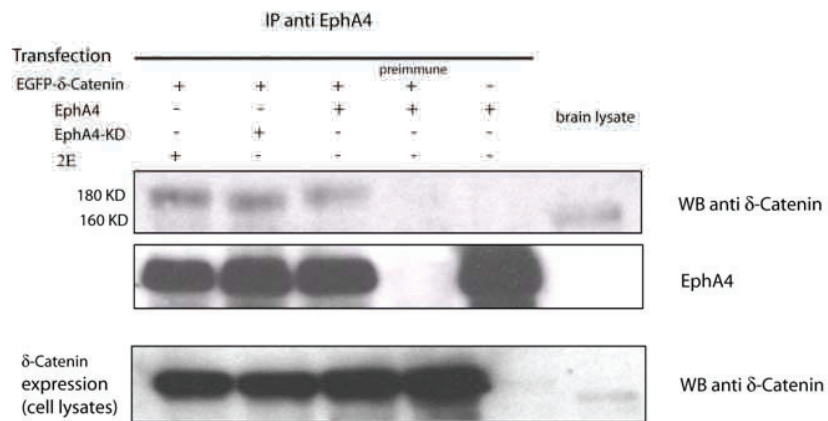


Figure 6.6 δ -Catenin and EphA4 co-immunoprecipitate in cell lines and brain lysate. A: IP anti EphA4 shows co-immunoprecipitation δ -Catenin from co-transfected HeLa cell lysates. The

difference of δ -Catenin apparent molecular weights is due to the EGFP-tag of transfected full length δ -Catenin. **B:** IP anti EphA4 shows co-immunoprecipitation of δ -Catenin from E17 brain lysates. **C:** IP anti EphA4 shows co-immunoprecipitation of EphA4 and mutants 2E and Kinase Dead (KD) with δ -Catenin (HeLa cells).

Further evidence for the interaction between δ -Catenin and EphA4 in neurons was obtained from fluorescent protein imaging using rat hippocampal cultures. The switch to rat neurons was due to the ease of transfecting rat neuronal cultures as opposed to mouse cultures. Hippocampal neurons from E19 rats were kept in culture and then transfected with fluorescently tagged versions of δ -Catenin and Eph receptor. Both proteins appeared to be expressed and homogeneously distributed throughout the neurons with no difference in cellular localization. Upon stimulation with ephrin at different time-points, together with the expected gradual formation of fluorescent Eph receptor clusters, a striking intracellular redistribution of fluorescent δ -Catenin was also noticed. δ -Catenin appeared to form aggregates that grow in size overtime, as the stimulation time proceeded. The first aggregates appeared after 30 minutes of ephrin application and they grew in size and number for 2 hours after stimulation. Strikingly, δ -Catenin aggregates and Eph receptor clusters appeared to co-localize, even if the dynamics of formation differed. Eph receptor clusters appeared after a few minutes from stimulus application while δ -Catenin aggregates became clearly visible only after about 30 minutes, hinting at the fact that one event may precede the other. A second interesting event that ephrin stimulation triggered in neurons over-expressing fluorescent δ -Catenin was a marked change in cellular morphology, specifically involving cellular processes: with dynamics similar to those of the formation of δ -Catenin clusters, neurites appeared to retract, markedly decrease in length, become thicker in diameter, and assume a much more irregular shape (**figure 6.7**).

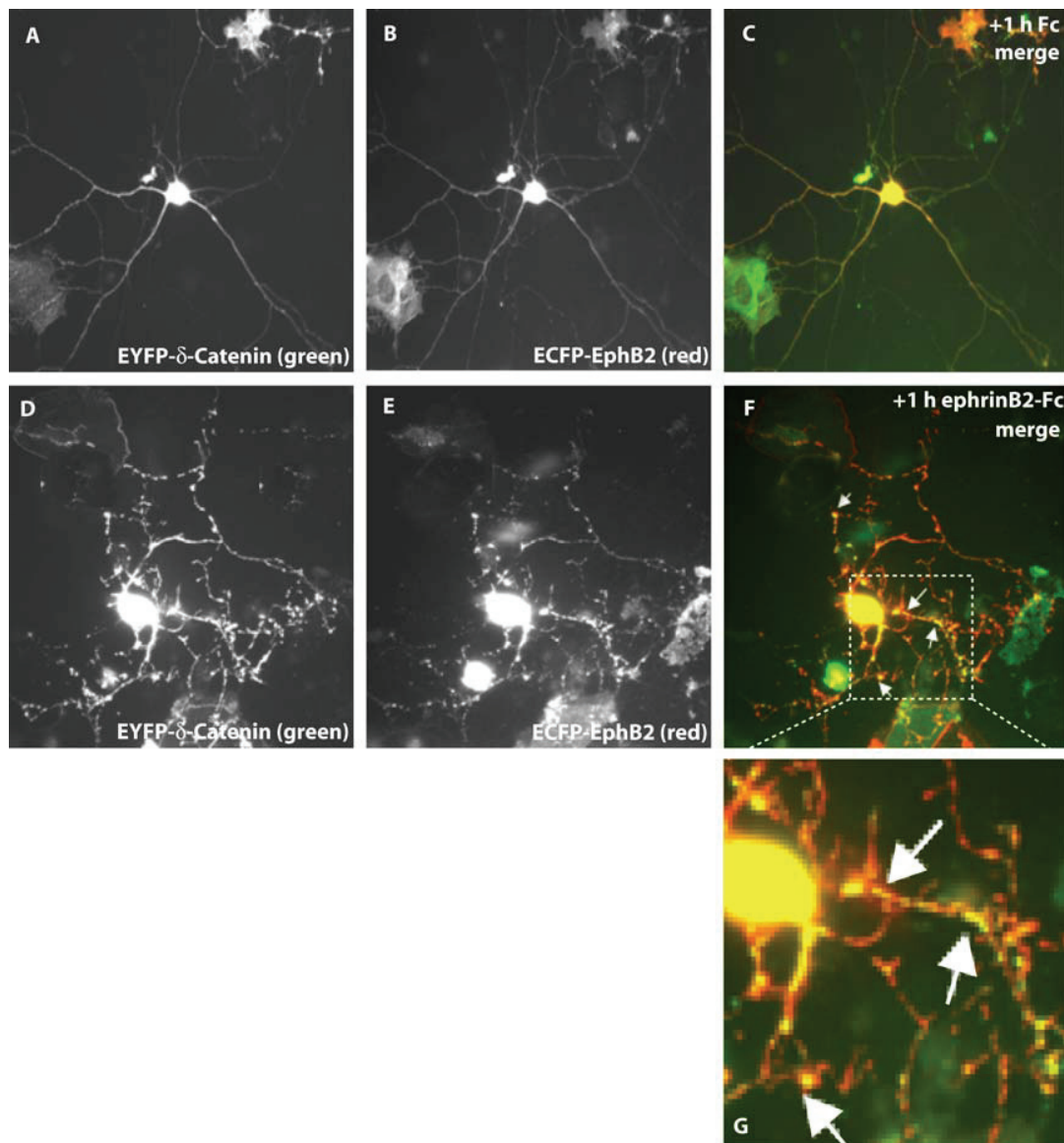


Figure 6.7: Fluorescently tagged δ -Catenin changes its intracellular distribution upon stimulation with ephrin. Rat hippocampal neurons in culture transfected with fluorescently tagged EphB2 receptor (ECFP) and δ -Catenin (EYFP) were stimulated for 2 hours with Fc as a control (panels **A**, **B**, **C**) and with ephrinB2-Fc (panels **D**, **E**, **F**, **G**). Upon stimulation, δ -Catenin strikingly changes its cellular distribution, forming aggregates that tend to become bigger overtime (other time points not shown). δ -Catenin aggregates co-localize with EphB2 clusters (see panels **F** and **G**, arrows). Note that stimulated neurons appear to have shorter neurites and a more irregular shape if compared to control neurons. (Transfection at 3DIV and imaging after 2 days)

The intracellular re-localization of δ -Catenin upon stimulation and the formation of aggregates which co-localize with Eph receptor clusters were also observed in NIH3T3 cell lines co-expressing fluorescently tagged versions of the two molecules. δ -Catenin forms aggregates upon ephrin stimulation and these appear to co-localize with Eph receptor clusters (**figure 6.8**).

Similar results were obtained with HeLa cells that co-expressed EGFP- δ -Catenin and EphA4 and were stimulated with pre-clustered ephrinB3-Fc: EGFP- δ -Catenin undergoes a striking redistribution, forming aggregates that colocalize with EphA4 clusters (**figure 6.9**). The EGFP- Δ C208 mutant on the other hand has a mislocalization problem, appearing to be unevenly distributed, already forming aggregates, independent of any stimulation. Some of the aggregates appear to partially co-localize with EphA4, raising the question whether EphA4 and EGFP- Δ C208 actually interact. For technical reasons it was not possible to prove this interaction with biochemical methods.

The co-immunoprecipitation results and the data from fluorescence imaging provide evidence that δ -Catenin and Eph receptor do interact with each other in cell lines but also in neurons. Whether they interact directly or via some adaptor protein remains to be clarified. The activation of Eph-ephrin signaling has a strong effect on δ -Catenin subcellular distribution, leading to the formation of large aggregates that co-localize with Eph receptor clusters. This hints to the possibility that δ -Catenin may be recruited by Eph receptor in response to receptor activation, is then phosphorylated and is subsequently involved in the downstream signaling cascade. The Δ C208 mutant, on the other hand, as a non phosphorylatable version of δ -Catenin (or due to its poor expression and mislocalization), may not be able to take part in the phosphorylation relay downstream of the activated receptor.

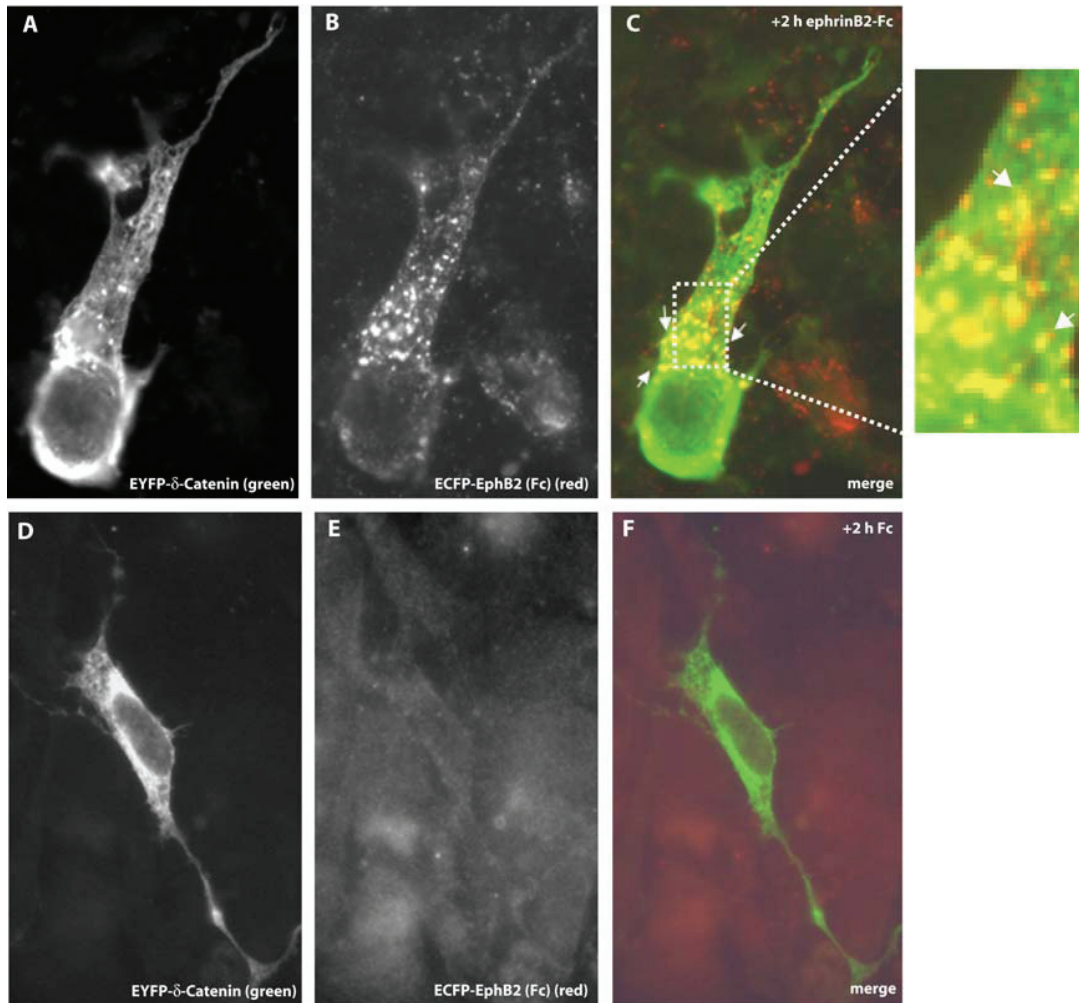


Figure 6.8. Ephrin induced δ -Catenin aggregates and EphB2 clusters co-localize in NIH3T3 fibroblasts. Co-localization (arrows) of co-transfected EYFP- δ -Catenin and ECFP-EphB2 upon stimulation with ephrinB2-Fc (**A, B, C**) or Fc (**D, E, F**) for 2 hours. EYFP-Delta Catenin, green; anti Fc immuno-staining (stains clustered ephrin-Fc bound to Eph receptor), red.

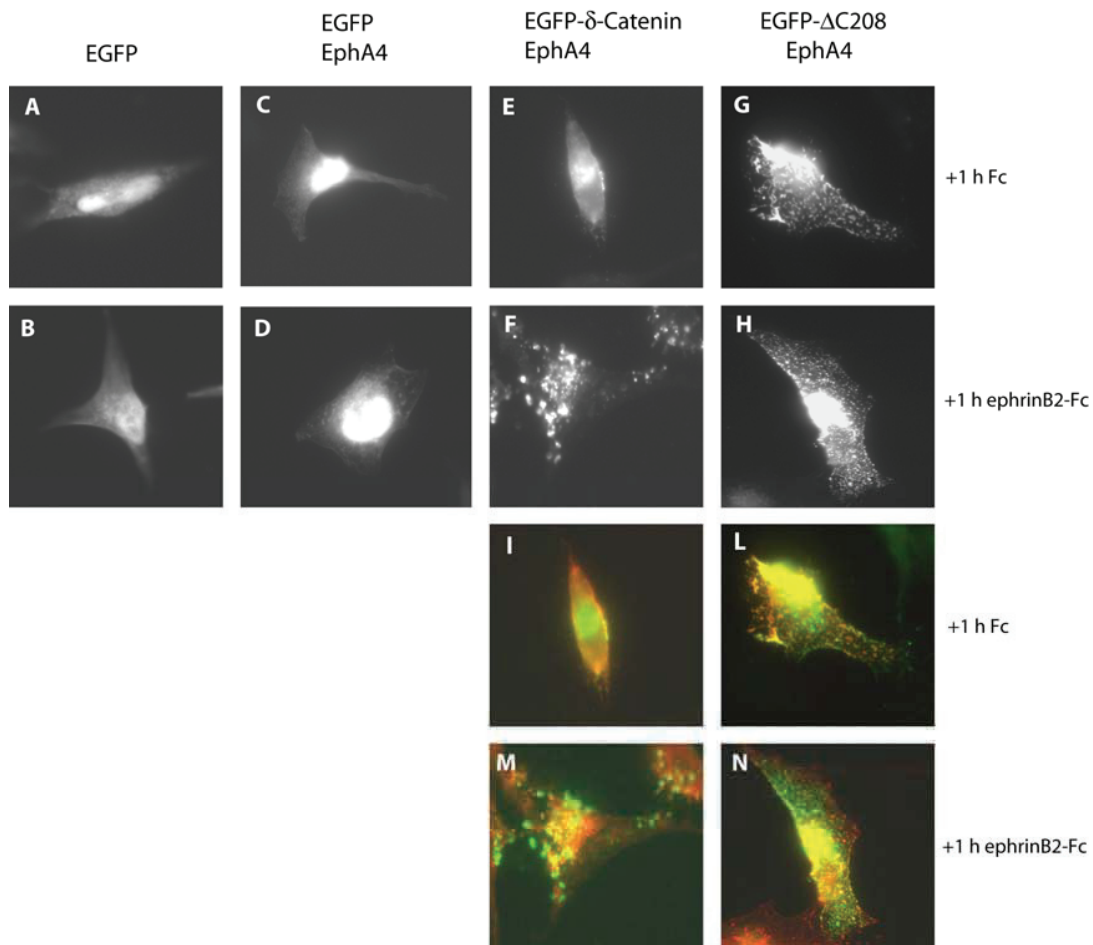


Figure 6.9. Relocalization of EGFP- δ -Catenin and co-localization with EphA4 after 1 hour stimulation with ephrinB3-Fc in HeLa cells. **A** and **B**, EGFP-transfected cells. **C** and **D**, cells co-transfected with EGFP and EphA4. **E** and **F**, cells co-transfected with EGFP- δ -Catenin and EphA4. **G** and **H**, cells co-transfected with EGFP- Δ C208 and EphA4. In **A** to **G** cells were stimulated with Fc as a control; in **B** to **H** with ephrinB3-Fc. All images show EGFP-fluorescence. Panels **I**, **L**, **M**, **N** show respectively **E**, **F**, **G**, **H** images (EGFP fluorescence in green) merged with anti EphA4 staining (red). EGFP- δ -Catenin undergoes an intracellular redistribution upon stimulation with ephrinB3-Fc, forming clusters which co localize with EphA4 clusters (**F**, **L**). EGFP- Δ C208 shows an uneven distribution, even under control conditions. Stimulation with ephrinB3-Fc does not have any visible effect. EGFP- Δ C208 clusters seem to partially co-localize with EphA4 clusters (**G**, **H**, **M**, **N**) (anti EphA4 staining alone is not shown).

6.3 Eph receptor forward signaling, but not ephrin reverse signaling, leads to the formation of δ -Catenin aggregates

In order to further investigate the dynamics of formation of δ -Catenin aggregates and the interaction with ephrinBs, rat hippocampal neurons were transfected with EGFP- δ -Catenin and imaged at different timepoints after stimulation with Fc as a control, ephrinB3-Fc or EphB1-Fc. As shown before, stimulation with ephrin induced an intracellular rearrangement of EGFP- δ -Catenin, causing the formation of aggregates that start to be visible at 30 - 60 minutes after stimulation, and become larger overtime (**figure 6.10 C and D**). Formation of δ -Catenin aggregates was not observed with Fc control stimulation (**figure 6.10 A and B**) and interestingly, with EphB1-Fc stimulation (**figure 6.10 E and F**). This led to the conclusion that δ -Catenin aggregated as a specific response to activation of forward signaling. These data correlate with δ -Catenin phosphorylation (also forward signaling specific), hinting at the fact that the activation of Eph receptor could lead to the recruitment and phosphorylation of δ -Catenin, which would then form aggregates at sites where active Eph receptors cluster. As mentioned before, the dynamics of δ -Catenin aggregates formation are slightly delayed from those of Eph receptor clusters and of Eph receptor activation, suggesting that the two events occur sequentially. Interestingly, δ -Catenin phosphorylation and aggregate formation dynamics are almost overlapping, about 30 – 60 minutes after stimulation as the two events first become detectable.

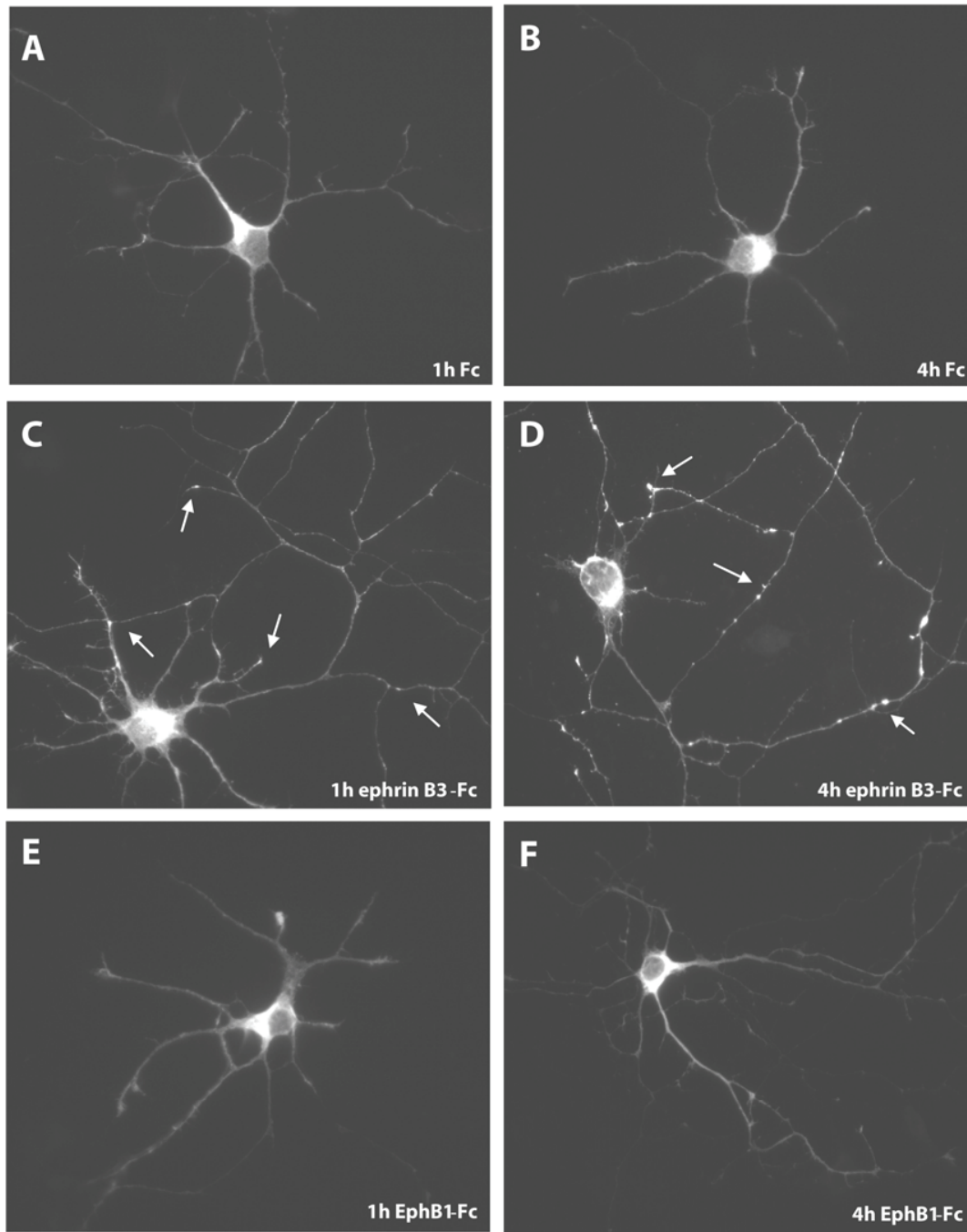


Figure 6.10. Eph receptor forward signaling, but not ephrin reverse signaling, leads to the formation of δ -Catenin aggregates. EGFP- δ -Catenin re-localization upon stimulation of transfected rat hippocampal neurons: δ -Catenin forms aggregates that increase in size overtime (arrows) only in neurons stimulated with ephrinB3-Fc (C and D) but not with Fc or EphB1-Fc (panels A and B and E and F respectively), (transfection at 3DIV and imaging after 2 days).

In order to better visualize the dynamics of δ -Catenin aggregate formation, rat hippocampal neurons expressing EGFP- δ -Catenin were imaged live for up to 125 minutes. Neurons were kept in culture and filmed for 60 minutes (1 image/5 min) before the stimulus was applied, then time lapse images were taken for 60 additional minutes. The stimuli used were ephrinB3-Fc and Fc as a control, being these two cases the most interesting in the set of fixed neurons described above. Application of ephrinB3-Fc clearly triggers EGFP- δ -Catenin aggregation in addition to causing changes in neurite shape; neurites retract and appear less regular in shape (**figure 6.11**). δ -Catenin aggregates are visible not only all along the cellular processes but also in the cell body. Control neurons stimulated with Fc do not show any change in δ -Catenin distribution overtime (**figure 6.12**). The time lapse experiments therefore confirm and reinforce the conclusions drawn from the fluorescence analysis of fixed hippocampal neuron cultures; fluorescently tagged δ -Catenin undergoes a dynamic redistribution upon stimulation with ephrinBs.

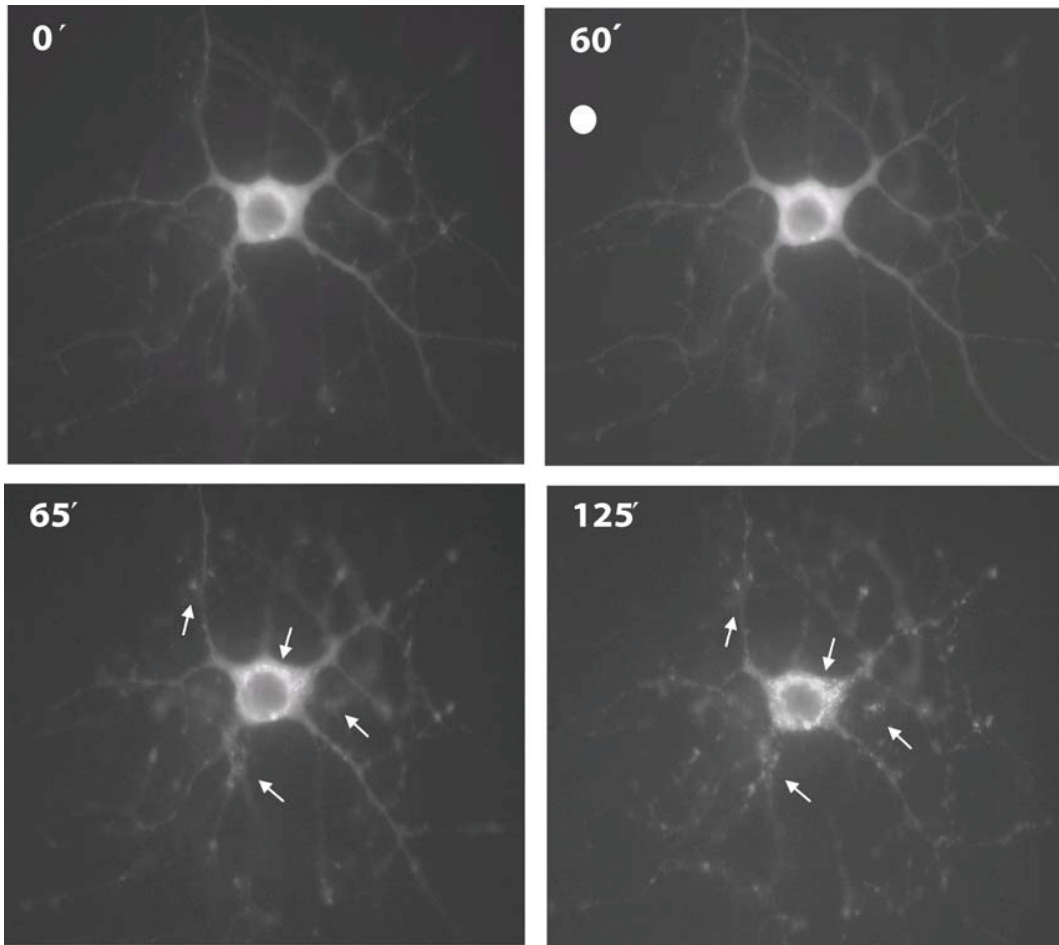


Figure 6.11. Live imaging of a EGFP- δ -Catenin transfected hippocampal neuron upon stimulation with ephrinB3-Fc. EphrinB3-Fc was added 60 minutes after imaging start. EGFP- δ -Catenin fluorescence undergoes an intracellular redistribution forming aggregates (**arrows**) that increase in size overtime. The aggregates can first be observed 5 minutes after stimulation and become more evident after about 1 hour stimulation. Time intervals: 5 minutes, exposure 100 msec. Transfection at 3DIV and imaging after 2 days (also see multimedia support).

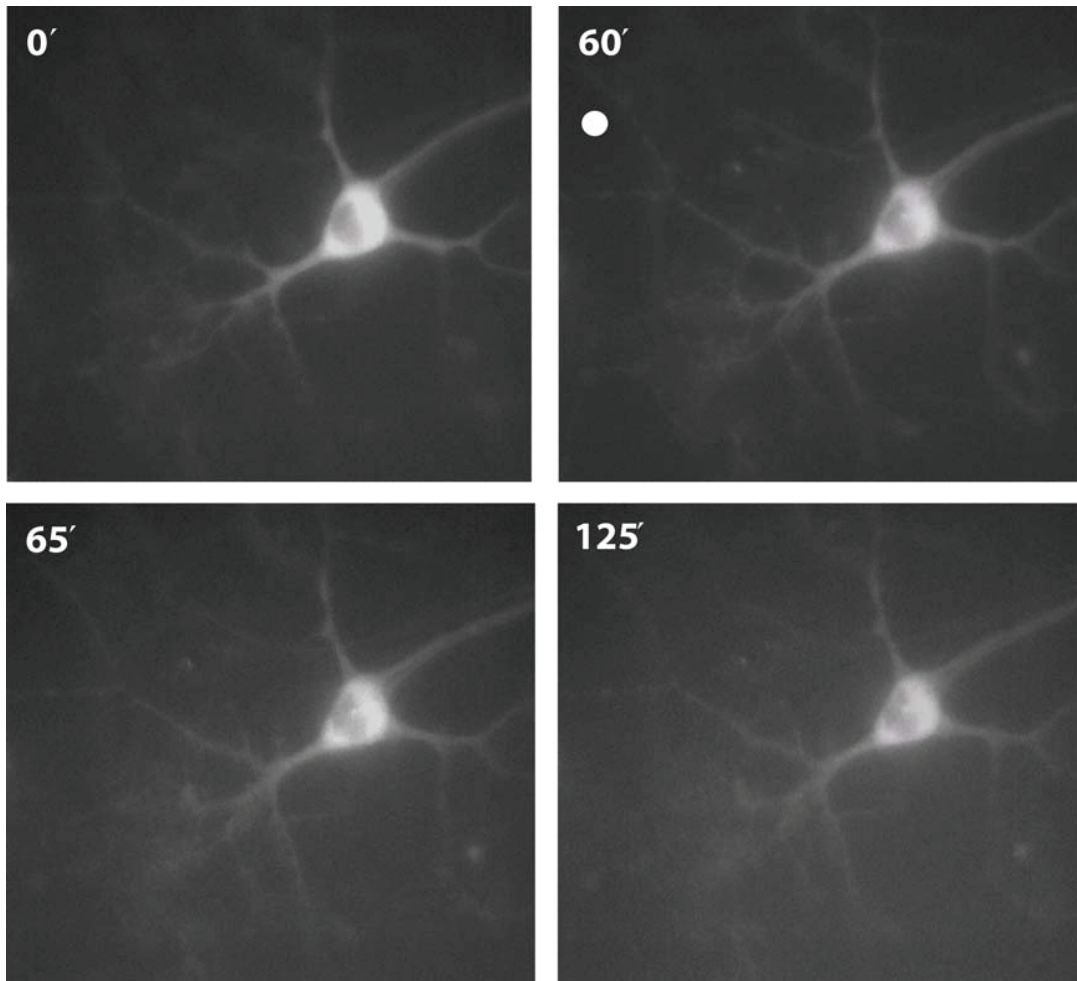


Figure 6.12. Live imaging of a EGFP- δ -Catenin transfected hippocampal neuron upon stimulation with Fc as a control. Fc was added 60 minutes after imaging start. EGFP- δ -Catenin fluorescence distribution is unchanged. Time intervals: 5 minutes, exposure 100 msec. Transfection at 3DIV and imaging after 2 days (also see multimedia support).

6.4 δ -Catenin and Eph-ephrin signaling are required for the establishment of proper dendritic morphology

Having shed some light on the nature of the δ -Catenin and Eph receptor interaction, the next question was to clarify what kind of cellular response and biological function was downstream of δ -Catenin and Eph-ephrin signaling. It has already been shown that over-expression of δ -Catenin in cultured hippocampal neurons alters dendritic morphology, causing a massive dendritic overgrowth (Lu et al., 2002). It was shown before that hippocampal neurons expressing EGFP- δ -Catenin display marked changes in neurite shape upon stimulation with ephrin ligand in addition to the re-localization and aggregation of EGFP- δ -Catenin protein. In order to study ephrin-induced changes in dendritic morphology, control neurons expressing EGFP, neurons expressing EGFP- δ -Catenin, and neurons expressing EGFP- Δ C207 were analyzed upon stimulation with different factors. As mentioned before, δ -Catenin COOH terminus deletion mutant Δ C207 lacks the PDZ binding motif and most of the 17 potentially phosphorylatable tyrosines. Δ C207 was shown to act as a dominant negative version of δ -Catenin as it can multimerize and sequester the endogenous protein (Lu et al., 2002). It also prevents the full length construct from causing the characteristic increase dendrite complexity if co-expressed in neurons. EGFP- Δ C207 expressing neurons appear to be much less complex than control neurons, being markedly less branched and having shorter dendrites. A very similar phenotype is caused by the depletion of endogenous δ -Catenin with RNAi interference (unpublished data, personal communication with Qun Lu, ECU, USA). Control EGFP, EGFP- δ -Catenin or EGFP- Δ C207 neurons were stimulated with Fc, ephrinB3-Fc, BDNF or NGF for 24 hours in order to visualize any long term effects on dendritic morphology. BDNF and NGF were chosen because of their well known promoting effect on dendritic outgrowth, therefore providing a reference and a control. The study of dendritic morphology was carried out using the Sholl analysis method in which a grid of concentric circles is centered on the cell body of a neuron and the number of times the dendritic tree intersects the grid is measured. The resulting figures show the

degree of complexity of the dendritic tree analyzed (Sholl, 1953). For statistical analysis of the following experiments, each condition is represented by 8 different neurons, with a total of 106 neurons imaged.

Figure 6.13 shows a summary of the effects of Fc, ephrinB3-Fc, BDNF and NGF on EGFP-transfected neurons as a reference for a control condition in which only endogenous δ -Catenin is present. Rat hippocampal neurons in culture express a basal level of δ -Catenin as shown by immuno-fluorescence staining (data not shown). Interestingly, long term stimulation with ephrinB3-Fc has an effect on the overall complexity of the neurons. Dendrites appear to shorten, to have fewer branches and to generate a number of short, filopodia-like cellular processes if compared to neurons treated with control Fc. An effect of Eph-ephrin signaling in shaping dendritic morphology was so far unreported even if the effect is mild. The stimulation with both BDNF and NGF on the other hand, causes a marked increase in dendritic complexity, enhancing, as expected, dendritic branching and length. The effects were quantified with a Sholl analysis and reported in tables of figure 6.14.

Figure 6.15 shows a summary of the effects of Fc, ephrinB3-Fc, BDNF and NGF on EGFP/EGFP- δ -Catenin co-transfected neurons. The co-transfection with EGFP was necessary to better visualize cellular contours and fine processes possibly devoid of fluorescent δ -Catenin. As mentioned before, δ -Catenin over-expression alone is able to increase dendritic complexity. Upon stimulation with ephrinB3-Fc, though, the dendritic tree undergoes a massive reorganization, in a similar fashion to that observed in EGFP-neurons but much more pronounced: dendrites appear much shorter and the number of dendritic branches was lower. On the other hand, BDNF and NGF do not have any specific additional effect to δ -Catenin induced dendritic complexity. Figure 6.16 shows the Sholl analysis for these neurons.

Figure 6.17 shows a summary of the effects of Fc, ephrinB3-Fc, BDNF and NGF on EGFP/EGFP- Δ C207 co-transfected neurons. As mentioned before, the deletion mutant alone induces a simplification of dendritic architecture; dendrites appear unbranched and short. The number of primary dendrites directly sprouting from the

cell body is very elevated, as compared to control neurons and additionally they show a higher number of short filopodia-like processes whose number or formation does not appear to be influenced by any of the stimuli applied, appearing unchanged in their morphology. Figure 6.18 shows the Sholl analysis data for these neurons.

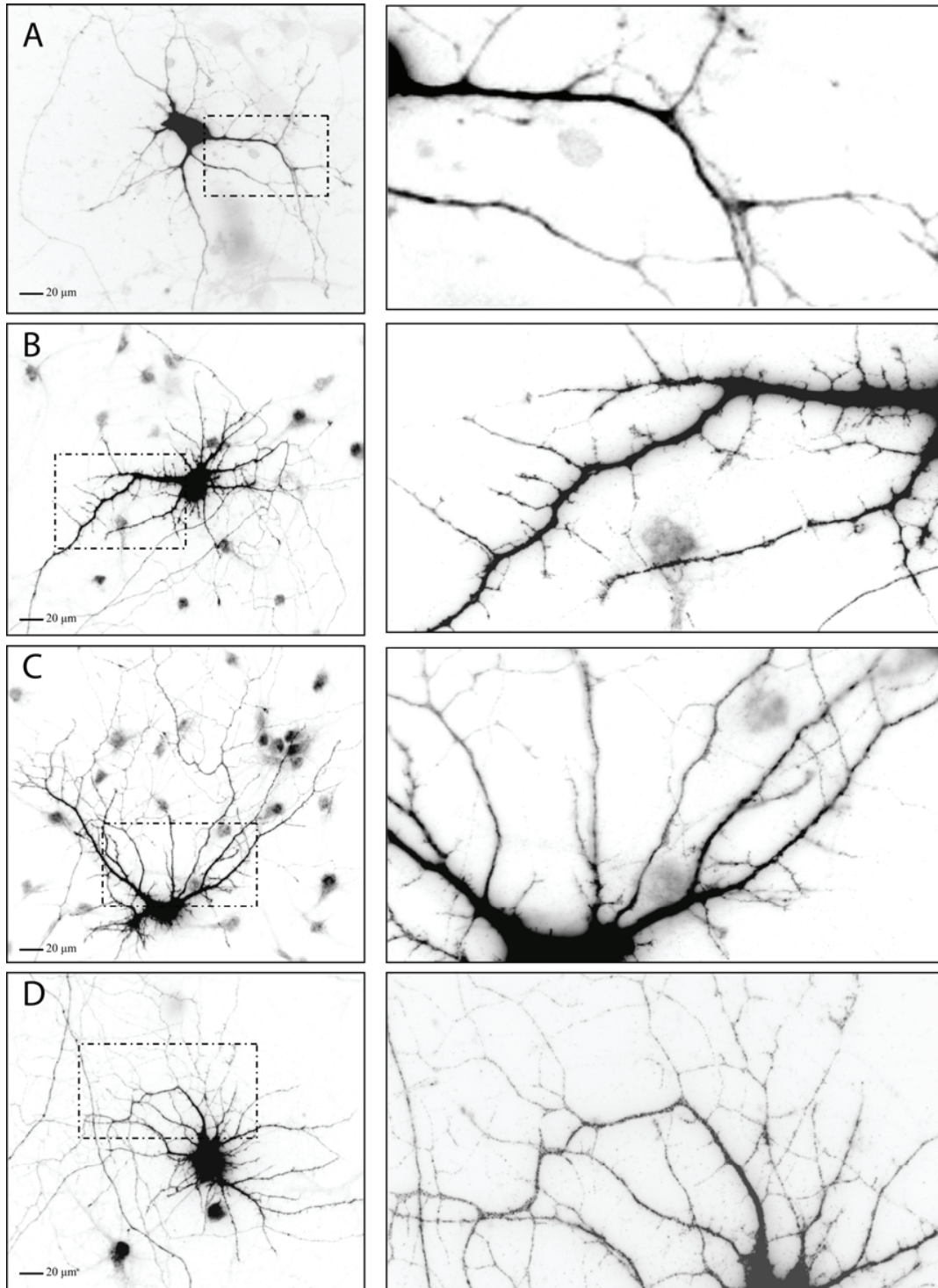


Figure 6.13. Effects of long-term ephrinB3-Fc, BDNF, or NGF on dendritic morphology of EGFP-transfected hippocampal neurons. A. Neuron stimulated with Fc for 24 hours. B. Neuron stimulated with ephrinB3-Fc; the cell appears to have shorter and less branched dendrites and show a higher number of small filopodia-like cellular processes. C and D. Neurons

stimulated with BDNF or NGF, respectively: both factors increase neuronal complexity promoting dendritic branching and elongation. Transfection at 3DIV and imaging after 2 days.

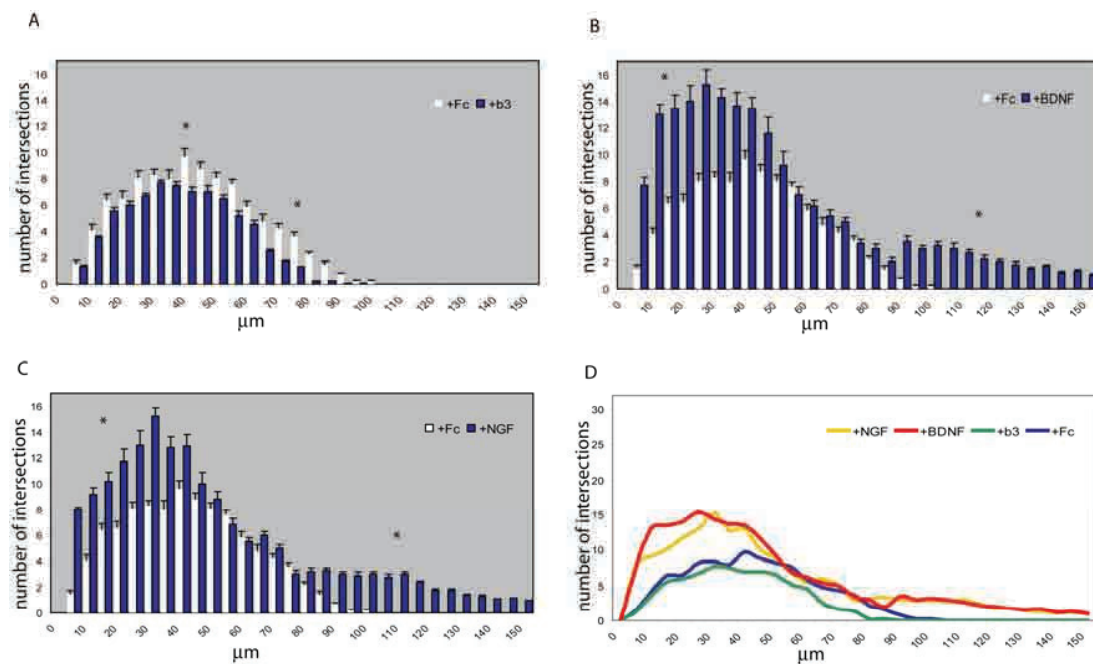


Figure 6.14 Sholl analysis of EFGP-transfected hippocampal neurons stimulated with Fc, ephrinB3-Fc, BDNF or NGF for 24 hours. The number of intersections between dendrites and Sholl circles is plotted as a function of the distance from the cell body. **A.** EphrinB3-Fc stimulation (blue bars) induces a simplification of the dendritic arbor as compared to Fc treated control neurons (white bars). The effect is evenly distributed all along the dendritic tree ($p < 0.05$ for areas neighboring asterisks). **B.** BDNF stimulation causes a marked increase in the complexity of the dendritic arbor, especially in regions close to the cell body and in regions most distal from it (asterisks indicate broad areas of statistical significance; $p < 0.01$). **C.** NGF stimulation causes very similar effects to BDNF (asterisks indicate broad areas of statistical significance; $p < 0.01$). **D.** Overall comparison view of Fc, ephrinB3-Fc, BDNF and NGF effects (3DIV+2 days after transfection), ($n=8$), (for simplicity ephrinB3-Fc = b3).

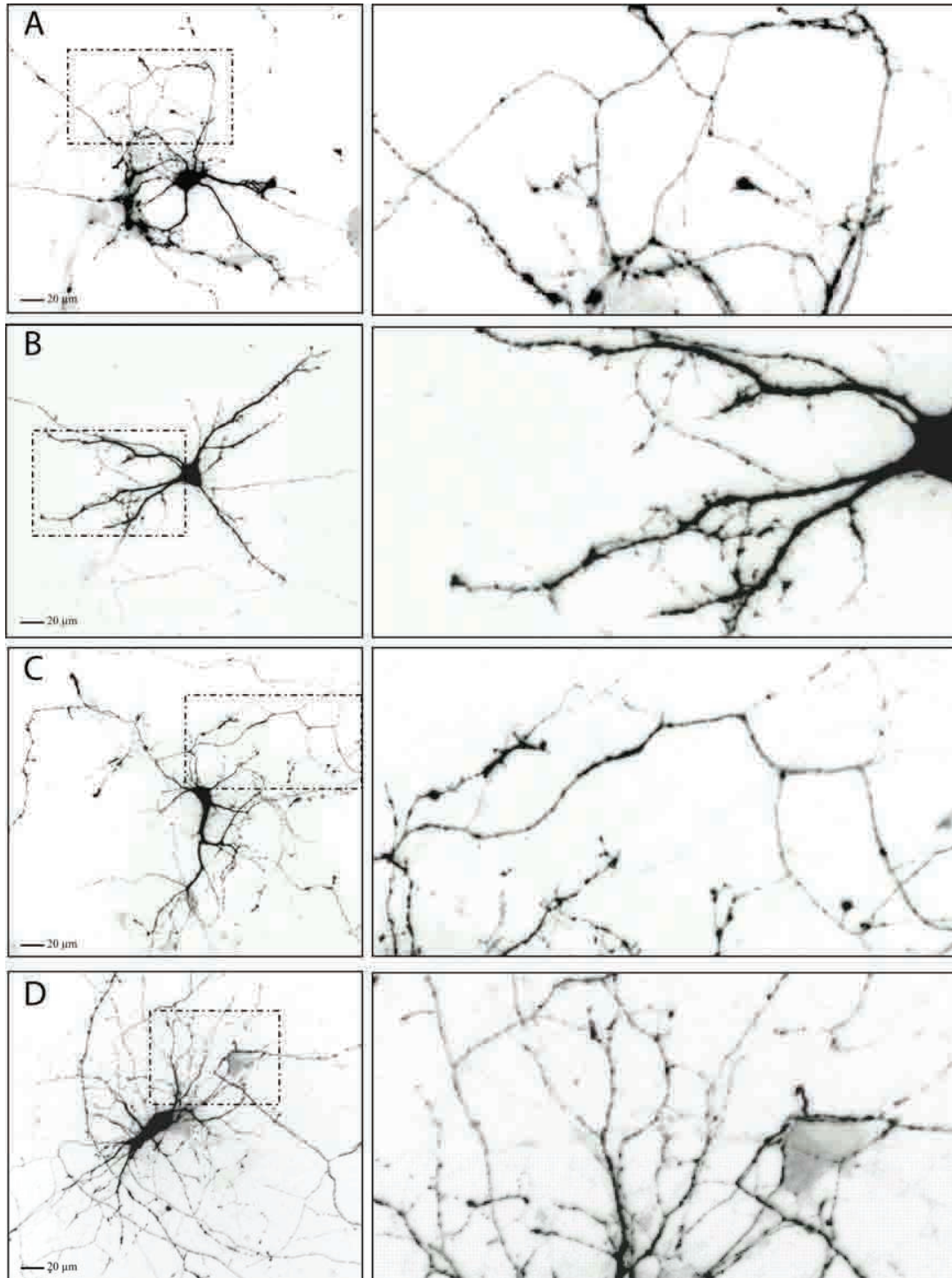


Figure 6.15. Effects of long term ephrinB3-Fc, BDNF, or NGF application on dendritic morphology of EGFP/EGFP- δ -Catenin transfected hippocampal neurons. A. Neuron stimulated with Fc for 24 hours. B. Stimulation with ephrinB3-Fc. Similarly to EGFP neurons, they display shorter and less branched dendrites, however, the effect induced by ephrin is even more pronounced. C and D. Neurons stimulated with BDNF or NGF, respectively: both factors

increase neuronal complexity promoting dendritic branching and elongation. Transfection at 3DIV and imaging after 2 days.

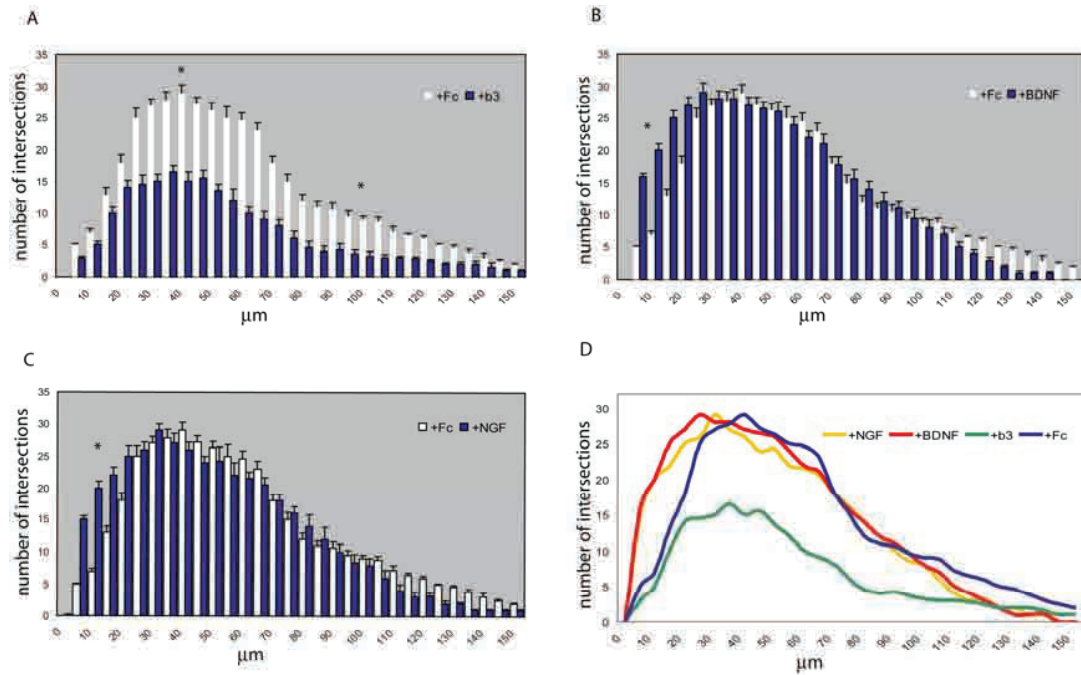


Figure 6.16. Sholl analysis of EGFP/EGFP- δ -Catenin transfected hippocampal neurons stimulated with Fc, ephrinB3-Fc, BDNF or NGF for 24 hours. **A.** EphrinB3-Fc stimulation induces a marked simplification of the dendritic arbor as compared to Fc treated control neurons. The effect is evenly distributed all along the dendritic tree (asterisks indicate broad areas of statistical significance; $p < 0.01$). **B.** BDNF stimulation does not seem to influence neuronal morphology in a dramatic way but it affects primary dendrites and processes close to the cell body (asterisks; $p < 0.05$). **C.** NGF stimulation causes very similar effects to BDNF. **D.** Overall comparison view of Fc, ephrinB3-Fc, BDNF and NGF effects (3DIV+2 days after transfection).

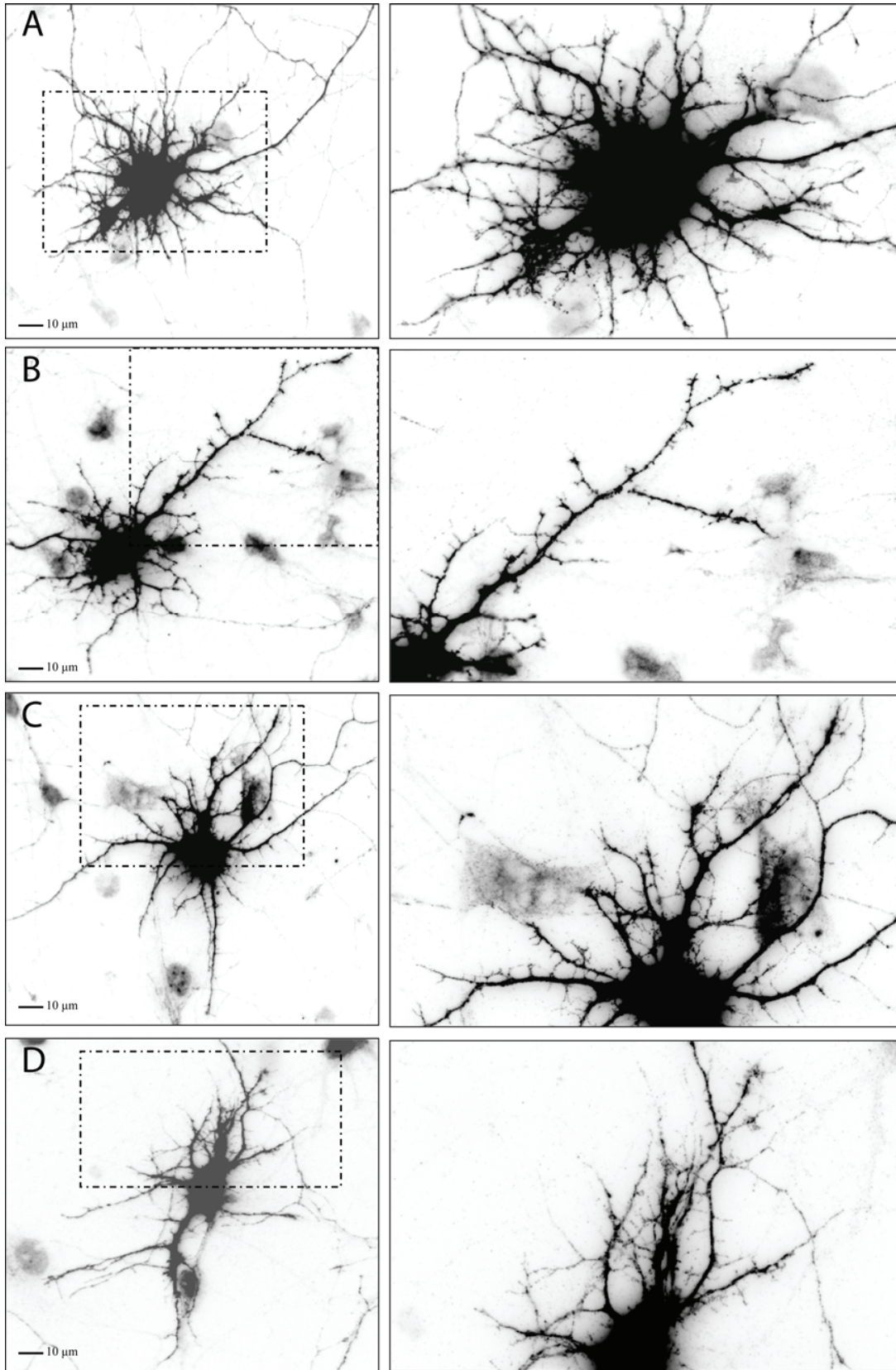


Figure 6.17. Effects of long term ephrinB3-Fc, BDNF or NGF on dendritic morphology of EGFP/EGFP- Δ C207 transfected hippocampal neurons. Δ C207 expressing cells show a very simplified dendritic architecture with very little dendritic branching, short dendrites but a higher number of primary dendrites and short filopodia-like processes whose formation is not affected by any of the stimuli. A. Neuron stimulated with Fc for 24 hours. B. Neuron stimulated with ephrinB3-Fc; the stimulation does not influence dendritic morphology. C and D. Neurons stimulated with BDNF and NGF, respectively: both factors partially rescue the Δ C207 mutant phenotype by increasing dendritic branching and elongation. (3DIV+2 after transfection).

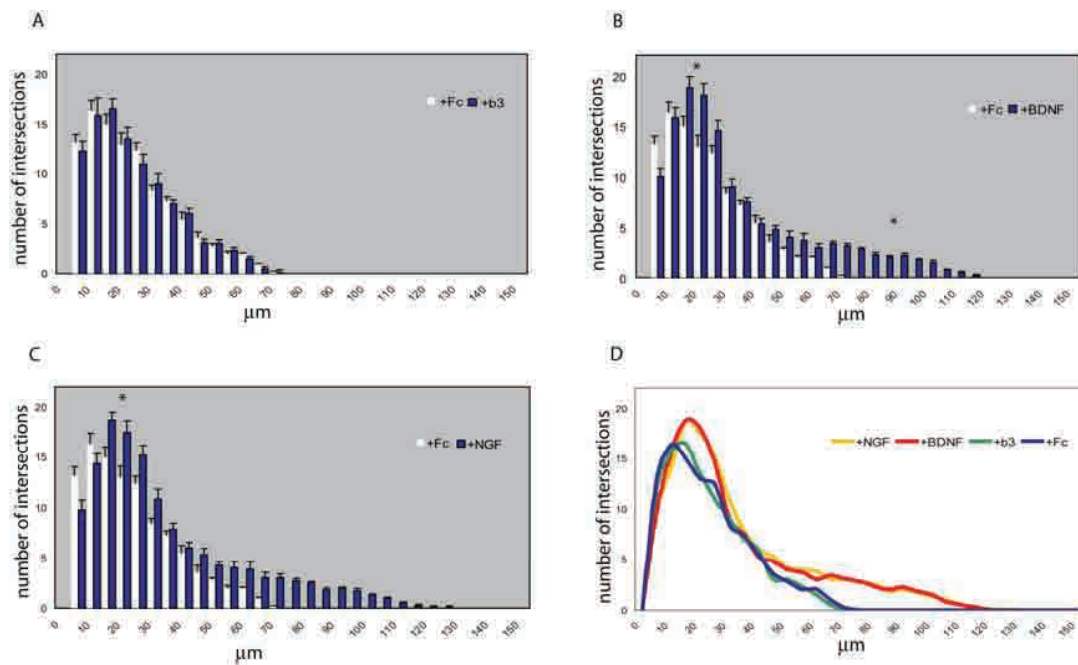


Figure 6.18. Sholl analysis of EGFP/EGFP- Δ C208 transfected hippocampal neurons stimulated with Fc, ephrinB3-Fc, BDNF or NGF for 24 hours. A. EphrinB3-Fc stimulation does not affect neuronal morphology. B. BDNF stimulation partially rescues the phenotype by increasing dendritic complexity in areas most proximal and distal from the cell body (asterisks, $p < 0.05$). C. NGF stimulation causes very similar effects to BDNF. D. Overall comparison view of Fc, ephrinB3-Fc, BDNF and NGF effects (3DIV+2 days after transfection).

Several other morphological parameters can be useful to evaluate the complexity of a dendritic tree. One of them is the dendritic order. The dendritic order refers to the degree of branching from a “primary” dendrite that sprouts directly from the cell body. A dendrite of the “secondary” order therefore generates as a branch from the primary dendrite and a branch extending from a secondary branch is then termed “tertiary”, and so on; the higher the dendrite order, the more complex the dendritic tree. As shown in **figure 6.19**, stimulation with ephrinB3-Fc markedly reduced dendritic orders in both EGFP-neurons (-37%, $p<0.05$) and, in a more striking way, in EGFP/EGFP- δ -Catenin neurons (-46%, $p<0.05$) as compared to control Fc treatment. EGFP/EGFP- Δ C208 neurons show no response to ephrinB3-Fc stimulation.

BDNF and NGF treatment causes an expected increase in dendrite order in EGFP-neurons but no additional effect in EGFP/EGFP- δ -Catenin neurons. On the other hand, they are able to increase dendrite order in EGFP/EGFP- Δ C208 neurons.

Another useful parameter to study dendritic tree complexity is the number of primary dendrites. As shown in **figure 6.20**, stimulation with ephrinB3-Fc causes a reduction in the number of primary dendrites in EGFP/EGFP- δ -Catenin neurons ($p<0.05$), more striking than in the case of EGFP neurons. EGFP/EGFP- Δ C208 neurons show no such response to ephrinB3-Fc. In this case, BDNF and NGF treatment also causes an increase in number of primary dendrites in EGFP-neurons but no additional effect in EGFP/EGFP- δ -Catenin neurons. Strikingly, EGFP/EGFP- Δ C208 neurons show an already elevated number of primary dendrites and they do not specifically respond to any of the stimuli.

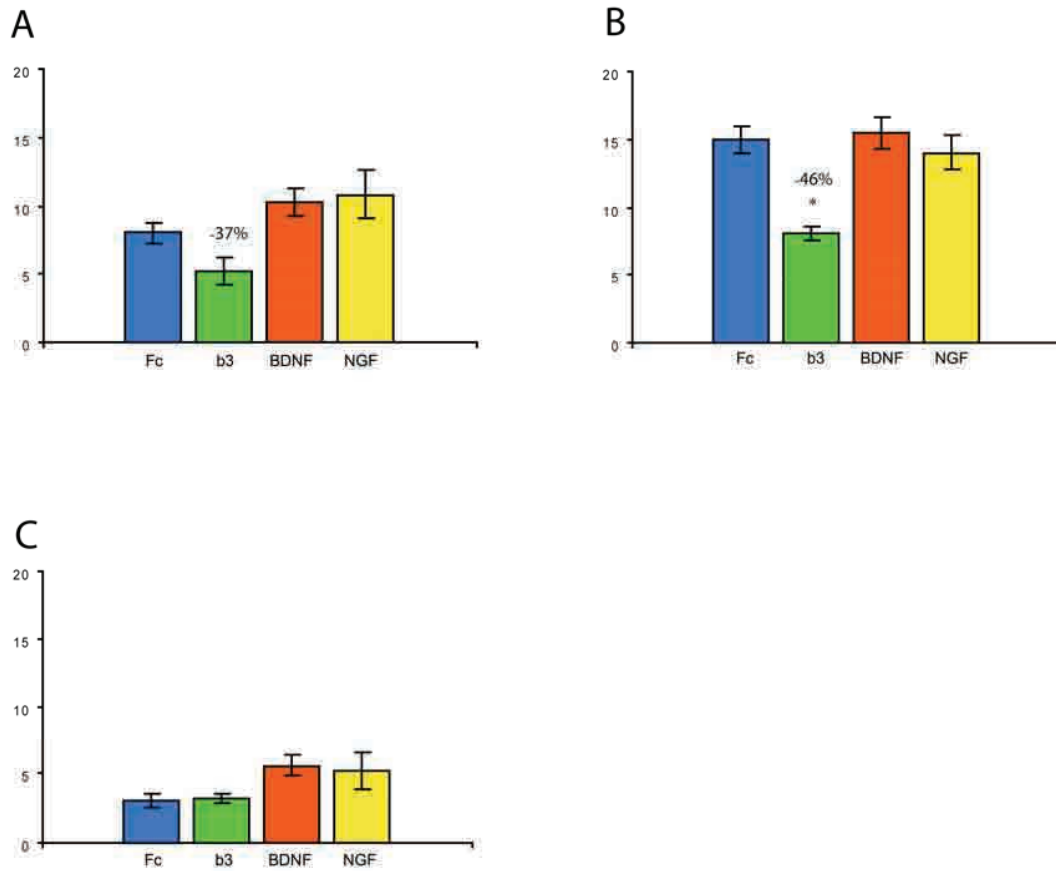


Figure 6.19. Dendrite order analysis of EGFP-, EGFP/EGFP δ -Catenin- and EGFP/EGFP- Δ C208 transfected neurons upon stimulation with Fc, ephrinB3-Fc, BDNF or NGF for 24 hours. **A.** EGFP neurons show a decrease in the order of dendritic branching upon ephrinB3-Fc stimulation (green) whereas BDNF (red) and NGF (yellow) have an opposite effect, causing an increase in branching order as compared to Fc control (blue). **B.** EGFP/EGFP δ -Catenin neurons show an overall increase in the order of dendritic branching. Whereas ephrinB3-Fc stimulation causes a marked decrease in the dendrite order, BDNF and NGF have no additional effect. **C.** EGFP/EGFP- Δ C208 neurons all show a lower order of branching, partially rescued by BDNF and NGF stimulation (for simplicity, “ephrinB3-Fc” stimulation is indicated as “b3”).

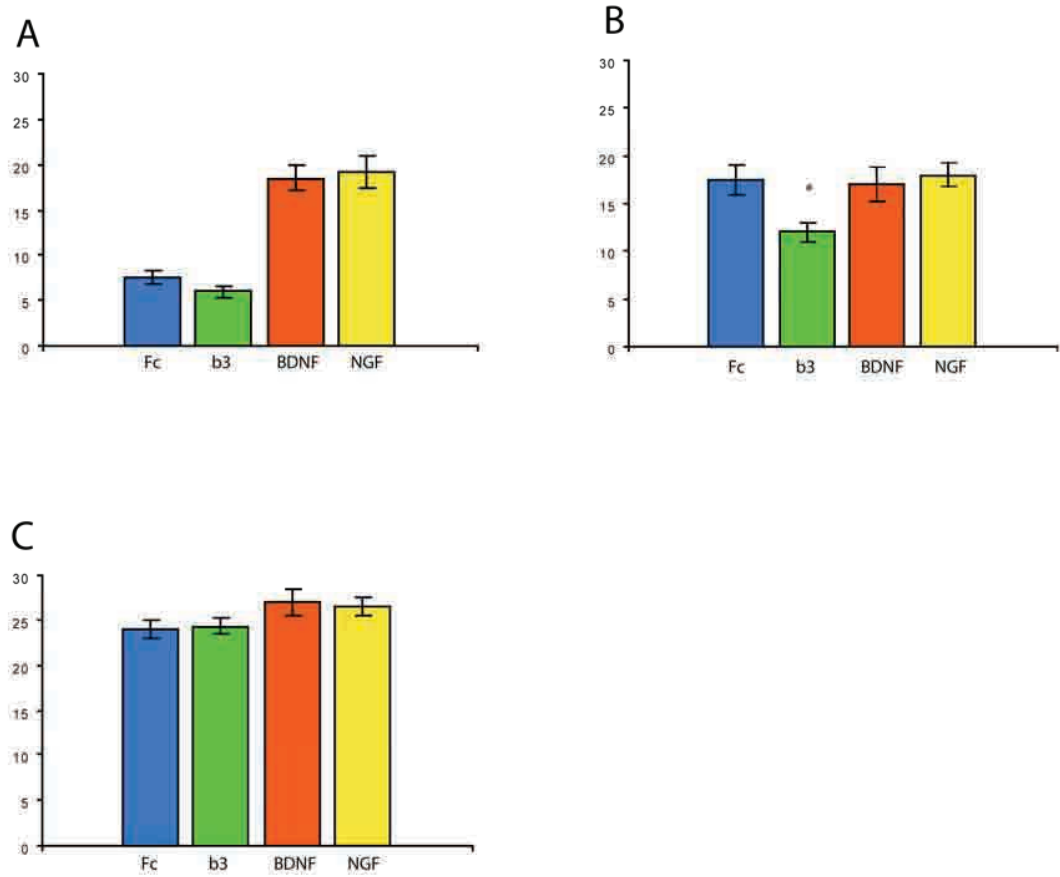


Figure 6.20. Primary dendrite analysis of EGFP-, EGFP/EGFP δ -Catenin- and EGFP/EGFP- Δ C208 transfected neurons upon stimulation with Fc, ephrinB3-Fc, BDNF or NGF for 24 hours. A. EGFP neurons show a trend towards a decrease in the number of primary dendrites upon ephrinB3-Fc stimulation (green). BDNF (red) and NGF (yellow) cause an increase in the number of primary dendrites as compared to Fc controls (blue). **B.** EGFP/EGFP δ -Catenin neurons show an overall increase in the number of primary dendrites independently of the stimulus. While ephrinB3-Fc stimulation causes a decrease in the number of primary dendrites, BDNF and NGF have no effect. **C.** EGFP/EGFP- Δ C208 neurons all show a very high number of primary dendrites unaffected by the stimulus applied.

A dendritic node is referred to as the point where a dendrite branches generating a process of a higher order. The number of nodes in a dendritic tree is therefore another indicator of complexity. As shown in **figure 6.21**, stimulation with ephrinB3-Fc has the slight effect of reducing the number of nodes in EGFP-neurons but more strikingly in EGFP/EGFP- δ -Catenin neurons as compared to control Fc treatment ($p < 0.05$). EGFP- Δ C208 neurons show no response to ephrinB3-Fc stimulation. BDNF and NGF treatment causes an increase in the number of nodes in EGFP-neurons but have no additional effect on EGFP/EGFP- δ -Catenin neurons. On the other hand, they are able to slightly increase node numbers in EGFP/EGFP- Δ C208 neurons.

Finally, another useful parameter is the total length of all dendrites in the tree. **Figure 6.22** shows that stimulation with ephrinB3-Fc has the effect of clearly shortening the average dendritic length of EGFP-neurons (-33% compared to control, $p < 0.05$). The effect is enhanced in EGFP/EGFP- δ -Catenin where the decrease in total length is -48% ($p < 0.05$) compared to the respective control. EphrinB3 stimulation has no effect on EGFP/EGFP- Δ C208 neurons. BDNF and NGF treatment on the other hand, cause an expected increase in dendritic length in EGFP-neurons but have no additional effect on EGFP/EGFP- δ -Catenin neurons which show an increased total dendritic length due to the effect of δ -Catenin over-expression. BDNF and NGF, similarly to what was observed in the case of dendrite order, partially rescue the phenotype, increasing the overall dendritic length of about 50% ($p < 0.05$).

The total dendritic length gives an idea of the overall extension of the dendritic tree, with no hint though to the complexity and the extent of branching. In order to have a very precise picture of a dendritic tree it is therefore necessary to take all the above described parameters in consideration.

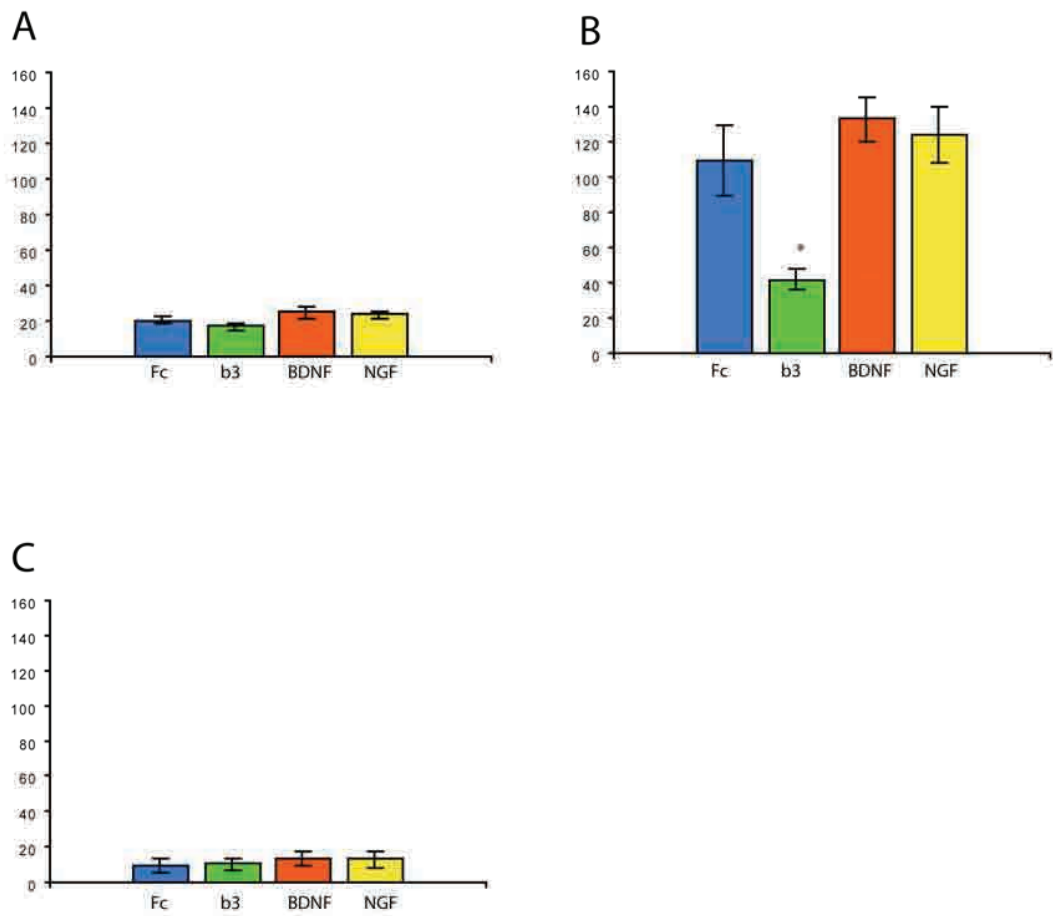


Figure 6.21. Analysis of the number of nodes in EGFP-, EGFP/EGFP δ -Catenin- and EGFP/EGFP- Δ C208 transfected neurons upon stimulation with Fc, ephrinB3-Fc, BDNF or NGF for 24 hours. A. EGFP neurons show a trend towards a decrease of the number of nodes upon ephrinB3-Fc stimulation (green). BDNF (red) and NGF (yellow) cause an increase in the number of nodes as compared to Fc control (blue). **B.** EGFP/EGFP- δ -Catenin neurons show much more marked differences; ephrinB3-Fc stimulation causes a marked decrease in the number, BDNF and NGF have no effect. **C.** EGFP/EGFP- Δ C208 neurons all show a low number of nodes; the phenotype is partially rescued by BDNF and NGF stimulation.

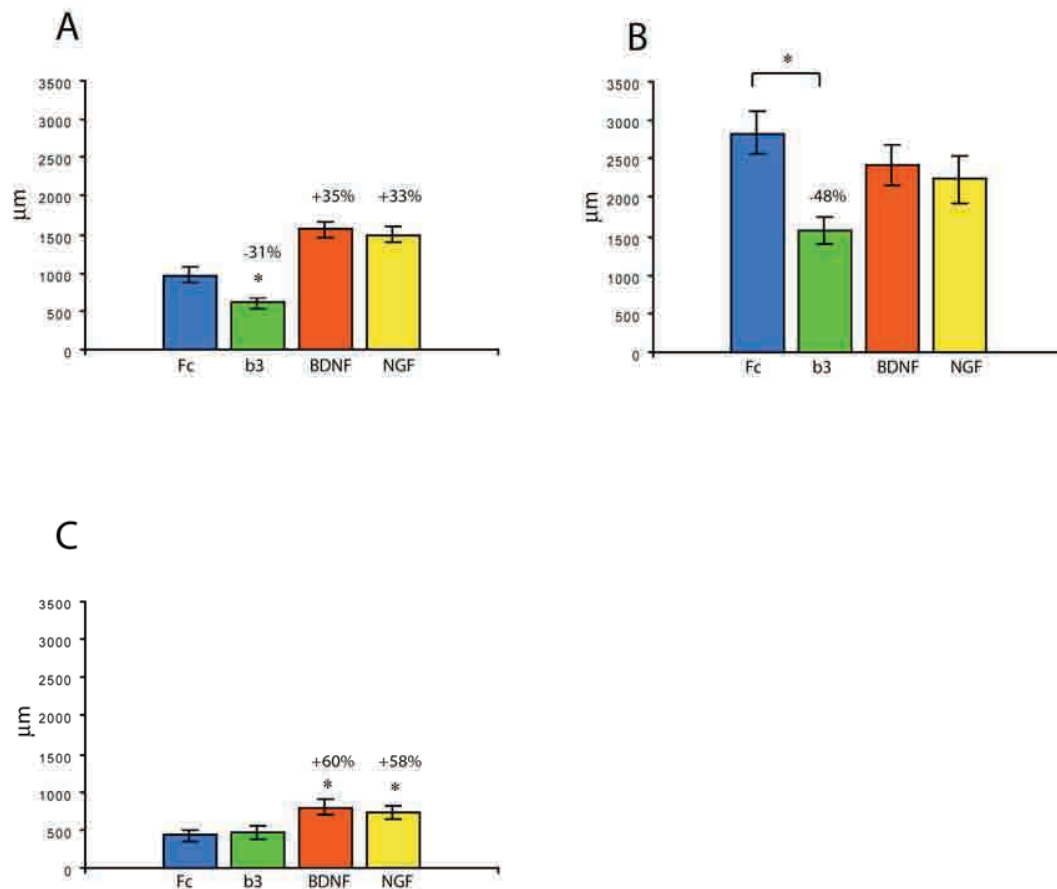


Figure 6.22. Analysis of total dendritic length in EGFP-, EGFP/EGFP δ -Catenin- and EGFP/EGFP- Δ C208 transfected neurons upon stimulation with Fc, ephrinB3-Fc, BDNF, NGF for 24 hours. A. EGFP neurons show a 31% decrease in total dendritic length upon ephrinB3-Fc stimulation whereas BDNF and NGF have an opposite effect, causing an increase total dendritic length as compared to Fc control. **B.** EGFP/EGFP δ -Catenin neurons show an overall increase in the order of dendritic branching as an effect of δ -Catenin over-expression. While EphrinB3-Fc stimulation causes a marked decrease in dendritic length (-48%), BDNF and NGF have no additional effect. **C.** EGFP/EGFP- Δ C208 neurons all show a decrease in dendritic length, compared to control neurons. The phenotype is partially rescued by BDNF and NGF stimulation which both cause an increase of 60 and 58% in total dendrite length whereas ephrinB3-Fc treatment has no evident effect ($p < 0.05$).

Taken together, the information resulting from the Sholl analysis and the analysis of various neuronal parameters presents a complex picture about the effect of various stimuli on δ -Catenin and Δ C208 neurons. The parameters establishing the complexity of a dendritic tree vary and most likely they are not influenced by the stimuli in the same way. **Figure 6.23** illustrates synoptically the results obtained from the morphological studies.

Overall, expression of full length δ -Catenin causes an increase in dendritic complexity whereas expression of Δ C208 causes a marked decrease if compared to control neurons, suggesting that functional δ -Catenin is essential for proper dendritogenesis. The effect of ephrinB3 stimulation has the general effects of reducing dendrite length, dendrite branching and the number of primary dendrites. These effects are greatly enhanced when neurons over-express δ -Catenin. The effect does not seem to be due to the higher complexity that δ -Catenin neurons have from the start since the differences between Fc and ephrinB3-Fc treatments between control neurons and EGFP- δ -Catenin neurons are higher in percentage. Δ C208 neurons do not respond to ephrinB3. Interestingly, Δ C208 neurons also have an extraordinary amount of primary dendrites sprouting from the cell body, even if these processes are short and not branched.

transfection	stimulus	primary dendrites	neurite extension	branching	overall complexity
EGFP	Fc	++	++	++	++
	ephrinB3	++	+	+	+
	BDNF NGF	+++	+++	+++	+++
δ-Catenin	Fc	+++	+++	+++	+++
	ephrinB3	+	+/-	-	-
	BDNF NGF	+++	+++	+++	+++
ΔC208	Fc	++++	-	-	-
	ephrinB3	++++	-	-	-
	BDNF NGF	++++	+	+	+

Figure 6.23. Synoptic scheme illustrating the effect of Fc, ephrinB3-Fc, BDNF and NGF stimulation on variously transfected neurons. For simplicity, EGFP-neurons are indicated as “EGFP”, EGFP/EGFP-δ-Catenin neurons are indicated as “δ-Catenin” and EGFP/EGFP-ΔC208 neurons as “ΔC208”. Similarly, stimulation with ephrinB3-Fc is indicated as “ephrinB3” and stimulations with BDNF and NGF have been grouped together due to the similarity of effects that they produce. The category “neurite extension” correlates with the total dendritic length mentioned in the previous section. “Pluses” are to be intended with as a comparison to EGFP neurons stimulated with Fc. – indicates a strong decrease, +/- indicates an intermediate situation. Note that the scheme has no statistical value but it is intended as a simplified summary of the data presented in the section above.

6.4.1 δ -Catenin and the dynamics of filopodia formation

Filopodia formation is a very important process during dendritic development as they are crucial intermediates for the initiation of dendritic branching and, although still not clearly, spine formation. In young neurons, when dendrites still do not have mature spines and are not engaged in synaptic relationships, filopodia presumably work as sensors, rapidly growing and retracting in response to specific signals with the aim of directing further growth or differentiation where it is appropriate (Davenport et al., 1993). Eph-ephrin signaling was shown to be a positive regulator of spinogenesis and the commitment of filopodia to spines (Penzes et al., 2003; Ma et al., 2003). In order to assess a potential role of δ -Catenin and its mutant Δ C208 in filopodia formation, the same neurons used in the Sholl analysis were further studied for filopodia formation. The age of the culture used (2 to 3DIV) did not allow discriminating between filopodia-like processes and nascent spines as spines appear as mature processes with a distinct neck and head only after one week or more in culture. Because of the lack of filopodia markers, the filopodia-like processes will be here referred to as “filopodia” based on morphological criteria. One interesting observation was that EGFP-transfected neurons seemed to respond to ephrinB3-Fc treatment by increasing the number of filopodia (see **figure 6.13**) and Δ C208, on the other hand, showed a massive filopodial growth independently of the stimulus applied (see **figure 6.17**). EGFP-, EGFP/EGFP- δ -Catenin- and EGFP/EGFP- Δ C208-transfected neurons stimulated with Fc, ephrinB3-Fc, BDNF or NGF were imaged and filopodia-like structures labeled and counted. The maximal length accepted for filopodia was of 2 μ m, longer processes were automatically considered as a nascent branch and excluded from the statistics. **Figure 6.24** shows an example of filopodia quantification using the programs NeuroLucida and Neuroexplorer in combination. The total number of filopodia is given as filopodial density or as a ratio by division with total dendritic length. The example shows the comparison between two EGFP-transfected neurons: one stimulated with Fc as a control and the other stimulated with ephrinB3-Fc. The stimulation with ephrinB3-Fc induced a marked increase in filopo-

dial density. The data from all neuronal transfections in all the applied stimulation conditions are summarized in **figure 6.25**.

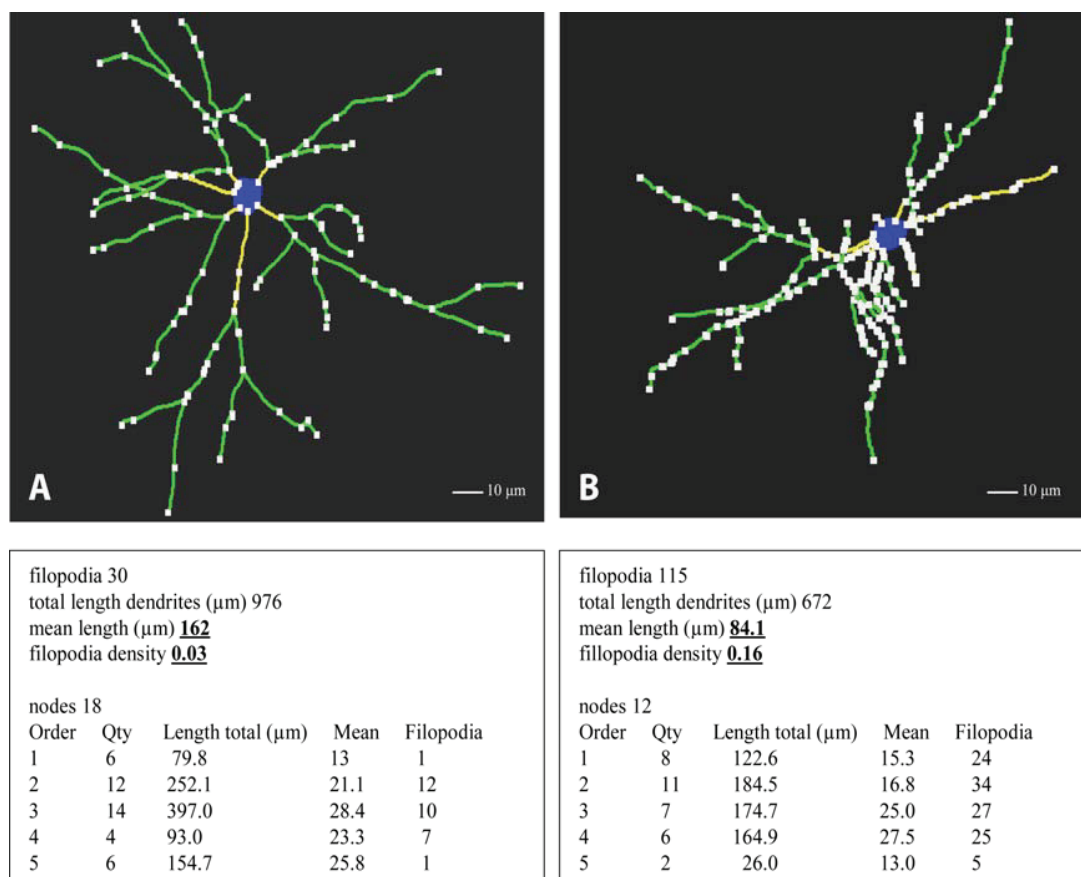


Figure 6.24. Examples of filopodial analysis using the programs NeuroLucida and Neuroexplorer. Neurons were traced and filopodia marked along the length of the dendrites (white squares) followed by software-based numeric analysis. The corresponding tables show the total number of filopodia as distributed along each dendritic branch, dendritic lengths and filopodia density calculated as a ratio between the total number of filopodia and the total length of the dendrites. **A.** EGFP- transfected neuron stimulated with Fc for 24 hours. **B.** EGFP-transfected neuron stimulated with ephrinB3-Fc for 24 hours. Together with a simplification of dendritic morphology (compare mean dendritic lengths in A and B), ephrinB3-Fc treatment brings along a marked increase in filopodial density (note that the white squares also indicate nodes).

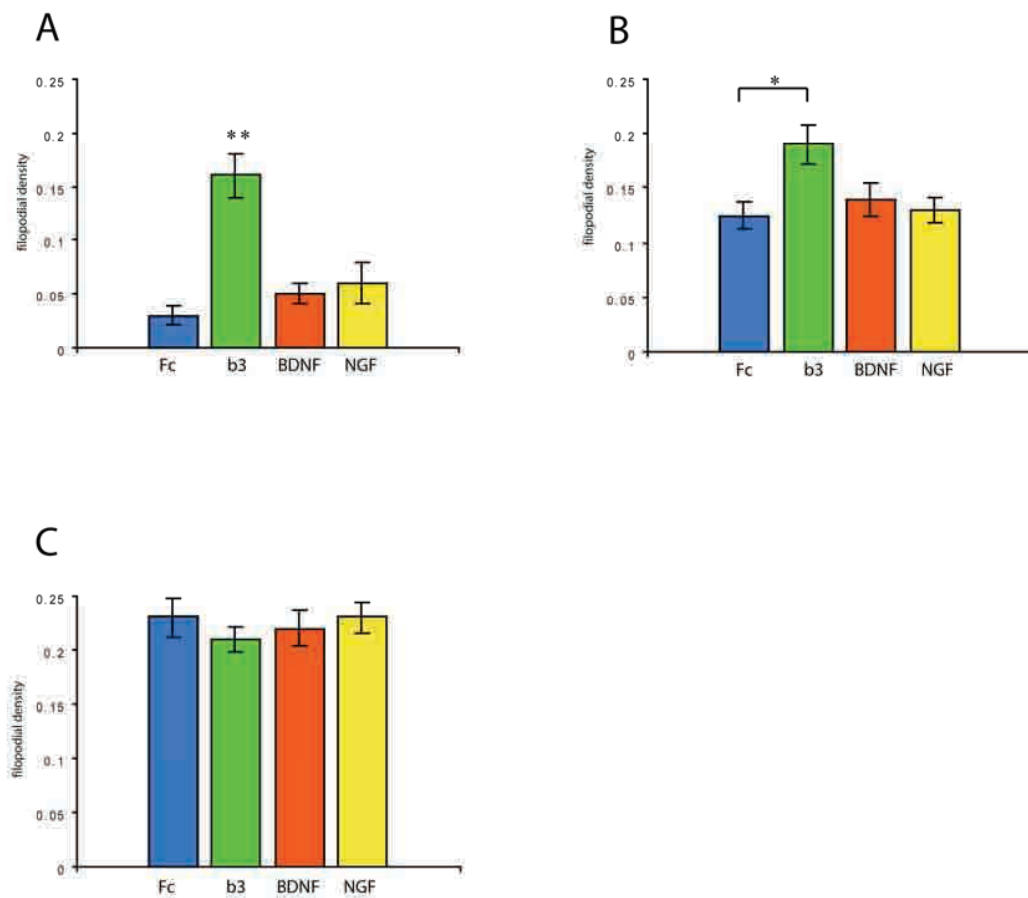


Figure 6.25. Filopodial analysis of EGFP-, EGFP/EGFP- δ -Catenin-, EGFP/EGFP- Δ C208 transfected neurons stimulated with Fc, ephrinB3-Fc, BDNF or NGF.

A, EGFP transfected neurons show a marked increase in filopodia density upon stimulation with ephrinB3-Fc ($p < 0.01$). **B**, EGFP/EGFP- δ -Catenin neurons show an overall increase in filopodia density, stimulation with ephrinB3-Fc further increases the effect ($p < 0.05$). **C**, EGFP/EGFP- Δ C208 neurons show a very high filopodial density and they were unresponsive to any of the stimuli.

As mentioned before, EGFP-neurons (**figure 6.25 A**) showed a marked increase in the number of filopodia upon stimulation with ephrinB3-Fc. Treatment with BDNF and NGF also showed a slight increase in filopodial density. EGFP/EGFP- δ -Catenin transfectants (**figure 6.25 B**) also displayed an increase in filopodial number upon stimulation with ephrinB3-Fc but not as striking as in the case of EGFP neurons. Moreover, they appeared to be far richer in filopodia even before stimulation, probably as a further effect of the δ -Catenin induced “complexing” phenotype. BDNF and NGF had no significant effect. EGFP/EGFP- Δ C208-transfected neurons (**figure 6.25 C**) have a striking and homogeneous filopodial overgrowth, uninfluenced by any of the stimuli applied.

In order to better visualize the two most interesting cases: the increase of filopodial density in EGFP-transfected neurons upon stimulation with ephrinB3-Fc and the filopodial overgrowth in EGFP/EGFP- Δ C208 transfectants, neurons were imaged over a long time. Neurons were kept in culture for 3 days + 2 after transfection and then filmed for 17 hours.

Figure 6.26 A and B show a GFP transfected neuron upon stimulation with Fc for 17 hours as a control. The neuron appears moderately branched, displays a fair amount of filopodia and is highly dynamic over time. Processes extend and retract and even the cell body appears quite motile in respect to the initial position at 0 minutes.

Figure 6.26 C and D show a neuron stimulated with ephrinB3-Fc. The stimulation has a clear effect in promoting filopodia and filopodia-like processes outgrowth. At the same time, the neuron retracts several branches, dendrites shorten and become thinner. Interestingly the neuronal cell body appears quite fixed and not as dynamic as in the case of the control, as if it was “frozen” on the spot when the ephrinB3-Fc stimulus was applied.

Figure 6.27 shows an EGFP/EGFP- Δ C208 transfected neuron upon stimulation with Fc (**A and B**) and one stimulated with ephrinB3-Fc (**C and D**). As shown in previous experiments, neurons are much less branched, with short dendrites but a high number of short and thin primary dendrites and several filopodia whose number does not appear to vary. Also in this case, the neurons appear to be fixed on the substrate and

show very little changes in morphology independently of the time in culture and stimulation.

Taken together, the information from the filopodial studies suggests a general involvement of long-term ephrinB3-Fc stimulation in the generation of filopodia-like structures. The effect is already strong in EGFP control neurons. Whether these filopodia will all mature into spines or if the result of this event will shift the ratio between filopodia and spines towards more filopodia and consequently mature less spines, is still not clear. In EGFP/EGFP- Δ C208 transfected neurons the number of filopodia is very high, independently of the stimulus applied, suggesting that the presence of inactive δ -Catenin (or perhaps the presence of phosphorylated δ -Catenin, similar to GFP neurons expressing endogenous and active δ -Catenin) may remove inhibition that allows the outgrowth of filopodia. The data from EGFP/EGFP- δ -Catenin transfectants partially support this as they also show some increase in numbers of filopodia even if the overall number, before stimulation, is already high, complicating the conclusions to be drawn from these experiments. Another complication in the interpretation of the EGFP/EGFP- Δ C208 data is the lack of effect of BDNF and NGF, making the correlation of the filopodial phenotype with δ -Catenin and Eph-ephrin signaling not so specific.

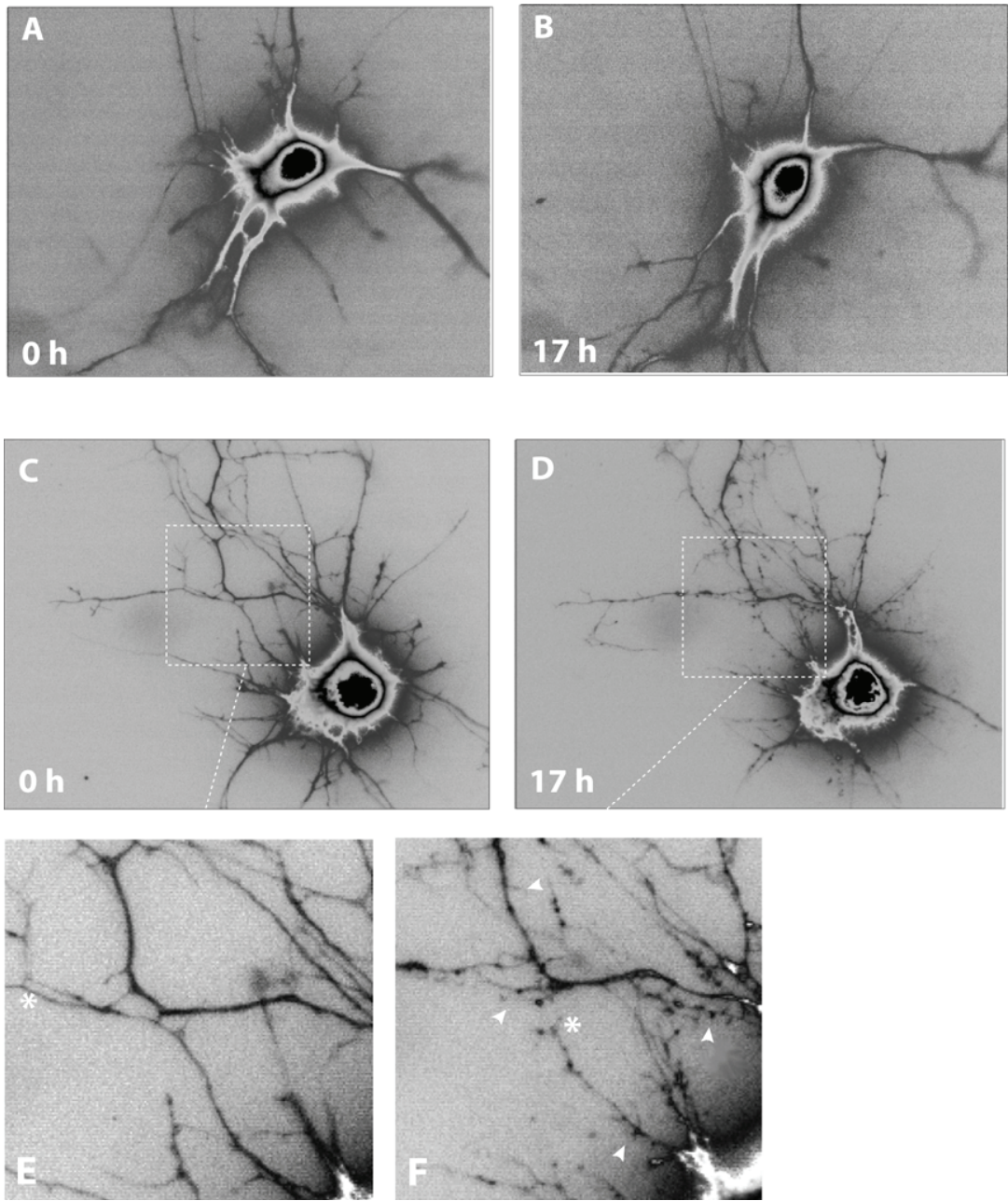


Figure 6.26. Live imaging of EGFP-transfected hippocampal neurons during long term stimulation with Fc (A and B) and ephrinB3-Fc (C and D). Pseudo colors indicate different fluorescence intensities. E and F represent detail magnifications of C and D, respectively. EphrinB3-Fc stimulation causes the outgrowth of numerous filopodia-like processes (D and F, arrows). In parallel, dendrites retract and appear simpler (asterisk in E and F indicates the retraction of a dendrite). On the other hand, the Fc-stimulated neuron (A and B) is much more dynamic and displayed a higher turnover of branching and process outgrowth. Nevertheless, the number of filopodia stays unchanged overtime (exposure: 100 msec) (3DIV+2 after transfection)

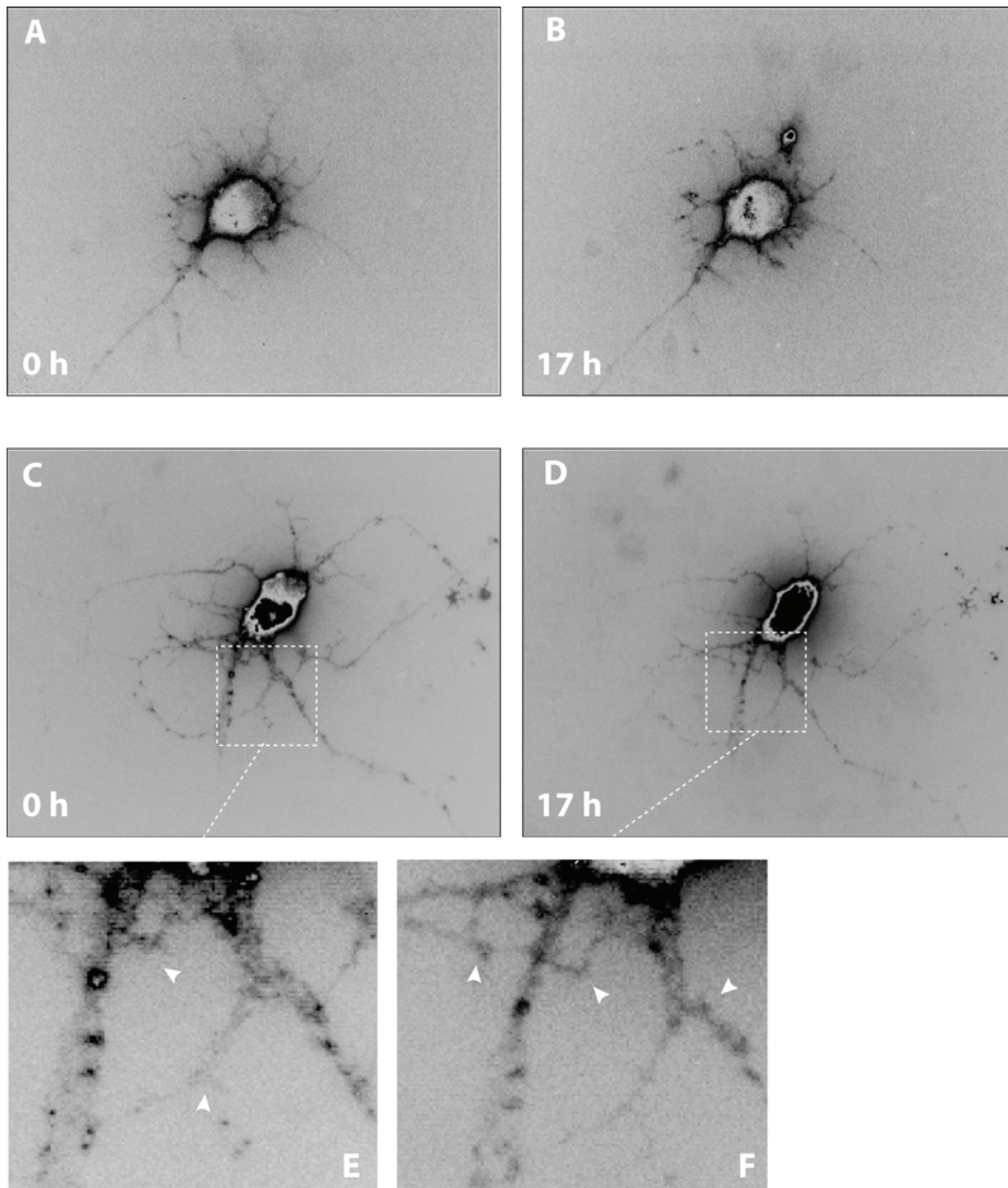


Figure 6.27. Live imaging of EGFP/EGFP-AC208 transfected hippocampal neurons upon long term stimulation with Fc (A and B) and ephrinB3-Fc (C and D). E and F show detail magnification of figures C and D respectively. Both neurons show a high number of filopodia-like processes already before stimulation with ephrinB3-Fc or Fc and no major differences are observed after 17 hours (E and F, arrows). Both neurons have a simple dendritic morphology (exposure: 100 msec), (3DIV+2 after transfection).

6.5 δ -Catenin and HeLa cell migration

The nature and strength of cell junctions is a parameter that directly influences the motility of cells; tighter junctions favour a compact and packed multicellular organization and weaker junctions favour the detachment and motility of the cells. It has been shown that a switch in cadherin subtypes in the adherens junctions, for example, has important developmental effects: during neurulation, some ectodermal cells change cadherin expression from E- to N-cadherin and the shift allows neural precursor cells to segregate from other cells derived from the ectoderm. Subsequently, neural crest cells, which down-regulate N-Cadherin expression, migrate from the dorsal ectoderm to specific locations in different germ layers (Hatta et al., 1987). The intracellular domains of Cadherins and specifically the juxtamembrane region appear to be crucial in the regulation of junction strength, in fact, in the case of E-Cadherin, it has been shown that the juxtamembrane region negatively regulates adhesion by preventing lateral dimerization of the Cadherin extracellular domain (Ozawa and Kemler, 1998). A switch in the intracellular components of the plaque may also influence the properties of the junctions in response to extracellular cues could be a key mechanism through which changes in cell motility are accomplished. For example, it has been shown that the activation of Wnt signalling leads to the dissociation of β -Catenin from N-cadherin influencing cell motility (Polakis, 2000 and Bienz et al., 2000) δ -Catenin binds to the juxtamembrane region of Cadherins and is a component of the adherens junction. Its ectopic expression in MDCK cells has been shown to influence the response of the cells to HGF stimulation, markedly increasing the already documented cell scattering (Lu et al., 1999). Eph-ephrin signalling has also been shown to be important in the regulation of adhesive properties and in cell migration with somewhat different effects according to the system used the Eph-ephrin subtypes. In order to investigate a possible role of δ -Catenin in a system in which cellular migratory properties are regulated by Eph-ephrin signalling, δ -Catenin or Δ C208 constructs were co-transfected with EphA4 in He La cells and the migratory properties of the cells in response to ephrin stimulation

were studied. A two-chamber system was used (see **figure 6.28**); cells were transfected and seeded in the upper chamber on a porous membrane that separates the upper chamber and the lower chamber. The surface of the membrane on the lower chamber side is priority treated with a ligand (Fc as a control or ephrinB3-Fc). Cells migrate from the upper chamber to the lower chamber in response to (or independently from) the cue present on the other side of the membrane. The membranes are then fixed and cells are counted on both sides of the membrane (they can be visualized with fluorescent dyes or by their own fluoresce i.e. if they express EGFP). Ratios between migrated and non migrated cells indicate migratory properties.

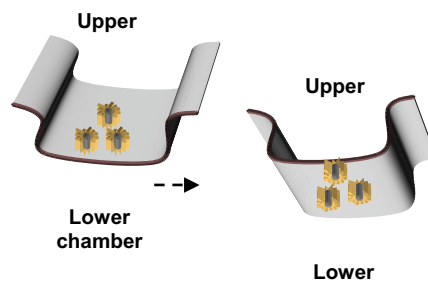


Fig 6.28 Diagram illustrating the two chamber system used in migration assays.

Cells are grown on a porous membrane that separates an upper and lower chamber. The lower chamber side of the membrane is pre-treated with the molecule whose effect on migratory properties of the cells is to be tested. The cells are allowed to migrate for an interval of time and then the filter is fixed. Cells are counted on both sides of the membrane and migration ratios are calculated.

In the following experiments EGFP-only and EGFP/EphA4 transfected cells were used as a control. The EGFP construct was used in order to fluorescently visualize the control cells. EGFP- δ -Catenin and EGFP- Δ C208 constructs were both co-transfected with EphA4. Each transfectant was allowed to migrate for 17 hours in low serum and in the presence of Fc or ephrinB3, the membrane were fixed and the cells were coun-

ted. The experiments were done in triplicate and cells from 5 different sections of each membrane were counted and plotted as percentage of migrated cells which indicates the number of cells counted on the filter of the low chamber against the total number of cells counted between the upper and the lower chamber. An aliquot of the transfected cells was seeded in parallel on glass coverslips and changes in EGFP fluorescence in response to Fc or ephrinB3 stimulation can be seen in **figure 6.9**

Nearly 65% of EGFP-expressing cells migrate through the membrane independently of the stimulus applied. HeLa cells do not express EphA4 endogenously. This parameter indicates the migratory properties of HeLa cells in the system used, and was used as a control (**figure 6.29** and **6.9 A** and **B**)

Cells co-expressing EGFP and EphA4 migrated at a ratio of approximately 65% in presence of Fc. In presence of ephrinB3-Fc the number of migrated cells increases significantly to 86%. The stimulation with ephrinB3-Fc therefore has the effect of increasing the migration rates of approximately 20% (**figure 6.29** and **6.9 C** and **D**). Approximately 78% of cells co-expressing EGFP- δ -Catenin and EphA4 migrate through the filter in the presence of Fc. The figure decreases significantly though when ephrinB3-Fc is present; in this case only 51% of the cells migrate (**figure 6.29** and **figure 6.9 E** and **F**). The presence of δ -Catenin in the system has the effect of decreasing cell motility but the effect is only detectable upon stimulation with ephrinB3. This effect correlates with the redistribution of EGFP- δ -Catenin in the cells upon stimulation with ephrinB3 (**figure 6.9 E** and **F**), shifting from a smooth and homogeneous distribution in the control to a markedly irregular and aggregated one.

Cells co-expressing EGFP- Δ C208 and EphA4 appear to be unresponsive to ephrinB3-Fc stimulation. The percentage of migrated cells ranges in this case between 58 and 55% (**figure 6.29**). Interestingly and similarly to the previous case, both Fc and ephrinB3-Fc treated cells show aggregates of EGFP- Δ C208 (**figure 6.9 G** and **H**).

These results suggest a possible interaction of δ -Catenin and Eph-ephrin signalling in regulating cell migration. The expression of δ -Catenin alone, differently from what was previously seen in hippocampal neurons, has no major effect. Only in the presence of

ephrinB3-Fc does the presence of δ -Catenin affect migratory properties of the cells. The presence of the functionally inactive Δ C208 mutant does not affect mi-

gration properties of the cells. Interestingly, the EGFP- Δ C208/EphA4 co-transfectants share a similar aggregated pattern of EGFP fluorescence with the EGFP- δ -Catenin/EphA4 co-transfectants in the presence of ephrinB3.

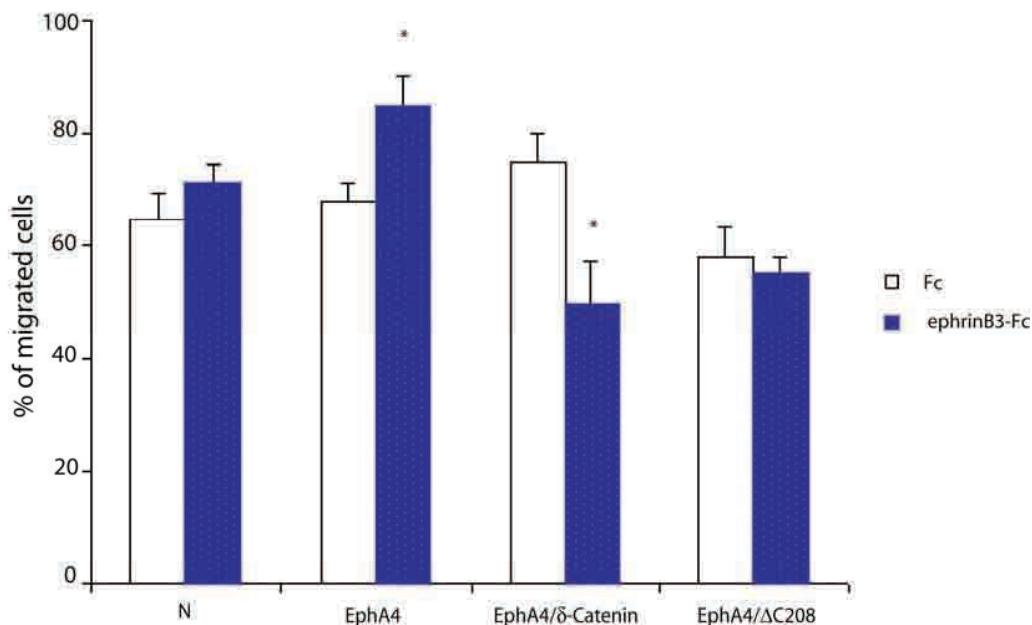


Figure 6.29. Co-expression of δ -Catenin and EphA4 influences migratory properties of HeLa cells upon stimulation with ephrinB3-Fc. Percentage of migrated cells is expressed as the ratio between migrated cells versus the total number of cells seeded. EGFP control transfectants (N) migrate at a rate of 65% and 70% upon treatment of the filter with Fc or ephrinB3-Fc respectively. The difference is not significant. EGFP/EphA4 co-transfectants (EphA4) show a significant ($p < 0.05$) 20% increase in migratory properties in the presence of ephrinB3-Fc. EphA4/EGFP- δ -Catenin co-transfectants (EphA4/ δ -Catenin) show a markedly different response to ephrinB3-Fc stimulation, appearing significantly less motile than the respective Fc treated control ($P < 0.05$). EphA4/EGFP- Δ C208 co-transfectants (EphA4/ Δ C208) show no response to ephrinB3 stimulation and their migratory properties are comparable to those of control cells.

7. DISCUSSION

Dendrites are, together with axons, distinctive structural features of neurons. They are primary sites for synaptic contact and therefore the proper development of the dendritic arbor is crucial to neuronal circuit formation and synaptic input processing in the nervous system. Although many proteins have been identified as regulators of dendritic morphogenesis, much remains to be elucidated about its molecular mechanism. δ -Catenin seemed to be an interesting candidate in the study of dendritic morphogenesis as it is a nervous system specific protein and, even if originally found as a component of the intracellular cadherin-catenin adherens junction plaque, it also distributes to neuronal processes and plays a role in the establishment of dendritic complexity. Its activity appears to be closely correlated with cytoskeletal processes and in particular with actin dynamics. This is in accordance with recent data showing that other members of the Arm repeat family involved in the formation of cellular junctions like β -Catenin, also play an important role in dendritic morphogenesis (Yu and Malenka, 2003).

The aim of this project was to find a link between Eph-ephrin signaling and δ -Catenin cellular function and demonstrate that Eph and ephrin, together with mediating several well characterized cellular effects, could also play a role in the complex events that lead to the correct development of the dendritic tree. The hypothesis for such a link initially arose as δ -Catenin mRNA and protein levels were found to be up-regulated in cortical neuron cultures in response to activation of Eph-ephrin signaling, in microarray experiments and Western blots respectively. The up-regulation of δ -Catenin followed the activation of both Eph-forward and ephrin-reverse signaling, suggesting that δ -Catenin is involved in the cellular response to both stimuli. It has been shown that the over-expression of δ -Catenin in hippocampal neurons promotes dendritic complexity, favors dendrite branching and increases dendritic length (Kim et al., 2002; Martinez et al., 2003). Conversely, neurons expressing a truncated form of δ -Catenin with dominant negative activity, or neurons treated with RNA interference in order to specifically knock down δ -Catenin levels in the cells, all led to a marked simplification of the dendritic tree (Kim et al., 2002; Jones and Lu, personal communication). A signal that induced the up-regulation of δ -Catenin in neurons, like the activation of Eph-ephrin, would

herefore have the predictable effect of instructing neurons to increase their dendritic complexity.

The interaction between Eph-ephrin signaling and δ -Catenin though, proved to be more complex than just a variation in gene expression levels, as endogenous δ -Catenin turned out to also be phosphorylated in response to ephrinB stimulation of cortical neuron cultures. Phosphorylation of cell junction molecules is a common event in the cell but the significance of these events is still not completely understood. δ -Catenin highly homologous protein p120ctn is a prominent target of both non-receptor and receptor tyrosine kinases (Daniel and Reynolds, 1997) and β -Catenin too can be phosphorylated upon activation of the Wnt pathway. δ -Catenin itself has been found to be a substrate of cAbl non receptor tyrosine kinase; the phosphorylation could be induced by the treatment with H₂O₂ (Lu et al., 2002) but no physiological stimulus has so far been shown to induce tyrosine phosphorylation in δ -Catenin. The phosphorylation of δ -Catenin induced by ephrinB is therefore a novel phenomenon, and it reinforces the idea that the molecule may mediate more complex events in the cell than just structural functions, taking part, for example in signaling cascades. δ -Catenin phosphorylation shows long term dynamics, it appears first around 30 minutes after stimulation and is then sustained for at least 24 hours. The most interesting aspect that emerges from the phosphorylation data is that the phosphorylation of δ -Catenin is an event specifically downstream of the activation of Eph-forward signaling. Activation of ephrin-reverse signaling (i.e. stimulation with clustered forms of Eph receptor) resulted in the above mentioned induction of δ -Catenin protein levels but it did not affect the phosphorylation state of the molecule. This suggests a different involvement of δ -Catenin in the two responses; in one case the increase in protein levels is accompanied by a second and more complex event, in the other, the response appears to be simpler.

As mentioned before, the over-expression of δ -Catenin in neurons has the effect of complicating dendritic architecture, favoring the development of dendritic branches and increasing dendritic length. The effect is most likely dependent on the unphosphorylated form of δ -Catenin, as it has been shown that the phenotype produced by the over-

expression is dependent on the interaction of unphosphorylated δ -Catenin with cortactin, which, as a complex with Arp2/3 induce local actin polymerization events (Martinez et al., 2003). An increase in the levels of endogenous (unphosphorylated) δ -Catenin, induced by reverse signaling, may therefore have the meaning to instruct neurons to locally increase their dendritic complexity. On the other hand, it has also been shown that the phosphorylation of δ -Catenin causes the complex with cortactin to disassemble, resulting in the disengagement of Arp2/3 and subsequently in the arrest of actin polymerization activity. Activation of the forward signaling therefore has the apparently contradictory double effect of inducing the synthesis of new δ -Catenin and at the same time to phosphorylate it. The contradiction arises from the fact that an increase of unphosphorylated δ -Catenin goes in the direction of higher complexity via the synthesis of actin filaments whereas δ -Catenin phosphorylation goes in the opposite direction, that is, towards a decrease in complexity due to the disruption of its complex with cortactin and Arp2/3. This observation could be explained by extrapolating to a more physiological context: i.e. during the development and guidance of a dendritic branch. Upon encounter of the branch with ephrinB, the phosphorylation of endogenous δ -Catenin may have the early effect of temporarily deactivating actin polymerization in order to immediately stop process growth or to mediate a repulsive response. The synthesis of new δ -Catenin protein is a later effect meant to “re-start” dendrite branching (perhaps in a different direction) when the repulsive cue subsides and to thus close the loop (see **figure 7.1**). Such a repulsive response mediated by ephrin cues has been well characterized in axonal growth cone collapse and its involvement in dendritic guidance could also be possible. Interestingly, under certain circumstances ephrin reverse signaling has opposite effects, rather working as an attractant than as a repellent. This would correlate with the absence of δ -Catenin phosphorylation in EphB-stimulated neurons and with the increase in dendritic complexity in neurons over-expressing the protein, or in neurons in which δ -Catenin expression is up-regulated, as in the case of EphB stimulation.

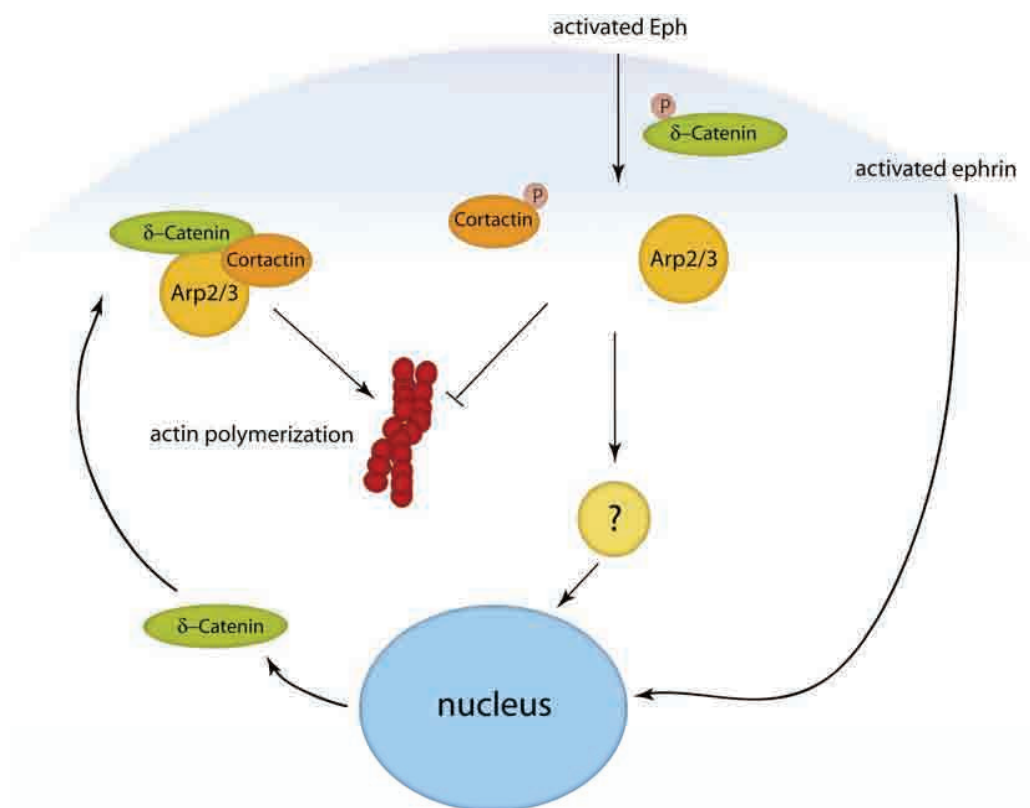


Figure 7.1. Differential engagement of δ -Catenin in Eph-forward and ephrin-reverse signaling. δ -Catenin forms a complex with cortactin and Arp2/3 and positively regulates actin polymerization. Activation of Eph-receptor leads to δ -Catenin phosphorylation and to the disassembly of the complex, resulting in a local inhibition of actin polymerization. The activation of Eph receptor also has the effect to promote δ -Catenin transcription and increase the pool of unphosphorylated δ -Catenin. This contributes to the formation of new δ -Catenin/cortactin/Arp2/3 complexes so that the signalling loop is closed. Ephrin activation has no effect on δ -Catenin phosphorylation but it promotes δ -Catenin synthesis, enriching the cellular pool of unphosphorylated δ -Catenin and enhancing actin polymerization.

A very interesting phenomenon observed upon transfection of neurons with fluorescently tagged δ -Catenin is the formation of tiny fluorescent protein aggregates upon stimulation with ephrinB. The formation of δ -Catenin aggregates is an Eph-forward specific effect as the activation of ephrin-reverse signaling does not induce the formation of aggregates; this is in accordance with the phosphorylation dynamics of δ -Catenin so that the formation of aggregates in response of activation of Eph-ephrin seems to be closely correlated. The recruitment to Eph of various factors, kinases and adaptor proteins is a

well known and documented phenomenon that follows the activation of the receptor. Put together, the experimental information presented so far suggests a possible mechanism involving the phosphorylation and sequestration of endogenous δ -Catenin by the activated Eph receptor, forming aggregates, so that δ -Catenin may not be able to bind its cellular partner cortactin and therefore promote actin polymerization. In support of this hypothesis is the fact that δ -Catenin and Eph receptor do physically interact in neurons and cell lines as it was shown in co-immunoprecipitation experiments. Additionally δ -Catenin aggregates co-localize with Eph receptor clusters induced by the stimulation with ephrinB. The two events happen simultaneously but differ slightly, being Eph-receptor cluster formation a somewhat earlier event than δ -Catenin aggregate formation, this in accordance with the fact that δ -Catenin phosphorylation and recruitment to the membrane is an effect mediated by the activated Eph receptor. Activation of Eph-ephrin and the changes in cytoskeletal dynamics in the direction of process collapse and repulsion are well studied. At the molecular level most of the already known mechanisms involve the Rho family of GTPases. In general, activation of Eph signaling leads to the inhibition of Rac and Cdc42. On the other end, the activation of GEF Ephexin favors RhoA-dependent signalling (Wahl et al., 2000; Shamah et al., 2001). An increase in the activity of RhoA has the well documented detrimental effect on the actin cytoskeleton, blocking polymerization of new actin and promoting the disassembly of existing filaments. The decrease in Rac and Cdc42 activity also has a detrimental effect on actin dynamics. Overall, the repression of Rac and Cdc42 pathways and the activation of RhoA play a crucial role in Eph-ephrin-mediated repulsive and retractive responses. The activity of δ -Catenin and its phosphorylation-dependent negative effect on actin polymerization could synergistically work (and perhaps even physically interact) with the signaling cascade that leads to the activation of RhoA, and subsequently to actin cytoskeleton disassembly (see **figure 7.2**)

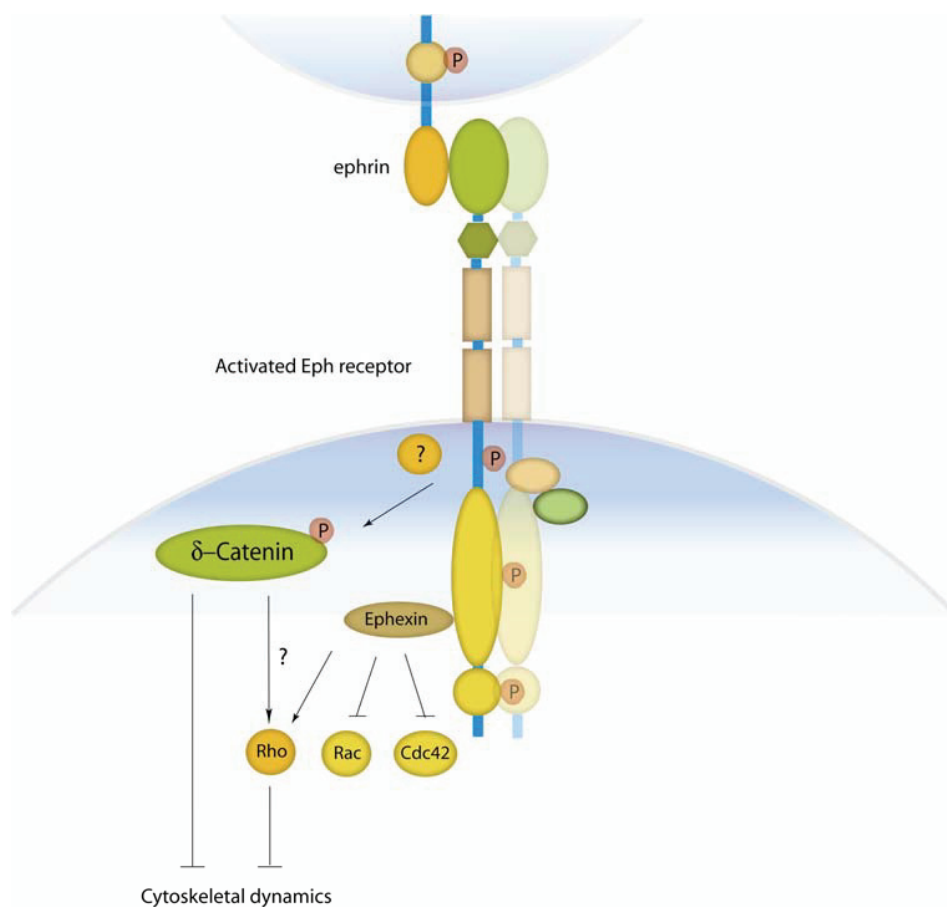


Figure 7.2. δ -Catenin as a new effector in Eph-forward signaling. The activation of Eph receptor mediates well described cellular responses like process retraction and cellular repulsion by negatively influencing cytoskeletal dynamics. Activation of Eph receptors leads, through ephexin, to the activation of RhoA which in turn has detrimental effects on cytoskeletal structures. The effect is enhanced by the repression of other factors like Rac and Cdc42 which normally have the opposite role of activating cytoskeletal dynamics. The phosphorylation of δ -Catenin following the activation of Eph receptor also negatively influences cytoskeletal dynamics by blocking actin polymerization, possibly interacting with the RhoA signalling pathway.

The morphological study of dendritic trees of hippocampal neurons was intended to shed some more light on the biochemical interaction between δ -Catenin and Eph-ephrin signaling in determining cytoskeletal dynamics in neurons. For this purpose and analysis, three main groups of neurons were chosen: control, in which both δ -Catenin and Eph receptor are involved as endogenous proteins; neurons over-expressing δ -Catenin; and

neurons with no functional δ -Catenin because of the concomitant expression of a dominant negative version of the molecule.

Relatively young neurons were chosen in the analysis because of the importance of dendritic differentiation in the study. Long stimulation times were chosen based on the observation that the effects induced on neurons were stronger and more clearly visualized in a 24h time frame, thus selecting also for late effects of stimulation. By comparison of the response of the three classes of neurons to ephrin stimulation it was possible to draw some interesting conclusions.

For clarity it is necessary to keep the two main parameters defining dendritic complexity separate: *dendritic branching* on one side and *primary dendrite outgrowth* on the other. The two developmental events are regulated differently (as mentioned before, dendritic branching is mediated by Rac/Cdc42 while outgrowth is a RhoA-dependent process) and in fact the presence of functional δ -Catenin or its absence has different effects on them.

- Control neurons respond to ephrin stimulation by decreasing the degree of branching. Primary dendrite outgrowth on the other hand is mostly unaffected.
- Neurons over-expressing δ -Catenin show an overall increase in dendritic complexity. Upon stimulation with ephrin a similar effect as in control neurons is observed, albeit much more pronounced: dendrite branching is decreased greatly whereas primary dendrite outgrowth is mildly reduced.
- Neurons lacking functional δ -Catenin are refractory to ephrin stimulation. They display a very scarcely branched dendritic arbor. Interestingly though, the outgrowth of primary dendrites is highly enhanced and is several magnitudes higher than in control neurons or neurons over-expressing δ -Catenin.

These observations hint to a scenario in which δ -Catenin is doubly implicated in controlling dendritic branching and dendrite outgrowth. The two mechanisms are in fact in an equilibrium which shifts to one side or another according to the specific requirements of a neuron. In some physiological contexts, for example under the

influence of an extracellular signal “A”, it is necessary for the cell to expand and branch its dendritic tree. In other cases for example under the influence of a signal “B” the neurons is instructed to arrest dendritic branching and rather trigger the outgrowth of new primary dendrites, possibly in a different direction. These shifts in the equilibrium find their molecular basis in the fact that the effects of Rac1 and Cdc42 on dendritic branching and the effects of RhoA on dendrite outgrowth are alternative and opposed to each other. A stimulus that positively activates Rac1 and Cdc42, negatively influences RhoA activity and vice versa. As mentioned before, it has been shown that the activation of EphBs represses Rac1 and Cdc42 activity and positively regulates RhoA activity, thus promoting actin disassembly and repulsive responses. In this respect, δ -Catenin could be a link between Eph-ephrin signaling and Rho GTPases-mediated changes in the actin cytoskeleton. The role of δ -Catenin in influencing the equilibrium between dendritic branching and outgrowth could depend on the two different forms of the molecule. Unphosphorylated δ -Catenin acts as a dendrite branching promoting factor. The phosphorylated and clustered δ -Catenin, in response to Eph activation, is not able to carry out its branch promoting activity. At the same time the aggregation and phosphorylation of δ -Catenin removes a blockade to the outgrowth of new primary processes, finally favoring outgrowth against dendritic branching. This is supported by the fact that in the absence of functional δ -Catenin neurons appear to be scarcely branched but with a very high number of primary dendrites. In this case the equilibrium is shifted towards primary dendrite outgrowth.

The use of Δ C208 deletion mutant of δ -Catenin though, still leaves some open questions. The deletion mutant of the 208 COOH terminal amino acids of δ -Catenin is not able to form a complex with cortactin and furthermore it has been described to sequester wild type δ -Catenin and prevent it from exerting its function (Kim et al., 2002); therefore the mutant has been described as a dominant negative and its over-expression results in the above mentioned phenotype. The phosphorylation data in the result section, on the other hand, show that Δ C208 is only weakly phosphorylated by the Eph receptor, partly because the tyrosine residues which are targets of Eph mediated phosphorylation lie in the C terminus of the molecule, and partly because the mutant is expressed less

efficiently than the full length protein. Whether the effect on dendritic architecture is due to the dominant negative activity of $\Delta C208$ or rather to the fact that the mutant has a possible effect of its own, i.e. due to its compromised role in signaling, is still not clear. The conclusion is that a functionally inactive form of δ -Catenin promotes dendritic outgrowth and clearly blocks dendritic branching (see **figure 7.3**).

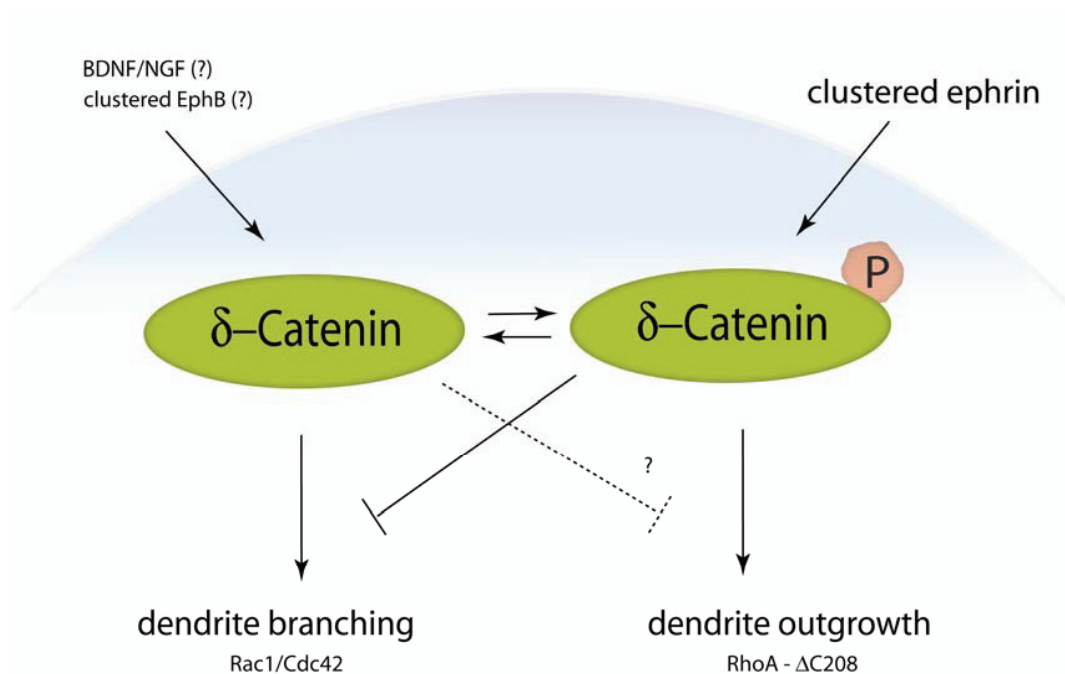


Figure 7.3. The role of δ -Catenin phosphorylation in the equilibrium between dendrite branching and dendrite outgrowth. The state of δ -Catenin phosphorylation regulates the equilibrium between dendrite branching and dendrite outgrowth: a prevalence of unphosphorylated δ -Catenin favors branching while a prevalence of phosphorylated δ -Catenin favors outgrowth. The factors that may help shift the balance towards the unphosphorylated form are BDNF and NGF but also clustered EphB which has been shown to induce new δ -Catenin synthesis. Rac1 and Cdc42 pathways may interact to promote dendrite branching. The factors that favor the phosphorylated form include clustered ephrin. The phosphorylated form of δ -Catenin promotes dendrite outgrowth and at the same time inhibits dendrite branching, acting as both an activator and a repressor, possibly with RhoA as a signaling partner. Cells expressing the $\Delta C208$

mutant seem to lack the dynamic branching/outgrowth equilibrium which is permanently shifted towards dendrite outgrowth independently of the extracellular stimulus applied.

BDNF and NGF also have interesting effects on the three categories of neurons. Control neurons stimulated with BDNF and NGF increase all parameters of dendritic complexity very much resembling neurons over-expressing δ -Catenin (before stimulation with ephrinB). Neurons over-expressing δ -Catenin on the other hand show no further increase in their already high dendritic complexity when BDNF or NGF are added. This may hint to the fact that over-expressing neurons have already reached the highest degree of dendritic complexity, or, more intriguingly that the effect of high levels of unphosphorylated δ -Catenin in the cell is equivalent to the stimulation of control neurons with BDNF or NGF, or, in other words, that BDNF and NGF could work in the same pathway and be above hypothesized factor or “A” that promotes unphosphorylated δ -Catenin-mediated dendritic branching. Another interesting observation comes from neurons expressing the non functional form of δ -Catenin. In this case, the neuronal phenotype, which consists in a simplified dendritic tree, is rescued and dendrites increase their branching upon stimulation with BDNF or NGF. This hints to the fact that δ -Catenin may be dispensable downstream of BDNF and NGF and that, at least in part, other molecular mechanisms control dendritic branching. Interestingly though, they have no additional positive effect on the number of primary dendrites and on the massive outgrowth visible in Δ C208 transfectants, confirming the process to be a phenotype generated by inactive δ -Catenin (see **figure 7.3**).

Parallel to the analysis of dendritic architecture, the results from the study of filopodial density in the three classes of neurons upon stimulation with ephrin, BDNF or NGF, add more complexity to the story. It has previously been shown that Eph-ephrin signaling is important for the generation and maintenance of spines (Irie and Yamaguchi 2002; Penzes et al. 2003). On the other hand the correlation between filopodial processes in young neurons and spines in adult neurons is not yet clear. If the hypothesis according to which a filopodium is a precursor of a spine is true, an increase in the number of filopodia upon a certain stimulus would mean that the neuron is instructed to generate

more spines. On the other hand, if filopodia formation and spinogenesis are unrelated processes, a stimulus that increases filopodia numbers may shift the equilibrium towards the filopodia with the final effect that the neurons develops less spines. At the molecular level, once more, Rho GTPases appear to have a major role in the formation of filopodia. Activation of Rac1 and Cdc42 pathways has been shown to positively influence spine formation. On the other hand mutants of important downstream effectors of Rac1 and Cdc42 like N-WASP, intersectin-1 and Cdc42 itself seem to inhibit spine formation and instead increase filopodia (Tashiro et al., 2000; Nakayama et al., 2000; Irie and Yamaguchi 2002; Pilpel and Segal 2004). This is consistent with the hypothesis that filopodia and spines indeed are two unrelated forms of fine dendritic processes, each with distinct cellular functions. The results presented in this thesis show that control neurons highly increase the number of filopodia upon long term stimulation with ephrin. Whether the effects will result in an increase of spine numbers or an overall decrease is not possible to say at this stage. The effect seems to be specific for ephrin treatment as BDNF and NGF have no effect on filopodial density. Filopodia also increase in neurons over-expressing δ -Catenin when they are stimulated with ephrin. δ -Catenin over-expression alone though, already has the effect of increasing filopodial density if compared to control neurons; this suggests that δ -Catenin up-regulation (in an unphosphorylated form), together with promoting dendritic branching, also promotes filopodia formation. As mentioned before, the major mechanism leading to dendritic branching is the so called “interstitial branching” where a branch arises laterally from the dendritic shaft as a small filopodium-like process, then it stabilizes and elongates. The increase in the number of filopodia could therefore be part of that late event induced by ephrin stimulation that leads to the restoration of dendritic complexity after the repulsive extracellular signal has exerted its effect. The newly generated filopodia could therefore represent the “sensing” organs of the dendritic tree, and the points from where the new branching, perhaps in a different direction, will take place. Another interesting observation comes from the filopodial analysis of $\Delta C208$ mutant. Filopodial density is in this case very high and not influenced by any of the stimuli applied. The filopodial phenotype of $\Delta C208$ partially resembles that of control and δ -Catenin neurons when stimulated with ephrinB. Since $\Delta C208$ is a dominant negative/inactive form of δ -Catenin, neurons lack the actin

promoting activity of unphosphorylated δ -Catenin and the potentially counteracting effects of phosphorylated δ -Catenin. There are two possible explanations for the phenotypes observed: first, the effects are due to the absence of δ -Catenin (because of the expression of the dominant negative mutant); second, the dominant negative mutant does not just act as a dominant negative, but it has effects of its own. More precisely, the effects of the Δ C208 mutant on dendritic architecture and filopodial formation may be due to the deletion of the tyrosine-rich C terminal portion of the molecule, where Eph receptor-mediated phosphorylation likely takes place and not only to the physical sequestration of endogenous δ -Catenin. The signaling-deficient δ -Catenin would then be responsible for the phenotypes observed. To distinguish between these two scenarios, the employment of RNAi knock-down experiments would be required.

The stimulation with BDNF and NGF could partially rescue the effect of Δ C208 on dendritic architecture, but the two growth factors showed no effect on filopodial dynamics. On the other hand, such an effect would not be expected since the application of BDNF and NGF does not have any influence in promoting filopodial outgrowth in control neurons. If filopodia are an intermediate for dendrite branching, then the BDNF and NGF induction of branching may also follow different pathways and signaling machineries.

Eph-ephrin signalling has been shown to be important in the regulation of adhesive properties and in cell migration with somewhat different effects according to the system used the Eph-ephrin subtypes. The two chambers migration assay gives another example of the functional interaction between δ -Catenin and Eph-ephrin signaling although the data still do not allow drawing definitive conclusions. The co-expression of δ -Catenin and EphA4 in HeLa cells has no effect on cell migration until cells are stimulated with ephrinB3. In this case they markedly decrease their motility and migrate approximately 30% less efficiently than the control cells. The use of the Δ C208 construct in the presence of EphA4 has no effect on migratory properties of the cells. The phosphorylation state of δ -Catenin and the formation of aggregates may again provide an explanation for these results. In cells co-expressing δ -Catenin and EphA4 the distribution of δ -Catenin fluorescence markedly changes upon stimulation with ephrinB3, leading to the formation

of aggregates. The phosphorylation state of δ -Catenin was not determined in the cells used for the migration assays; on the other hand, as it was shown before, the phosphorylation state of the molecule is correlated with the number of its aggregates and vice versa. In these cells, activation of the receptor may lead to phosphorylation, aggregation and sequestering of δ -Catenin. This, in accordance with what was observed in neurons, could possibly negatively influence cytoskeletal dynamics making cells less motile. In this case then, δ -Catenin may act as a repressor of migration when present in the phosphorylated form. Differently from neurons, its unphosphorylated form does not seem to have a specific effect. The data derived from Δ C208 and EphA4 co-transfectants are consistent with this idea. In this case migratory properties are not influenced by ephrinB3 stimulation. Interestingly though, the distribution of Δ C208 fluorescence also shows an aggregated pattern in both control and stimulated cells. Δ C208 is a non functional version of δ -Catenin which most likely lacks key residues implicated in the regulation of the phosphorylation state of the molecule. Its aggregates form independently of any stimulus. HeLa cells with clustered Δ C208 therefore migrate as if no δ -Catenin were present in the cells, as the activity of the full length protein is dependent on the fine regulation of its phosphorylation state and aggregation. Another hypothesis could be that Δ C208 does indeed behave as the clustered/phosphorylated δ -Catenin in repressing cell migration. What argues against this hypothesis is the fact that migration rates of Δ C208/EphA4 co-transfectants are slightly but not significantly lower than those of control cells.

Taken together the experimental data presented in this thesis propose δ -Catenin as a novel interactor of Eph-ephrin signaling, involved in mediating cytoskeletal responses upon activation of the signaling cascade. A few points require further investigation. It is still not clear if the biochemical interaction between δ -Catenin and EphA4 is direct or indirect. In the case of a direct interaction, still to be determined are the domains involved in both δ -Catenin and EphA4 sequences. In the case of δ -Catenin phosphorylation, it is also not clear which residues are involved, even if the data shown suggest that they may be concentrated near the COOH terminus of the molecule. The analysis of the

phosphorylatable tyrosine residues via the generation i.e. of deletion mutants proved to be difficult due to the high number of potentially important residues and their concentration in a relatively short sequence of δ -Catenin structure. This is in accordance with other members of the Arm family; β -Catenin stability and association with cadherins, for example, are highly regulated through multiple phosphorylation sites (Polakis et al., 2000; Bienz et al., 2000; Roura et al., 1999; Murase et al., 2002).

The role of the up-regulation of endogenous δ -Catenin in the context of dendritogenesis is still in apparent contradiction with the local effect that ephrin stimulation has on neurons. For this reason it would be important to find an extracellular cue capable of increasing dendritic complexity mediated by δ -Catenin but that at the same time keeps the phosphorylation state of the molecule unchanged, or, in other words, a signal that shifts the equilibrium towards the unphosphorylated state of δ -Catenin, increasing its activity in promoting dendritic branching. Natural candidates are BDNF and NGF but their effects on δ -Catenin expression and protein levels and on δ -Catenin phosphorylation still need to be tested before the two growth factors can be associated with δ -Catenin activity. An important control will also include EphB-Fc as a stimulus in the Sholl analysis of dendritic complexity. EphB-Fc stimulation induces δ -Catenin expression and protein levels but does not lead to δ -Catenin phosphorylation and aggregation. If the equilibrium model hypothesized before were correct, activation of reverse signaling should positively regulate dendritic branching by enriching the pool of unphosphorylated δ -Catenin. Preliminary data show that both control and δ -Catenin over-expressing hippocampal neurons stimulated with Eph-Fc for 24 hours indeed seem to increase their dendritic complexity (data not shown).

Finally, further experiments need to be done in order to shed more light on the role of δ -Catenin and Eph-ephrin signaling in HeLa cell migration. Also in this case it would be interesting to evaluate the role of ephrin-reverse signaling by using δ -Catenin/ephrin co-transfectants and stimulate with clustered Eph.

7.1 Outlook

A potentially interesting yet unexplored field is the role of δ -Catenin in regulating gene transcription. Other members of the Arm family with important structural roles in the cell junction and in dendritic development like β -Catenin have also been shown to influence gene transcription. Upon activation of the Wnt pathway, β -Catenin changes its intracellular distribution and migrates from the cell junction to the nucleus. Interestingly, recent data (Yu and Malenka, 2003) indicate that the intracellular re-localization of β -Catenin from the cell junction to the nucleus is also important for the modulation of β -Catenin mediated effect on dendrite branching. The study suggests that β -Catenin bound to Cadherins is required for dendritic outgrowth and a cue diverting β -Catenin from its normal distribution negatively influences the branching. Conversely, all manipulations that enhance dendritic branching can be effectively blocked by sequestering intracellular β -Catenin. This information nicely fits with the hypothesis of the sequestration of δ -Catenin by the activated Eph receptor and the subsequent decrease of dendritic branching. Whether phosphorylated δ -Catenin once re-localized is able, like β -Catenin, to migrate to the nucleus and have any activity in gene transcription is not known. Like β -Catenin though, δ -Catenin has a nuclear localization sequence in its molecular structure, suggesting that indeed the two molecules could share more than just a few functional analogies.

δ -Catenin KO mice have recently been described in Israely et al., 2004. Although KO mice appear to be viable and fertile and they do not show any major defect in CNS morphology so far identified, they have severe but specific learning, synaptic plasticity, and synaptic composition deficits that cannot be compensated for by other catenin family members in the brain, such as p120ctn or β -Catenin. This suggests a critical and specific role for δ -Catenin in experience-dependent synaptic modifications and cognitive function. Given the implication of Eph-ephrin signalling in synaptic plasticity and synapse formation, the study of the relationship between δ -Catenin and Eph-ephrin in this field could prove to be quite interesting.

8. MATERIALS AND METHODS

8. 1 Buffers and solutions

10X PBS	1.3M NaCl 70mM Na ₂ HPO ₄ 30mM NaH ₂ PO ₄ , pH 7.2
TE buffer	10mM Tris/HCl 1mM EDTA, pH 8
50X TAE	2M Tris-Acetate 50mM EDTA
20XSSC	3M NaCl 0.3M NaCitrate, pH 7.5/4.5
1X MOPS	0.418% MOPS 2mM Na-Acetate 1mM EDTA pH 8
RNA loading buffer	13.4% formamide 4.4% of 37% formaldehyde 80ug Blue Bromophenol 1X MOPS
5X Denhardt solution	1% Ficoll 400 1% polyvinylpyrrolidone 1% BSA H ₂ O
Microarray hybridization buffer	50% formaldehyde

	6X SSC
	0.5% SDS
	5X Denhardt solution
<i>In situ</i> pre-hybridization solution	50% formamide
	5X SSC pH4.5
	0.1% tween 20
	0.5% CHAPS
	2% blocking reagent
	50 μ g/ml tRNA
	50 μ g/ml heparin
	5mM EDTA pH 8.1
<i>In situ</i> hybridization buffer	0.19M NaCl
	10mM Tris pH7.2
	5mM NaH ₂ PO ₄ *2H ₂ O
	50% formamide
	10% dextrane sulphate
	1mg/ml Yeast rRNA
	1X Denhardt solution
<i>In situ</i> washing buffer	50% formamide
	2X SSC
	0.1% tween 20

8.2 Media and antibiotics for bacterial culture

LB (Luria-Bertani-) medium	10g Bacto-Trypton 5g Yeast extract 5g NaCl add H ₂ O to 1l, adjust pH to 7.5
----------------------------	--

LB plates	supplement with 15g/l agar
-----------	----------------------------

Antibiotics	diluted 1:1000
Ampicillin	Stock 100mg/ml in H ₂ O
Kanamycinsulfate	Stock 50mg/l in H ₂ O

8.3 Bacterial strains

DH5 α <i>hsdR17</i>	<i>supE44 ΔlacU169 (Φ80 lacZ ΔM15)</i> <i>recA1 endA1 gyrA96 thi-1 relA1</i>
K12 (dam minus) <i>hsdR17</i>	<i>supE44 ΔlacU169 (Φ80 lacZ ΔM15)</i> <i>recA1 endA1 gyrA96 thi-1 relA1</i>

8.4 Media and supplements for tissue culture

DMEM	Dulbecco's Modified Eagle medium (Invitrogen) Supplemented with 10% (0.5% or 0.25% for starving media) Calf serum/ Foetal bovine serum 0.292mg/ml L-glutamine, 100U/ml penicillin, 100μg/ml streptomycin
DMEM CS G418	DMEM, 10% Calf serum, 0.292mg/ml L-glutamine, 100U/ml penicillin, 100μg/ml streptomycin, 350μg/ml geneticin sulfate (G418).

DMEM FBS G418	DMEM, 10% Foetal bovine serum, 0.292mg/ml L-Glutamine, 100U/ml Penicillin, 100µg/ml Streptomycin, 350µg/ml geneticin sulfate (G418).
---------------	--

8.5 Media and supplements for primary culture of neurons

Neurobasal medium/B27	500ml of neurobasal medium (Invitrogen) were supplemented with 10ml of B27 supplement (Invitrogen).
MEM	Minimal essential medium (Invitrogen)
N-MEM	MEM, 0.6% glucose, 110µg/ml pyruvic acid, 0.292mg/ml L-glutamine
N2 supplement	MEM containing: Insulin (500µg/l), human transferrin (10mg/l), progesterone (0.63µg/l), putrescin (1611µg/l), selenite (0.52µg/l).
N2-MEM	N-MEM, 10%N2, 0.1g/ml chicken egg albumin.
HS-MEM	MEM, 10% HS, 0.6% glucose, 0.292mg/ml L-glutamine.
Borate Buffer	1.24g boric acid, 1.9g Borax ad 400ml H ₂ O, pH8.5.
HBSS	500ml of Hank's buffered salt solution (Invitrogen) were supplemented to final concentrations of 100U/ml penicillin, 100µg/ml streptomycin and with 3.5ml 1M HEPES (pH7.2) and 3.5ml 1M MgCl ₂ when used as a dissection medium.

8.6 Cell lines

NIH3T3 (Bristol Mayer Squibbs)	Mouse fibroblasts	DMEM CS
COS	Simian fibroblasts derived from kidney	DMEM FBS

PC12	Rat adrenal pheochromocytoma cells	DMEM FBS
HeLa	Human cervix carcinoma cells	DMEM FBS

8.7 Solutions for cell transfection

1M CaCl₂

2× BES-buffered saline (2×BBS)	50 mM BES
	280 mM NaCl
	1.5 mM Na ₂ HPO ₄ ·2H ₂ O
	(pH 6.96-7.22)

8.8 Solutions for Biochemistry

Laemmli stacking gel (10ml):	1.3ml	30% w/v acrylamid/bis 25:1
	2.6ml	0.5M Tris HCl pH6.8, 0.4% SDS
	6.1ml	H ₂ O
	100µl	10% APS
10% Laemmli separating gel (10ml):	10µl	TEMED
	3.3ml	30% w/v acrylamid/bis 25:1
	2.6ml	1.5M Tris HCl pH8.8, 0.4% SDS
	4ml	H ₂ O
	50µl	10% APS
	5µl	TEMED

5x Laemmli electrophoresis buffer (10l):	154.5g	Tris base
	721g	glycine
	50g	SDS
10x Transfer buffer (2.5l):	60.5g	tris base
	281.5g	glycine
	25g	SDS
Anderson stacking gel buffer (7.45ml):	1.25ml	30% w/v acrylamide
	1ml	1% bisacrylamide
	0.9ml	1M Tris HCl pH6.8
	4.3ml	H ₂ O
	50μl	10% APS
	5μl	TEMED
15% Anderson separating gel (20ml):	10ml	30% w/v acrylamide
	1.7ml	1% bisacrylamide
	5ml	1.5M Tris HCl pH8.8
	3.15ml	H ₂ O
	200μl	10% APS
	20μl	TEMED
5x Anderson electrophoresis buffer (2l):	60g	Tris Base
	288g	glycine
	10g	SDS
Stripping buffer:	5mM	PBS pH7.2
	2mM	β-mercaptoethanol
	2%	SDS
4x Sample buffer for non-reducing conditions:	4ml	10% SDS
	16.ml	1M Tris pH6.8
	2ml	glycerol
	1.9ml	H ₂ O
	0.1%	bromophenol blue
4x Sample buffer for reducing conditions:	50μl β-mercaptoethanol /ml	4x sample buffer

8.9 Plasmids

pE(G/Y)FP-C1

Becton Dickson

pSPORT 1

Lifetech

8.9.1 Expression constructs

Full length δ -Catenin-EGFP-tagged	From Qun Lu
Full length δ -Catenin-EYFP -tagged into	Insert (BglIII and XmaI ends) was cloned pEYFP-C1 vector
Δ C208-EGFP-tagged	From Qun Lu
Δ C208-YGFP-tagged	Insert (BglIII and XmaI ends) was cloned into pEYFP-C1 vector
Δ N250-EGFP-tagged	From Qun Lu
EphA4	From Joaquin Egea
EphA4-Kinase Dead	From Joaquin Egea
EphA4-2E	From Joaquin Egea
EphB2-ECFP-tagged	From Jenny Koehler

8.10 Antibodies

Primary antibodies

Anti-tubulin	Sigma, mouse WB: 1:2000
Anti-phosphotyrosine (4G10)	Upstate Biotechnology, mouse WB: 1:5000

Anti-EphB2	R&D, goat WB: 1:200 Immunocytochemistry: 4 μ g/ml
Anti-EphA4 globular domain	(J. Egea, R.K., unpublished) rabbit serum Immunocytochemistry: 1:100 WB: 1:2000
Anti-Sek (EphA4)	Transduction Laboratories, mouse WB: 1:1000 IP: 2 μ g/mg protein
Anti-GFP	RDI, rabbit WB: 1:2000 IP: 1-4 μ g/mg protein Immunocytochemistry: 1:100
Anti- δ -Catenin	Transduction Laboratories, mouse WB: 1:1000 IP: 4 μ g/mg protein Immunocytochemistry: 1:100
Anti-Calsyntenin	Gift from P. Sonderegger's Lab
Anti-Smad4	Santa Cruz, mouse WB: 1:2000
Anti-human Fc γ FITC- or TR-conjugated	Jackson ImmunoResearch, goat polyclonal Immunocytochemistry: 7.5 μ g/ml

Anti-human Fc_γ
proteins
Jackson ImmunoResearch, goat
1/10 (w/w) for preclustering of Fc-fusion

Secondary antibodies

Anti-mouse HRP	Amersham, goat polyclonal WB: 1:2000
Anti-rabbit HRP	Amersham, goat polyclonal WB: 1:2000
Anti-mouse Texas Red	Sigma, goat polyclonal IF: 1:200
Anti-mouse-Cy3, -Cy5 polyclonal	Jackson ImmunoResearch, donkey IF: 1:200
Anti-mouse-Alexa488	Molecular Probes, goat polyclonal IF: 1:200

8.11 Chemicals and commercial kits

100x L-glutamine (Invitrogen)
100x penicillin / streptomycin. (Invitrogen)
30% Acrylamid/Bis 25:1 (Biorad)
Aprotinin (Sigma)
Benzamidine (Sigma)
Biorad D_c Protein Assay (Biorad)

β -Mercaptoethanol (Sigma)
Calf serum (CS) (Invitrogen)
Chicken albumin (Sigma) 1g/ml in N-MEM
Dimethyl sulfoxide (DMSO) (Sigma)
Dithiothreitol (DTT)
ECL Western Blot detection reagent (Amersham)
EDTA (Sigma)
EphB1-Fc, EphrinB3-Fc, EphrinB2-Fc, EphrinB1-Fc (R&D)
Foetal bovine serum (FBS) (Invitrogen)
Geneticin sulfate (G418) (Invitrogen)
Human Fc fragment (Dianova)
Human transferrin (Sigma)
Isopropyl- β -D-thiogalactopyranoside (IPTG) (Sigma)
LightCycler DNA Master SYBRGreen I system (Roche)
Lipofectamine (Invitrogen)
Lipofectamine plus reagent (Invitrogen)
Lysozyme (Sigma)
Mouse-laminin (Invitrogen)
Normal Donkey Serum (Dianova)
Normal Goat Serum (Dianova)
Papain (Sigma), 1mg/ml, stored at 4°C.
phenylmethylsulfonyl fluoride (PMSF) (Sigma)
Poly-D-lysine (Sigma)
Poly-L-lysine (Sigma)
PonceauS solution (Serva)
Progesterone (Sigma)
Protein A-Sepharose 4B (Pharmacia)
Protein G-Sepharose 4B (Pharmacia)
Putrescin (Sigma)
Pyruvic acid (Sigma)
TEMED (Biorad)
Triton X-100, analytical grade (Serva)
Trypsin inhibitor (Roche)
Trypsin/EDTA (Invitrogen)
Tween 20 (Biorad)

Methods

8.12 Molecular biology

8.12.1 Preparation of plasmid DNA

Plasmid DNA was purified from small-scale (5 ml, minipreparation) or from large-scale (300

ml, maxipreparation) bacterial cultures. Single colonies from transformed bacteria or bacterial glycerol stocks were picked into LB medium containing 100 $\mu\text{g/ml}$ ampicillin or kanamycin and grown overnight (ON) at 37°C with vigorous shaking. The bacterial suspension was pelleted by centrifugation at 4,000 rpm for 5 min at RT. The pellet was resuspended in buffer P1 (QIAGEN). Mini- and Maxipreparations of plasmid DNA were carried out according to the QIAGEN protocol using lysis of the cells and binding of the plasmid DNA to a special resin. After washing, elution and precipitation the plasmid DNA was re-dissolved in a suitable volume of EB buffer (QIAGEN) for minipreparation or pure water (Sigma) for maxipreparation. DNA concentration was measured in a UV spectrometer at 260 nm. The following formula was used: dsDNA: $\text{OD} \times 50 \times \text{dilution factor} = X \mu\text{g/ml}$

8.12.2 Enzymatic treatment of DNA

Cleavage of plasmid DNA: Approximate 2-6 μg of DNA was cut in 30 μl of the appropriate buffer and 2 to 5 U restriction enzyme for 1 to 2 hours (hrs) at an appropriate temperature. De-phosphorylation of DNA fragments: For the dephosphorylation of DNA fragments 10 \times buffer, pure water (Sigma) and 1 U (1 μl) of calf intestine alkaline phosphatase (Roche) was added to the restriction enzyme reaction to get a total reaction volume of 40 μl , incubated for 20 min at 37°C and heat-inactivated at 75°C for 15 min. Subsequently the de-phosphorylated DNA fragments were purified from the reaction mix. Ligating vector and target DNA fragments: A 10 μl reaction containing purified linearized vector (approximate 0.1 μg) and DNA fragments (“insert”) in an 1:5 ratio, 0.5 μl of T4 DNA ligase (NEB), ligation buffer (10 \times T4 DNA ligase buffer, NEB) was

incubated over-night at 16°C or at RT for 2 hours, followed by 30 min at 37°C for sticky end ligations. The reaction was then used to transform competent bacteria.

8.12.3 Separation of DNA on agarose gels

The DNA mix and circa one sixth of the volume of 6× loading buffer were loaded onto a 0.8-2% agarose gel in TAE buffer containing ethidium bromide and run for approximately 30 to 35 min at 100-180 V. After electrophoresis a UV photograph of the gel was taken. In a preparative gel, the DNA band was excised from the agarose gel with a clean, sharp scalpel and purified.

8.12.4 Purification of DNA

From agarose gel: Following extraction, purification of DNA fragments from agarose gel was carried out using the QIAquick Gel Extraction Kit (#28704, QIAGEN) as recommended by the manufacturer. The DNA was eluted in 30 μ l of buffer EB (QIAGEN). From enzymatic reactions: to clean-up DNA fragments or oligonucleotides (>17 nucleotides) from salts, enzymes, unincorporated nucleotides, the QIAquick Nucleotide Removal Kit (#28104, QIAGEN) was used according to the protocol of QIAGEN. The DNA was eluted in 30 μ l of buffer EB (QIAGEN).

8.12.5 Transformation of competent E. coli by electroporation

50 μ l of electro competent bacteria were gently thawed on ice, mixed with 3-5 μ l of the ligation product and placed on ice for 1 min. Sterile 0.2 cm (green) cuvettes were placed on ice. The Gene pulser apparatus (Bio-Rad) was set at 25 μ F and to 2.5 kV; the pulse controller to 200 W. The mixture of bacteria and DNA was transferred to a cold electroporation cuvette. The cuvette was placed in the chamber slide, pushed into the chamber and pulsed once at the above settings. 1 ml LB medium was immediately added. The cells were resuspended, transferred to a reaction tube and incubated at 37°C for 15 to

60 minutes with shaking at 225-250 rpm. The bacteria were then plated on LB agar plates containing the appropriate antibiotic for the plasmid vector and incubated at 37°C ON.

8.13 Semi-quantitative real-time PCR

8.13.1 cDNA preparation

Total RNA was prepared from primary cortical neuron cultures in the same way as in the Microarray section (see below). Reverse transcription reactions were performed at 55°C with Superscript III reverse transcriptase (Invitrogen) according to the instructions. The reaction included the use of oligo d(T) primers. cDNA products were further processed by digesting RNA for 20 min with 4 U of RNase H (Biolabs), and then purified using a PCR cleanup kit (Qiagen).

8.13.2 PCR primers and templates

Specific oligonucleotides for each gene to be validated with RT-PCR were designed by the Oligo 6 Primer software. Only primers sets that formed very limited double stranded secondary structures were selected in order to avoid any double strand background. Blast searches were used to ensure that primers were specific for each individual gene. Primer sets amplified a single product of the correct size from a complex cDNA as measured by melting curve analysis on the light cycler system (Roche) and agarose gel electrophoresis.

8.13.3 LightCycler RT-PCR

Real-time PCR was performed with the LightCycler FastStart DNA Master SYBR Green I system (Roche). Master mixtures were prepared in accordance with the manufacturer's instructions by using the specific oligonucleotides for the genes of interest. After RT for 20 min at 50°C, the following temperature profile was utilized for amplification:

denaturation for 1 cycle at 95°C for 30 s; 45 cycles at 95°C for 1 s (temperature transition, 20°C/s), 55 to 50°C (step size, 1°C; step delay, 1 cycle) for 15 s (temperature transition, 20°C/s), and 72°C for 15 s (temperature transition, 2°C/s); and fluorescence acquisition at 55 to 50°C in single mode. Melting-curve analysis was performed at 45 to 90°C (temperature transition, 0.2°C/s) with step-wise fluorescence acquisition. Sequence-specific standard curves were generated by using 10-fold serial dilutions of the specific RNA standards. The relative abundance of each sample transcript was then determined with the aid of the LightCycler software based on the comparison with the G3PDH and S16 curves as a standard. The specificity of the PCR was verified by ethidium bromide staining on 3% agarose gels.

8.14 Primary culture of cortical neurons for biochemistry

Mass cultures of cortical neurons were prepared by a modified procedure based on (de Hoop et al., 1998). Forebrain hemispheres from mouse E14.5 embryos were dissected in warm HBSS as above. Cortices were washed with HBSS and then dissociated with Trypsin/EDTA solution for 15min at 37°C. Trypsin was blocked by 2 washes in prewarmed HS-MEM medium. Cells were triturated as above and plated in tissue culture dishes precoated with 1mg/ml poly-L-lysine in borate buffer over night at 37°C and HS-MEM for an additional over night period at 37°C. Approximately 4-6 hemispheres were used per 10cm dish. Cells were left for 5h to attach and then medium was changed to N2-MEM without insulin. Neurons were left for 2 days to differentiate, washed three times in warm HBSS and then stimulated.

8.14.1 Stimulation of cells

Neurons and cell lines (see below) were stimulated with ephrinB2-, ephrinB1-, EphB1-Fc Chimeras (R&D) or Fc (Dianova) which had been pre-clustered for 1h at room temperature using 1/10 (w/w) Fc fragment, goat anti-human IgG (Jackson

Immunoresearch). Before stimulation, all cell types except cortical neurons were starved for 16h in medium containing 0.5% serum.

Stimulation of hippocampal neurons with BDNF and NGF was carried out using the following concentrations: 50 ng/ml and 100ng/ml respectively

8.15 Primary culture of neurons for immunocytochemistry, cell imaging and time lapse imaging

Hippocampal and cortical neurons were taken from mouse E15 and rat E19 embryos. Embryos were taken out of the uterus and kept in ice cold HBSS buffer. Embryo heads were cut off and the skull opened to take out the brain. Brain cortices were cut off from the midbrain and brainstem and the meninges was pulled off. For hippocampal cultures the striatum was cut out and the hippocampus was separated from the cortex. Hippocampi and cortices were incubated in HBSS with 1/10 papain solution for 10min at 37°C. The digestion reaction was stopped using 10mg/ml trypsin inhibitor in HBSS. The tissue was washed 3 times in Neurobasal medium. Cells were dissociated by trituration with glass Pasteur pipettes with narrowed tips. 10ml of cell suspension was centrifuged for 3min at 800rpm to remove debris. The cell pellet was resuspended in Neurobasal medium supplemented with B27. Cells were plated on glass coverslips or on live-cell-dishes precoated with 1mg/ml Poly-D-lysine in borate buffer over night and 10µg/ml mouse laminin in PBS for 2h at 37°C. Cells were cultured in medium supplemented with 1/3 (v/v) of conditioned growth medium obtained from at least 7day old high density E17.5 cortical neuron cultures ($3 \cdot 10^6$ cells / 10cm dish) prepared the same way as above with the exception that the dishes were not coated with laminin. Depending on the length of culture and the experiment, different numbers of cells were plated and incubated for a number of days at 37°C, 5% CO₂ then transfected and imaged. For time lapse experiments of neurons live-cell-dishes with a glass bottom were used.

8.15.1 Transfection of cell lines and primary neurons

NIH3T3 cells were transiently transfected using Lipofectamine Plus (QIAGEN) according to the protocol. COS cells and HeLa cells were transfected with the calcium phosphate method.

For the calcium phosphate transfection method all solutions were warmed to room temperature. The plasmid DNAs were briefly spinned down in a mini centrifuge. For transfection of neurons growing (i) in time-lapse dishes, part of the medium was removed, leaving 0.9 ml medium in the dish and (ii) on glass coverslips in a 24-well plate, leaving 0.25 ml. The remaining medium was collected, filter-sterilized and kept at 37°C in a humidified incubator with an atmosphere of 5% CO₂. For 1 ml transfection solution 3-7.5 µg DNA (depending on the plasmid size) were slowly added to freshly diluted 250mM CaCl₂ solution by stirring with the pipette tip, the final volume being 50 µl. 50 µl of 2× BBS was added drop by drop to the DNACaCl₂ solution. The reaction tube was gently shaken each time after addition of three drops of 2× BBS. The solution was then thoroughly mixed. The CaCl₂-DNA-BBS mixture was added drop wise to the hippocampal neurons and the dishes gently swirled in order to mix medium and transfection mixture and to ensure a homogenous formation of the DNA-calcium phosphate precipitation.

For the transfection of neurons and HeLa cells on coverslips the CaCl₂-DNA-BBS mixture was added drop by drop to 0.9 ml medium in a polystyrene-tube while vortexing. 250 µl of the transfection solution was immediately added to each well. The collected medium was filter-sterilized and kept in the incubator. Cells were incubated at 37°C in a humidified incubator with an atmosphere of 5% CO₂ for the appropriate transfection time (30 min - 4 h). If the formation of the precipitate was too heavy, the transfection medium was removed and cultures were washed with pre-warmed HBSS (Invitrogen) until the DNA-calcium phosphate precipitation was completely washed off. After that the cells were incubated in the “old”, equilibrated culture medium. The expression time for time-lapse experiments was 2 to 3 days.

8.15.2 Time-lapse imaging

Live-cell imaging was performed with a Zeiss Axiovert 200M microscope equipped with a temperature-controlled CO₂-incubation chamber set to 37°C, 60-70% humidity, 5% CO₂ and a FluoArc system (Zeiss, Germany) set to 30-50%. Images were acquired using a 63×oil immersion objective with a CoolSNAP-fx camera. Fluorescence images were processed using MetaMorph (Visitron, Germany).

8.15.3 Immunocytochemistry and cell imaging

For immunocytochemistry of total protein distribution, neurons and cells grown on coverslips were fixed with 4% PFA, 4% sucrose in D-PBS for 13 min at RT, washed once with D-PBS, then incubated with 50 mM ammonium chloride in D-PBS for 10 min at RT and washed again before permeabilization for 5 min with ice-cold 0.1% TX-100 in D-PBS at 4°C. After washing, coverslips were blocked for about 30 min at RT or overnight at 4°C with 2% bovine albumin (A-3294, Sigma) and 4% serum (depending on the secondary antibody used: donkey, goat, sheep and/or rat serum, Jackson ImmunoResearch) in PBS. After blocking, coverslips were transferred into a dark moist chamber, face up. Primary antibodies for total stainings were incubated for at least 60 min at RT in 50 µl blocking solution. After 3 washing steps with D-PBS for 5 min, secondary antibodies, previously diluted in 50 µl of blocking solution, were added to the coverslips for 30 min at RT in the dark. After washing, samples were mounted in Gel/Mount media and dried at RT. For simple cell imaging of fluorescent proteins the same coverslip preparation procedure was done excluding the permeabilization and the antibody staining steps. Images were acquired using an epifluorescence microscope (Zeiss) equipped with a digital camera (SpotRT, Diagnostic Instruments) and the MetaMorph software (Visitron Systems).

8.16 Microarray

8.16.1 Microarray production

High density glass microarray chips were prepared at EMBL using the NIA 15K cDNA mouse clone set (Tanaka et al., 1997). The 15,247 cDNAs were first replicated inoculating 2 μ l of the original bacterial suspension into 50 μ l of LB broth. The replica plates were incubated for 18 hours at 37°C. 1 μ l of the bacterial replica culture was then amplified by PCR using two universal oligonucleotides. The 15,247 PCR products were further purified from unincorporated dNTPs and oligonucleotides using the PCR purification kit (Mecherey-Nagel). The purified PCR products were eluted in 100 μ l TE buffer. The size and quality of the PCR products were then checked by agarose gel electrophoresis and then spotted at high density on glass coverslips by a robot. The slides were then incubated at 50°C for 3 hours and the DNA was denatured at 100°C for 10 min. The microarray slides were then stored at room temperature in a dark place until use.

8.16.2 RNA extraction and preparation of fluorescent probes

Total RNA was extracted from cortical neuron cultures under different experimental conditions using the RNAClean protocol (Hybaid). The RNA was then purified using RNA purification kit (Qiagen) and 40 μ g were then retro-transcribed and fluorescently labelled using a mixture of 3 μ g poly-dT oligonucleotides (GIBCO), 6 μ l of retro-transcriptase superscript II (GIBCO), 0,1M DTT, 3 μ l of either Cy3-dUTP (Amersham) for the control sample or Cy5-dUTP for the test, and 25 μ M of dNTPs. The retro-transcription reaction was incubated for 4 hours at 42°C then stopped with 1,5 μ l of 1M NaOH/20 mM EDTA. The labelled cDNA was then purified using the PCR purification kit (Qiagen).

8.16.3 Microarray hybridization

The cDNA spotted on the array slide was denatured for 2 min in boiling water before the hybridization with the fluorescent probes took place. The Cy3- and Cy5-labelled cDNAs were pooled, dried out and resuspended in 30 μ l water. 2.4 μ g salmon sperm DNA, 10 μ g

poly-dA oligonucleotide (Invitrogen) and 24 μ l hybridization buffer were added to the cDNA probes and the mixture was then denatured by incubation for 2 min at 95°C. The probes were then hybridized to the microarray slide and incubated for 16 hours at 42°C in a water bath. After the hybridization, the microarray was washed twice with 0.1X SSC, 0.1% SDS for 10 min at room temperature and twice with 0.5X SSC for 10 min. Finally, the microarray was scanned with a fluorescence laser-scanning device (GenePix 400B, Axon instruments).

8.16.4 Microarray analysis

The hybridizations were performed in triplicate. The differential expression of each gene was calculated from the relative intensity of the Cy5 versus the Cy3 fluorescent signal. Two independent experiments were conducted comparing two control samples (background control). The data acquisition and initial data analysis was performed with GenePix Pro 3.0 and the resulting data tables were analysed further with Microsoft Excel. Scatter plots were used to visualize and select the genes. The GenePix Pro software calculates the normalization factor for each hybridization, based on the principle that the arithmetic mean of the ratios from each feature on the array should be equal to 1. Normalization was therefore performed by multiplying the factor for the ratio of medians in each gene. The genes were then sorted by the sum of medians which indicates the intensity of hybridization. In order to obtain the list of genes with higher abundance only the spots with sum of medians higher than 5000 were selected. Finally, the genes were sorted by their ratio of medians which ultimately reflects the folds of induction or repression.

8.16.5 Insert cloning and generation of probes for various uses

For the generation of probes from selected genes in the NIA library, clones were selected, amplified and plasmids isolated with the miniprep kit (Qiagen). 5 μ of the isolated

plasmids were digested using NotI and Sall restriction enzymes (Biolabs) which are universal cutters for the excision of the NIA library inserts. The restriction digest was then run on agarose gel and the excised insert recovered and purified using the Gel Extraction Kit (Qiagen).

8.17 Boyden chamber assay

HeLa cells were grown as above. One day before transfection the cells were trypsinized and 1×10^6 cells were plated on a 10 cm Petri dish (Falcon). The cells were then transfected with the appropriate constructs with the calcium phosphate method as described above. Cells were detached using PBS without Ca^{2+} and Mg^{2+} and supplemented with EDTA (final concentration 2mM). The cells were then centrifuged and resuspended in warm starving medium. Cells were then counted and 5×10^4 were seeded on the migration membranes. Prior to cell seeding the Boyden chambers ($8 \mu\text{m}$ pore size, Costar) were coated for 18 hours at 4°C with $0.15 \mu\text{g}/\text{cm}^2$ fibronectin plus (Sigma) $0.6 \mu\text{g}/\text{cm}^2$ anti-Fc (Jackson Immunoresearch). Membranes were then washed with PBS and blocked with 1% BSA (Sigma) in PBS for 1h at room temperature. Membranes were then incubated for 1h at room temperature with either Fc or ephrinB3-Fc at a concentration of $1.3 \mu\text{g}/\text{well}$. After washing in PBS, the membranes were kept in starving medium (serum $<0.5\%$). The transfected cells are then seeded and left migrating overnight. The membranes are then fixed by incubating them for 5 min in 4%PFA (Sigma), washed, DAPI stained if necessary then the membranes are carefully detached from the plastic support and mounted on a glass slide always in the correct orientation for fluorescence microscopy analysis.

8.18 Sholl analysis

Fluorescence pictures were taken with a 40x calibrated objective at a constant 1 sec exposure time in order to highlight even small or weak fluorescent details. The images

were converted into their negative to further accentuate the contrast between the background and the neuronal structures. Sets of images were then processed with the software NeuroLucida which allows manual tracing of dendritic processes. The cut-off for filopodia was set to $2\mu\text{m}$; any structure exceeding the threshold was considered to be a nascent dendritic branch. Traced images were then further analyzed with the software Neuroexplorer which automatically calculates a set of statistical parameters including dendritic length, number of filopodia etc and other important parameters defining dendritic complexity (i.e. the number of intersections between the dendritic tree and a set of concentric circles drawn on the neuron and centered on the cell body (Sholl, 1953). The tables generated by Neuroexplorer were then exported to Microsoft Excel and statistically analysed.

8.19 Biochemistry

8.19.1 Cell lysis

Cortical neurons and transiently transfected cells were washed once with ice-cold D-PBS and lysed in lysis buffer (50mM Tris-HCl, pH 7.5, 0.5-1% Triton X-100, 150mM NaCl, 10mM NaPPi, 20mM NaF, 1mM sodium orthovanadate, 1mM PMSF, 2.5mM benzamidine and

10 $\mu\text{g/ml}$ each leupeptin and aprotinin) on ice for approximately 5 min. Cell lysates were then collected and centrifuged at 10,000g for 15 min at 4°. Before loading, samples were boiled for 5 min in 2 \times sample buffer for 5 min.

8.19.2 Immunoblotting and immunoprecipitation

Protein samples were separated by 7,5 or 10% SDS-PAGE and transferred to nitrocellulose membranes. The membranes were blocked for 2h at room temperature in 7.5% non-fat milk in PBS plus 0.1% Tween-20.

For immunoprecipitation, cells were lysed in lysis buffer and centrifuged at 10000g for 10min. Lysates were then incubated with a variable amount (2 to 4 μ g) of antibody prebound to 20 μ l of proteinA or proteinG-Sepharose. After 2h at 4°C, immunoprecipitates were washed, denatured and analyzed by SDS-PAGE. After blotting, membranes were incubated either 1-3 hours at RT or overnight at 4°C with a primary antibody diluted in blocking solution. Membranes were washed three times for 10 min in PBST at RT. Secondary antibodies linked to horseradish peroxidase (HRPO) were used to specifically recognize the primary antibody diluted in blocking solution. After incubation for 1 hour at RT, membranes were washed three times for 10 min in PBST. To visualize signals, the membrane was incubated with ECl solution for 1 min at RT and exposed to films (BioMax MS/MS, Kodak). The films were developed in an Optimax (Typ TR, MS Laborgeräte. Anti-phosphotyrosine blots were performed using 4G10. For reprobing, membranes were stripped with 5mM sodium-phosphate buffer, pH 7.5, 2% SDS, 2mM β -mercaptoethanol, where indicated.

8.20 Histology

8.20.1 Vibratome sections for *in situ* hybridization

Dehydrated E15 mouse embryos were left overnight in 4% PFA at 4°C were washed three times with D-PBS and then immersed in a mixture of gelatine and ovoalbumine in acetate buffer (see embedding solution). For embedding, a 11-ml aliquot was thawed at 37°C and cooled down at RT. A base was prepared by adding 100 μ l of glutaraldehyde (25%, Sigma) to 2 ml embedding medium, mixed quickly and poured into the molds.

After polymerization the embryos were placed on top. 350 μ l of glutaraldehyde (25%, Sigma) were added to the remaining 7 ml of embedding medium, then mixed quickly and poured on the sample. Samples were stored 1 hour at 4°C in PBS. For vibratome sections the polymerised block was glued to the holder (Leica). 80 μ m and 100 μ m sections were cut on a microtome (VT1000S, Leica), immersed in D-PBS and immediately processed further for *in situ* hybridization.

8.20.2 *In situ* hybridization

Sections were collected in D-PBS and subsequently dehydrated in methanol diluted in D-PBS (25% for 5 min, 50% for 5 min, 75% for 5 min, 100% for twice 5 min). Sections were stored for up to several months at -20°C in 100% methanol or further processed after at least 2 hours at -20°C. Sections were then placed into a solution made out of 80% methanol and 20% of 30% H₂O₂ solution (final concentration of 6% H₂O₂) for 1 hour at RT. Rehydration was carried out in 50% methanol in D-PBS for 5 min followed by 25% methanol in D-PBS for 5 min. Samples were washed three times in PBST for 5 min at RT. Sections were treated with Proteinase K (20 μ g/ml in D-PBST) for 13 min at RT. In order to stop the reaction, sections were washed twice with PBST on ice. Subsequently, sections were fixed in fresh 4% PFA containing 0.2% glutaraldehyde for 40 min at RT. After two washes in PBST, sections were gently rocked in prehybridization buffer for at least 1 hour at 70°C. Labeled RNA probes (= 12.5 μ l/ml) were diluted in prehybridization buffer, preheated for 7 min to 70°C, and incubated with the sections overnight at 70°C. The next day, sections were first rinsed for 5 min and then washed three times for 30 min in Solution 1 at 70°C. Following 5-min rinsing and three 30-min washes in Solution 2 at 66°C, sections were first rinsed for 5 min and then washed three times for 30 min in Solution 3 once at 66°C and twice at 68°C. Subsequently, sections were washed twice with MABT for 5 min at RT and then twice for 30 min at 70°C. Unspecific antibody binding was prevented using blocking solution for 1.5 hour at RT. To detect DIG-labeled RNA, sections were incubated overnight at 4°C with an anti-DIG. Fab fragment conjugated with alkaline phosphatase (AP) (1:2000 in blocking solution, #1 093274,

Roche). The next day, sections were washed 8 to 10 times with MABT for 30 min to get rid of unbound or unspecifically bound Fab fragments and to prevent endogenous AP activity. After washing, sections were rinsed once in freshly made NTMT and then equilibrated in NTMT for 10 to 20 min. Developing solution was added (1.4 μ l nitroblue tetrazolium (NBT) and 1.1 μ l 5-bromo-4-chloro-3-indolyphosphate (BCIP) per ml NTMT) to give a dark purple color. Reaction and sample were kept in the dark. Sections were left in substrate solution at 37°C until enough staining was obtained. After development, sections were washed in PBST and postfixed in 4% PFA overnight. The sections were then mounted and stored in a solution made of 1 part 4% PFA and 1 part glycerol.

9. BIBLIOGRAPHY

Aberle, H., H. Schwartz, and R. Kemler. 1996. Cadherin-catenin complex: protein interactions

and their implications for cadherin function. *J. Cell. Biochem.* 61:514-523.

Aberle, H., S. Butz, J. Stappert, H. Weissig, R. Kemler, and H. Hoschuetzky. 1994. Assembly of

the cadherin-catenin complex in vitro with recombinant proteins. *J. Cell Sci.* 107:365-366.

Adams, R. H., F. Diella, S. Hennig, F. Helmbacher, U. Deutsch and R. Klein. The cytoplasmic domain of the ligand ephrinB2 is required for vascular morphogenesis but not cranial neural crest migration. *Cell* (2001). 104: 57-69.

- Adams, R. H., F. Diella, S. Hennig, F. Helmbacher, U. Deutsch and R. Klein. The cytoplasmic domain of the ligand ephrinB2 is required for vascular morphogenesis but not cranial neural crest migration. *Cell*(2001) 104: 57-69.
- Adams, R. H., G. A. Wilkinson, C. Weiss, F. Diella, N. W. Gale, U. Deutsch, W. Risau and R. Klein Roles of ephrinB ligands and EphB receptors in cardiovascular development: demarcation of arterial/venous domains, vascular morphogenesis and sprouting angiogenesis. *Genes and Development*(1999). 13: 295-306.
- Adams, R. H., G. A. Wilkinson, C. Weiss, F. Diella, N. W. Gale, U. Deutsch, W. Risau and R. Klein. Roles of ephrinB ligands and EphB receptors in cardiovascular development: demarcation of arterial/venous domains, vascular morphogenesis and sprouting angiogenesis. *Genes and Development*(1999) 13: 295-306.
- Altman, J. & Anderson, W. J. Experimental reorganization of the cerebellar cortex. I. Morphological effects of elimination of all microneurons with prolonged x-irradiation started at birth. *J. Comp. Neurol.* 146, 355–406 (1972).
- Amano, M., Ito, M., Kimura, K., Fukata, Y., Chihara, K., Nakano, T., Matsuura, Y., and Kaibuchi, K.. Phosphorylation and activation of myosin by Rho-associated kinase (Rho-kinase). *J. Biol. Chem* 1996. 271: 20246–20249.
- Anastasiadis, P.Z., and A.B. Reynolds. 2001. Regulation of Rho GTPases by p120-catenin. *Curr. Opin. Cell Biol.* 13:604–610.
- Anastasiadis, P.Z., S.Y. Moon, M.A. Thoreson, D.J. Mariner, H.C. Crawford, Y. Zheng, and A.B. Reynolds. 2000. Inhibition of RhoA by p120 catenin. *Nat. Cell Biol.* 2:637–644.
- Bamburg, J.R. Proteins of the ADF/cofilin family: Essential regulators of actin dynamics. *Annu. Rev. Cell Dev. Biol.* 1999. 15: 185–230
- Bayer SA, Altman J. 1991. Development of the endopiriform nucleus and the claustrum in the rat brain. *Neuroscience* 45:391–412.
- Becker, E., U. Huynh-Do, S. Holland, T. Pawson, T. O. Daniel and E. Y. Skolnik. Nck-interacting Ste20 kinase couples Eph receptors to c-Jun N-terminal kinase and integrin activation. *Mol Cell Biol* (2000). 20(5): 1537-45.
- Benson DL, Tanaka H. 1998. N-cadherin redistribution during synaptogenesis in hippocampal

- neurons. *J Neurosci* 18:6892–6904.
- Berry M, Rogers AW. 1965. The migration of neuroblasts in the developing cerebral cortex. *J Anat* 99:691–701.
- Bienz M, Clevers H. Linking colorectal cancer to Wnt signaling. *Cell*. 2000. 103(2):311-20.
- Boeckers, T.M., Bockmann, J., Kreutz, M.R., and Gundelfinger, E.D.. ProSAP/Shank proteins—
A family of higher order organizing molecules of the postsynaptic density with an emerging role in human neurological disease. *J. Neurochem* 2002. 81: 903–910.
- Bokoch, G.M. Biology of the p21-activated kinases. *Annu. Rev. Biochem* 2003. 72: 743–781.
- Bonhoeffer, T. and R. Yuste. Spine motility. Phenomenology, mechanisms, and function. *Neuron* (2002) 35(6): 1019-27.
- Bonhoeffer, T. and Yuste, R. Spine motility. Phenomenology, mechanisms, and function. *Neuron* 2002 35: 1019–1027.
- Bossing, T. and A. H. Brand Dephrin, a transmembrane ephrin with a unique structure, prevents interneuronal axons from exiting the *Drosophila* embryonic CNS. *Development* (2002).129(18): 4205-18.
- Bray, D. Branching patterns of individual sympathetic neurons in culture. *J. Cell Biol.* 56, 702–712 (1973).
- Brieher, W.M., A.S. Yap, and B.M. Gumbiner. 1996. Lateral dimerization is required for the homophilic binding activity of C-cadherin. *J. Cell Biol.* 135: 487–496.
- Brückner, K., E. B. Pasquale and R. Klein. Tyrosine phosphorylation of transmembrane ligands for Eph receptors. *Science* (1997)275: 1640-1643.
- Brückner, K., J. P. Labrador, P. Scheiffele, A. Herb, F. Bradke, P. H. Seeburg and R. Klein. EphrinB ligands recruit GRIP family PDZ adaptor proteins into raft membrane microdomains. *Neuron* (1999)22: 511-524.
- Caviness VS, Jr. 1982. Neocortical histogenesis in normal and reeler mice: a developmental study based upon [3H]thymidine autoradiography. *Brain Res* 256:293–302.

- Chin-Sang, I. D., S. E. George, M. Ding, S. L. Moseley, A. S. Lynch and A. D. Chisholm. The ephrin VAB-2/EFN-1 functions in neuronal signaling to regulate epidermal morphogenesis in *C. elegans*. *Cell* (1999) 99(7): 781-90.
- Chong, L. D., E. K. Park, E. Latimer, R. Friesel and I. O. Daar. Fibroblast growth factor receptor-mediated rescue of x-ephrin B1-induced cell dissociation in *Xenopus* embryos. *Mol Cell Biol* (2000) 20(2): 724-34.
- Contractor, A., C. Rogers, C. Maron, M. Henkemeyer, G. T. Swanson and S. F. Heinemann. Trans-synaptic Eph receptor-ephrin signaling in hippocampal mossy fiber LTP. *Science* (2002) 296(5574): 1864-9.
- Cooke, J. E. and C. B. Moens. Boundary formation in the hindbrain: Eph only it were simple. *Trends Neurosci*(2002) 25(5): 260-7.
- Cowan, C. A. and M. Henkemeyer. The SH2/SH3 adaptor Grb4 transduces B-ephrin reverse signals. *Nature* (2001) 413(6852): 174-9.
- Cruts M, Van Broeckhoven C. 1998. Presenilin mutations in Alzheimer's disease. *Hum Mutat* 11:183-190.
- Dailey, M. E. & Smith, S. J. The dynamics of dendritic structure in developing hippocampal slices. *J. Neurosci.* 16, 2983-2994 (1996).
- Dalva, M. B., M. A. Takasu, M. Z. Lin, S. M. Shamah, L. Hu, N. W. Gale and M. E. Greenberg. EphB receptors interact with NMDA receptors and regulate excitatory synapse formation. *Cell* (2000) 103(6): 945-56.
- Dan, C., Kelly, A., Bernard, O., and Minden, A.. Cytoskeletal changes regulated by the PAK4 serine/threonine kinase are mediated by LIM kinase 1 and cofilin. *J. Biol. Chem.* 2000 276: 32115-32121.
- Davenport RW, Dou P, Rehder V, Kater SB. A sensory role for neuronal growth cone filopodia. *Nature.* 1993 ;361(6414):721-4.
- Davy, A. and S. M. Robbins. Ephrin-A5 modulates cell adhesion and morphology in an integrin-dependent manner. *EMBO J*(2000) 19: 5396-5405.
- Davy, A., N. W. Gale, E. W. Murray, R. A. Klinghoffer, P. Soriano, C. Feuerstein and S. M. Robbins. Compartmentalized signaling by GPI-anchored ephrin-A5 requires

- the Fyn tyrosine kinase to regulate cellular adhesion. *Genes Dev*(1999) 13: 3125-3135.
- Edwards, D.C., Sanders, L.C., Bokoch, G.M., and Gill, G.N. Activation of LIM-kinase by Pak1 couples Rac/Cdc42 GTPase signalling to actin cytoskeletal dynamics. *Nat. Cell Biol* 1999. 1: 253–259.
- Ehlers, M.D. Synapse structure: Glutamate receptors connected by the shanks. *Curr. Biol* 1999. 9: R848–R850.
- Ellis, C., F. Kasmi, P. Ganju, E. Walls, G. Panayotou and A. D. Reith. A juxtamembrane autophosphorylation site in the Eph family receptor tyrosine kinase, Sek, mediates high affinity interaction with p59fyn. *Oncogene* (1996)12: 1727-1736.
- Engert F, Bonhoeffer T: Dendritic spine changes associated with hippocampal long-term synaptic plasticity. *Nature* 1999, 399:66-70.
- Ethell, I. M. and Y. Yamaguchi (1999). Cell surface heparan sulfate proteoglycan syndecan-2 induces the maturation of dendritic spines in rat hippocampal neurons. *J Cell Biol* (1999) 144(3): 575-86.
- Ethell, I. M., F. Irie, M. S. Kalo, J. R. Couchman, E. B. Pasquale and Y. Yamaguchi. EphB/syndecan-2 signaling in dendritic spine morphogenesis. *Neuron*(2001) 31(6): 1001-13.
- Funayama, N., F. Fagotto, P. McCrea, and B.M. Gumbiner. 1995. Embryonic axis induction by the armadillo repeat domain of beta-catenin: evidence for intracellular signaling. *J. Cell Biol.* 128:959Ð968.
- Gale, N. W., P. Baluk, L. Pan, M. Kwan, J. Holash, T. M. DeChiara, D. M. McDonald and G. D. Yancopoulos. Ephrin-B2 selectively marks arterial vessels and neovascularization sites in the adult, with expression in both endothelial and smooth-muscle cells. *Dev Biol*(2001) 230(2): 151-60.
- George, S. E., K. Simokat, J. Hardin and A. D. Chisholm. The VAB-1 Eph receptor tyrosine kinase functions in neural and epithelial morphogenesis in *C. elegans*. *Cell*(1998) 92: 633-643

- Gerety, S. S., H. U. Wang, Z. F. Chen and D. J. Anderson. Symmetrical mutant phenotypes of the receptor EphB4 and its specific transmembrane ligand ephrinB2 in cardiovascular development. *Mol Cell* (1999) 4: 403-414.
- Gerlai, R.. Eph receptors and neural plasticity. *Nat Rev Neurosci*(2001) 2(3): 205-9.
- Giger, R. J., Wolfer, D. P., De Wit, G. M. & Verhaagen, J. Anatomy of rat semaphorin III/collapsin-1 mRNA expression and relationship to developing nerve tracts during neuroembryogenesis. *J. Comp. Neurol.* 375, 378–392 (1996).
- Govek EE, Newey SE, Van Aelst L. The role of the Rho GTPases in neuronal development. *Genes Dev.* 2005 Jan 1;19(1):1-49.
- Grunwald, I. C. and R. Klein. Axon guidance: receptor complexes and signaling mechanisms. *Curr Opin Neurobiol* (2002) 12(3): 250-9.
- Grunwald, I. C., M. Korte, D. Wolfer, G. A. Wilkinson, K. Unsicker, H. P. Lipp, T. Bonhoeffer and R. Klein. Kinase-Independent Requirement of EphB2 Receptors in Hippocampal Synaptic Plasticity. *Neuron* (2001) 32(6): 1027-40.
- Gu, C. and S. Park (2003). The p110 gamma PI-3 kinase is required for EphA8-stimulated cell migration. *FEBS Lett* (2003) 540(1-3): 65-70.
- Gu, C. and S. Park. The EphA8 receptor regulates integrin activity through p110gamma phosphatidylinositol-3 kinase in a tyrosine kinase activity-independent manner. *Mol Cell Biol* (2001) 21(14): 4579-97.
- Hatta K, Takagi S, Fujisawa H, Takeichi M. 1987. Spatial and temporal expression pattern of N-cadherin cell adhesion molecules correlated with morphogenetic processes of chicken embryos. *Dev Biol* 120:215–227.
- Helmchen, F.. Raising the speed limit--fast Ca(2+) handling in dendritic spines. *Trends Neurosci* (2002) 25(9): 438-41.
- Henkemeyer, M., D. Orioli, J. T. Henderson, T. M. Saxton, J. Roder, T. Pawson and R. Klein. Nuk controls pathfinding of commissural axons in the mammalian central nervous system. *Cell* (1996) 86(1): 35-46.
- Hering, H. and M. Sheng. Dendritic spines: structure, dynamics and regulation. *Nat Rev Neurosci* (2001) 2(12): 880-8.

- Himanen, J. P., K. R. Rajashankar, M. Lackmann, C. A. Cowan, M. Henkemeyer and D. B. Nikolov. Crystal structure of an Eph receptor-ephrin complex. *Nature* (2001)414(6866): 933-8.
- Ho C, Zhou J, Medina M, Goto T, Jacobson M, Bhide PG, Kosik KS. Delta-catenin is a nervous system-specific adherens junction protein which undergoes dynamic relocalization during development.. *J Comp Neurol*. 2000 May 1;420(2):261-76.
- Holland, S. J., N. W. Gale, G. Mbamalu, G. D. Yancopoulos, M. Henkemeyer and T. Pawson. Bidirectional signaling through the EPH-family receptor Nuk and its transmembrane ligands. *Nature* (1996) 383: 722-725.
- Horch, H. W., Kruttgen, A., Portbury, S. D. & Katz, L. C. Destabilization of cortical dendrites and spines by BDNF. *Neuron* 23, 353–364 (1999).
- Hoschuetzky, H., H. Aberle, and R. Kemler. 1994. Beta-catenin mediates the interaction of the cadherin-catenin complex with epidermal growth factor receptor. *J. Cell Biol.* 127:1375–1380.
- Huai, J. and U. Drescher. An ephrin-A-dependent signaling pathway controls integrin function and is linked to the tyrosine phosphorylation of a 120-kDa protein. *J Biol Chem* (2001)276: 6689-6694.
- Huang, C., Y. Ni, T. Wang, Y. Gao, C.C. Haudenschild, and X. Zhan. 1997. Down-regulation of the filamentous actin cross-linking activity of cortactin by Src-mediated tyrosine phosphorylation. *J. Biol. Chem.* 272:13911–13915.
- Huynh-Do, U., C. Vindis, H. Liu, D. P. Cerretti, J. T. McGrew, M. Enriquez, J. Chen and T. O. Daniel. Ephrin-B1 transduces signals to activate integrin-mediated migration, attachment and angiogenesis. *J Cell Sci* (2002) 115(Pt 15): 3073-81.
- Ide, N., Hata, Y., Deguchi, M., Hirao, K., Yao, I., and Takai, Y. Interaction of S-SCAM with neural plakophilin-related Armadillo-repeat protein/delta-catenin. *Biochem. Biophys. Res. Commun.* (1999) 256, 456–461.
- Ide, N., Hata, Y., Deguchi, M., Hirao, K., Yao, I., Takai, Y., 1999. Interaction of S-SCAM with neural plakophilin-related Armadillo-repeat protein/delta-catenin. *Biochem. Biophys. Res. Commun.* 256, 456–461.

Irie, F. and Yamaguchi, Y. EphB receptors regulate dendritic spine development via intersectin,

Cdc42 and N-WASP. *Nat. Neurosci* 2002. 5: 1117–1118.

Israely I, Costa RM, Xie CW, Silva AJ, Kosik KS, Liu X. Deletion of the neuron-specific protein

delta-catenin leads to severe cognitive and synaptic dysfunction. *Curr Biol*. 2004

Sep

21;14(18):1657-63.

Jaffer, Z.M. and Chernoff, J. p21-activated kinases: three more join the Pak. *Int. J. Biochem. Cell*

Biol 2002. 34: 713–717.

Jan YN, Jan LY: The control of dendrite development. *Neuron* 2003, 40:229-242.

Jones SB, Lanford GW, Chen YH, Moribito M, Kim K, Lu Q. Glutamate-induced delta-catenin

redistribution and dissociation from postsynaptic receptor complexes.

Neuroscience.

2002;115(4):1009-21.

Jou, T., D. Steward, J. Stappert, W. Nelson, and J. MARRS. 1995. Genetic and biochemical dissection of protein linkages in the cadherin-catenin complex. *Proc. Natl. Acad. Sci. USA*. 92:5067–5071.

Kalo, M. S., H. H. Yu and E. B. Pasquale. In vivo tyrosine phosphorylation sites of activated ephrin-B1 and ephB2 from neural tissue. *J Biol Chem* (2001) 276(42): 38940-8.

Kim, A.S., Kakalis, L.T., Abdul-Manan, N., Liu, G.A., and Rosen, M.K.. Autoinhibition and

activation mechanisms of the Wiskott-Aldrich syndrome protein. *Nature* 2000 404: 151–158.

Kim K, Sirota A, Chen Yh YH, Jones SB, Dudek R, Lanford GW, Thakore C, Lu Q. Dendrite-

like process formation and cytoskeletal remodeling regulated by delta-catenin expression. *Exp Cell Res*. 2002 May 1;275(2):171-84.

Kim, K., Pang, K. M., Evans, M., and Hay, E. D. (2000). Overexpression of beta-catenin induces

- apoptosis independent of its transactivation function with LEF-1 or the involvement of major G1 cell cycle regulators. *Mol. Biol. Cell* 11, 3509–3523.
- Kimura, K., Ito, M., Amano, M., Chihara, K., Fukata, Y., Nakafuku, M., Yamamori, B., Feng, J., Nakano, T., Okawa, K., et al. Regulation of myosin phosphatase by Rho and Rho associated kinase (Rho-kinase). *Science* 1996 273: 245–248
- Koleske AJ, Gifford AM, Scott ML, Nee M, Bronson RT, Miczek KA, Baltimore D. 1998. Essential roles for the Abl and Arg tyrosine kinases in neurulation. *Neuron* 21:1259–1272.
- Lanier LM, Gates MA, Witke W, Menzies AS, Wehman AM, Macklis JD, Kwiatkowski D, Soriano P, Gertler FB. 1999. Mena is required for neurulation and commissure formation. *Neuron* 22:313–325.
- Lanier LM, Gertler FB. 2000. From Abl to actin: Abl tyrosine kinase and associated proteins in growth cone motility. *Curr Opin Neurobiol* 10: 80–87.
- Lee T, Winter C, Marticke SS, Lee A, Luo L: Essential roles of Drosophila RhoA in the regulation of neuroblast proliferation and dendritic but not axonal morphogenesis. *Neuron* 2000, 25:307-316.
- Lein, P., Johnson, M., Guo, X., Rueger, D. & Higgins, D. Osteogenic protein-1 induces dendritic growth in rat sympathetic neurons. *Neuron* 15, 597–605 (1995).
- Le Roux P, Behar S, Higgins D, Charette M OP-1 enhances dendritic growth from cerebral cortical neurons in vitro. *Exp Neurol.* 1999 Nov;160(1):151-63
- Leung, T., Chen, X.Q., Manser, E., and Lim, L.. The p160 RhoA-binding kinase ROK is a member of a kinase family and is involved in the reorganization of the cytoskeleton. *Mol. Cell. Biol.* 1996 16: 5313–5327.
- Leung, T., Manser, E., Tan, L., and Lim, L.. A novel serine/threonine kinase binding the Ras-related RhoA GTPase which translocates the kinase to peripheral membranes. *J. Biol. Chem* 1995. 270: 29051–29054.

- Levitt P, Rakic P. 1982. The time of genesis, embryonic origin and differentiation of the brain stem monoamine neurons in the rhesus monkey. *Brain Res* 256:35–57.
- Li Z, Aizenman CD, Cline HT: Regulation of Rho GTPases by crosstalk and neuronal activity in vivo. *Neuron* 2002, 33:741-750.
- Li Z, Van Aelst L, Cline HT: Rho GTPases regulate distinct aspects of dendritic arbor growth in *Xenopus* central neurons in vivo. *Nat Neurosci* 2000, 3:217-225.
- Lin, D., G. D. Gish, Z. Songyang and T. Pawson. The carboxyl terminus of B class ephrins constitutes a PDZ domain binding motif. *J Biol Chem*(1999) 274: 3726-3733.
- Lisman, J. Actin's actions in LTP-induced synapse growth. *Neuron* 2003 38: 361–362.
- Lu, Q., E. E. Sun, R. S. Klein and J. G. Flanagan. Ephrin-B reverse signaling is mediated by a novel PDZ-RGS protein and selectively inhibits G protein-coupled chemoattraction. *Cell*(2001) 105: 69-79.
- Lu Q, Mukhopadhyay NK, Griffin JD, Paredes M, Medina M, Kosik KS. Brain armadillo protein delta-catenin interacts with Abl tyrosine kinase and modulates cellular morphogenesis in response to growth factors. *J Neurosci Res.* 2002 Mar 1;67(5):618-24.
- Lu Q, Paredes M, Medina M, Zhou J, Cavallo R, Peifer M, Orecchio L, Kosik KS. delta-catenin, an adhesive junction-associated protein which promotes cell scattering. *J Cell Biol.* 1999 Feb 8;144(3):519-32.
- Luo L, Hensch TK, Ackerman L, Barbel S, Jan LY, Jan YN: Differential effects of the Rac GTPase on Purkinje cell axons and dendritic trunks and spines. *Nature* 1996, 379:837-840.
- Luo, Y., Raible, D. & Raper, J. A. Collapsin: a protein in brain that induces the collapse and paralysis of neuronal growth cones. *Cell* 75, 217–227 (1993). 31. Messersmith, E. K. *et al.* Semaphorin III can function as a selective chemorepellent to pattern sensory projections in the spinal cord. *Neuron* 14, 949–959 (1995).
- Ma, X.M., Huang, J., Wang, Y., Eipper, B.A., and Mains, R.E. Kalirin, a multifunctional Rho

- guanine nucleotide exchange factor, is necessary for maintenance of hippocampal pyramidal neuron dendrites and dendritic spines. *J. Neurosci.* 2003 23: 10593–10603.
- Machesky, L.M. and Insall, R.H. Signaling to actin dynamics. *J. Cell Biol* 1999. 146: 267–272.
- Maekawa, M., Ishizaki, T., Boku, S., Watanabe, N., Fujita, A., Iwamatsu, A., Obinata, T., Ohashi, K., Mizuno, K., and Narumiya, S. Signaling from Rho to the actin cytoskeleton through protein kinases ROCK and LIM-kinase. *Science* 1999. 285: 895–898.
- Marrs, J.A., and W.J. Nelson. 1996. Cadherin cell adhesion molecules in differentiation and embryogenesis. *Int. Rev. Cytol.* 165:159–205.
- Martinez MC, Ochiishi T, Majewski M, Kosik KS. Dual regulation of neuronal morphogenesis by a delta-catenin-cortactin complex and Rho. *J Cell Biol.* 2003 Jul 7;162(1):99-111. Epub 2003 Jun 30.
- Matsui, T., Amano, M., Yamamoto, T., Chihara, K., Nakafuku, M., Ito, M., Nakano, T., Okawa, K., Iwamatsu, A., and Kaibuchi, K.. Rho-associated kinase, a novel serine/threonine kinase, as a putative target for small GTP binding protein Rho. *EMBO J* 1996. 15: 2208–2216.
- May, R.C. 2001. The Arp2/3 complex: a central regulator of the actin cytoskeleton. *Cell. Mol. Life Sci.* 58:1607–1626.
- McAllister AK, Katz LC, Lo DC: Opposing roles for endogenous BDNF and NT-3 in regulating cortical dendritic growth. *Neuron* 1997, 18:767-778.
- McAllister AK, Lo DC, Katz LC: Neurotrophins regulate dendritic growth in developing visual cortex. *Neuron* 1995, 15:791-803.
- McAllister, A. K., Katz, L. C. & Lo, D. C. Neurotrophin regulation of cortical dendritic growth requires activity. *Neuron* 17, 1057–1064 (1996).

- McAllister, A. K., Lo, D. C. & Katz, L. C. Neurotrophins regulate dendritic growth in developing visual cortex. *Neuron* 15, 791–803 (1995).
- McLaughlin, T., R. Hindges and D. D. O'Leary. Regulation of axial patterning of the retina and its topographic mapping in the brain. *Curr Opin Neurobiol*(2003) 13(1): 57-69.
- Mellitzer, G., Q. Xu and D. G. Wilkinson. Eph receptors and ephrins restrict cell intermingling and communication. *Nature* (1999)400(6739): 77-81
- Miao, H., E. Burnett, M. Kinch, E. Simon and B. Wang. Activation of EphA2 kinase suppresses integrin function and causes focal-adhesion-kinase dephosphorylation. *Nat Cell Biol* (2000).2(2): 62-9.
- Miki, H., Suetsugu, S., and Takenawa, T. WAVE, a novel WASP-family protein involved in actin reorganization induced by Rac. *EMBO J* 1998. 17: 6932–6941
- Murai, K. K. and E. B. Pasquale. Can Eph receptors stimulate the mind? *Neuron*(2002) 33(2): 159-62.
- Nagafuchi, A., and M. Takeichi. 1988. Cell binding function of E-cadherin is regulated by the cytoplasmic domain. *EMBO (Eur. Mol. Biol. Organ.) J*.7:3679–3684.
- Nakagawa, O., Fujisawa, K., Ishizaki, T., Saito, Y., Nakao, K., and Narumiya, S.. ROCK-I and ROCK-II, two isoforms of Rho-associated coiled-coil forming protein serine/threonine kinase in mice. *FEBS Lett* 1996. 392: 189–193.
- Nakayama AY, Harms MB, Luo L: Small GTPases Rac and Rho in the maintenance of dendritic spines and branches in hippocampal pyramidal neurons. *J Neurosci* 2000, 20:5329-5338.
- Nakayama, A.Y., M.B. Harms, and L. Luo. 2000. Small GTPases Rac and Rho in the maintenance of dendritic spines and branches in hippocampal pyramidal neurons. *J. Neurosci.* 20:5329–5338.
- Nedivi, E., Wu, G. Y. & Cline, H. T. Promotion of dendritic growth by CPG15, an activity-induced signalling molecule. *Science* 281, 1863–1866 (1998).

- Neumann, H., R. Schweigreiter, T. Yamashita, K. Rosenkranz, H. Wekerle, and Y.A. Barde. 2002. Tumor necrosis factor inhibits neurite outgrowth and branching of hippocampal neurons by a rho-dependent mechanism. *J. Neurosci.* 22:854–862
- Noren, N.K., B.P. Liu, K. Burrige, and B. Kreft. 2000. p120 catenin regulates the actin cytoskeleton via Rho family GTPases. *J. Cell Biol.* 150:567–580.
- O’Leary, D. D. M. & Terashima, T. Cortical axons branch to multiple subcortical targets by interstitial axon budding: implications for target recognition and “waiting periods.” *Neuron* 1, 901–910 (1988).
- Ohashi, K., Nagata, K., Maekawa, M., Ishizaki, T., Narumiya, S., and Mizuno, K. Rho-associated kinase ROCK activates LIM-kinase 1 by phosphorylation at threonine 508 within the activation loop. *J. Biol. Chem* 2000. 275: 3577–3582.
- O’Leary, D. D. and D. G. Wilkinson. Eph receptors and ephrins in neural development. *Curr Opin Neurobiol*(1999) 9(1): 65-73.
- Orioli, D., M. Henkemeyer, G. Lemke, R. Klein and T. Pawson. Sek4 and Nuk receptors cooperate in guidance of commissural axons and in palate formation. *Embo J* (1996)15(22): 6035-49.
- Ozawa, M., and R. Kemler. 1998. The membrane-proximal region of the E-cadherin cytoplasmic domain prevents dimerization and negatively regulates adhesion activity. *J. Cell Biol.* 142:1605–1613.
- Ozawa, M., and R. Kemler. 1998. The membrane-proximal region of the E-cadherin cytoplasmic domain prevents dimerization and negatively regulates adhesion activity. *J. Cell Biol.* 142:1605–1613.
- Ozawa, M., H. Baribault, and R. Kemler. 1989. The cytoplasmic domain of the cell adhesion molecule uvomorulin associates with three independent proteins structurally related in different species. *EMBO (Eur. Mol. Biol. Organ.) J.* 8:1711–1717.
- Paffenholz R, Kuhn C, Grund C, Stehr S, Franke WW. 1999. The armrepeat protein NPRAP

- (neurojungin) is a constituent of the plaques of the outer limiting zone in the retina, defining a novel type of adhering junction. *Exp Cell Res* 250:452–464.
- Palmer, A. and R. Klein. Multiple roles of ephrins in morphogenesis, neuronal networking, and brain function. *Genes Dev*(2003) 17(12): 1429-50.
- Park, E., Na, M., Choi, J., Kim, S., Lee, J.R., Yoon, J., Park, D., Sheng, M., and Kim, E. The Shank family of postsynaptic density proteins interacts with and promotes synaptic accumulation of the γ -PIX guanine nucleotide exchange factor for Rac1 and Cdc42. *J. Biol. Chem* 2003. 278: 19220–19229
- Penzes, P., Beeser, A., Chernoff, J., Schiller, M.R., Eipper, B.A., Mains, R.E., and Huganir, R.L.. Rapid induction of dendritic spine morphogenesis by trans-synaptic ephrinB-EphB receptor activation of the Rho-GEF kalirin. *Neuron* 2003 37: 263–274.
- Penzes, P., Johnson, R.C., Alam, M.R., Kambampati, V., Mains, R.E., and Eipper, B.A. An isoform of kalirin, a brainspecific GDP/GTP exchange factor, is enriched in the postsynaptic density fraction. *J. Biol. Chem* 2000. 275: 6395–6403.
- Penzes, P., Johnson, R.C., Sattler, R., Zhang, X., Huganir, R.L., Kambampati, V., Mains, R.E., and Eipper, B.A. The neuronal Rho-GEF Kalirin-7 interacts with PDZ domain containing proteins and regulates dendritic morphogenesis. *Neuron* 2001 29: 229–242.
- Pilpel, Y. and Segal, M. Activation of PKC induces rapid morphological plasticity in dendrites of hippocampal neurons via Rac and Rho-dependent mechanisms. *Eur. J. Neurosci* 2004. 19: 3151–3164.
- Polakis, P. Wnt signalling and cancer. *Genes Dev.* 2000. 14(15):1837-51.
- Pollard, T.D., Blanchoin, L., and Mullins, R.D.. Molecular mechanisms controlling actin filament dynamics in nonmuscle cells. *Annu. Rev. Biophys. Biomol. Struct* 2000. 29: 545–576.
- Polleux, F., Giger, R. J., Ginty, D. D., Kolodkin, A. L. & Ghosh, A. Patterning of cortical efferent projections by semaphorin-neuropilin interactions. *Science* 282, 1904–1906 (1998).

- Polleux, F., Morrow, T. & Ghosh, A. Semaphorin 3A is a chemoattractant for cortical apical dendrites. *Nature* 404, 567–573 (2000).
- Rimm, D.L., E.R. Koslov, P. Kebraiaei, C.D. Cianci, and J.S. Morrow. 1995. Alpha1 (E)-catenin is an actin-binding and -bundling protein mediating the attachment of F-actin to the membrane adhesion complex. *Proc. Natl. Acad. Sci. USA*. 92:8813–8817.
- Rohatgi, R., Ma, L., Miki, H., Lopez, M., Kirchhausen, T., Takenawa, T. and Kirschner, M.W. The interaction between N-WASP and the Arp2/3 complex links Cdc42-dependent signals to actin assembly. *Cell* 1999 97: 221–231.
- Ruchhoeft ML, Ohnuma S, McNeill L, Holt CE, Harris WA: The neuronal architecture of *Xenopus* retinal ganglion cells is sculpted by rho-family GTPases in vivo. *J Neurosci* 1999, 19:8454-8463.
- Ruchhoeft ML, Ohnuma S, McNeill L, Holt CE, Harris WA: The neuronal architecture of *Xenopus* retinal ganglion cells is sculpted by rho-family GTPases in vivo. *J Neurosci* 1999, 19:8454-8463.
- Sanders, L.C., Matsumura, F., Bokoch, G.M., and de Lanerolle, P. Inhibition of myosin light chain kinase by p21-activated kinase. *Science* 1999 283: 2083–2085.
- Schuman EM: Neurotrophin regulation of synaptic transmission. *Curr Opin Neurobiol* 1999, 9:105-109.
- Scott EK, Luo L. How do dendrites take their shape? *Nat Neurosci*. 2001 Apr;4(4):359-65.
- Scully, A. L., M. McKeown and J. B. Thomas. Isolation and characterization of Dek, a *Drosophila* eph receptor protein tyrosine kinase. *Mol Cell Neurosci* (1999)13(5): 337-47.
- Shamah, S. M., M. Z. Lin, J. L. Goldberg, S. Estrach, M. Sahin, L. Hu, M. Bazalakova, R. L. Neve, G. Corfas, A. Debant and M. E. Greenberg. EphA receptors regulate growth cone dynamics through the novel guanine nucleotide exchange factor ephexin. *Cell*(2001) 105(2): 233-44.
- Shen J, Bronson T, Chjen DF, Xia W, Selkoe DJ, Tonegawa S. 1997. Skeletal and CNS defects in *presenilin-1*-deficient mice. *Cell* 89:629–639.

- Shin, D., G. Garcia-Cardena, S. Hayashi, S. Gerety, T. Asahara, G. Stavrakis, J. Isner, J. Folkman, M. A. Gimbrone, Jr. and D. J. Anderson. Expression of ephrinB2 identifies a stable genetic difference between arterial and venous vascular smooth muscle as well as endothelial cells, and marks subsets of microvessels at sites of adult neovascularization. *Dev Biol*(2001) 230(2): 139-50.
- Sholl, DA (1953) Dendritic Organization in the Neurons of the Visual and Motor Cortices of the Cat. *J. Anat.* 87:387-406.
- Simons, K. and D. Toomre. Lipid Rafts and signal transduction. *Nat Rev Mol Cell Biol*(2000) 1: 31-39.
- Sin WC, Haas K, Ruthazer ES, Cline HT: Dendrite growth increased by visual activity requires NMDA receptor and Rho GTPases. *Nature* 2002, 419:475-480.
- Sanyon, C.A. and Bernard, O. LIM-kinase1. *Int. J. Biochem. Cell Biol* 1999.. 31: 389–394.
- Stein, E., A. A. Lane, D. P. Cerretti, H. O. Schoecklmann, A. D. Schroff, R. L. Van Etten and T. O. Daniel. Eph receptors discriminate specific ligand oligomers to determine alternative signaling complexes, attachment, and assembly responses. *Genes Dev*(1998) 12(5): 667-78.
- Suetsugu, S., Miki, H., and Takenawa, T.. Identification of two human WAVE/SCAR homologues as general actin regulatory molecules which associate with the Arp2/3 complex. *Biochem. Biophys. Res. Commun*1999. 260: 296–302.
- Sumi, T., Matsumoto, K., and Nakamura, T. Specific activation of LIM kinase 2 via phosphorylation of threonine 505 by ROCK, a Rho-dependent protein kinase. *J. Biol.Chem* 2001. 276: 670–676.
- Sumi, T., Matsumoto, K., Takai, Y., and Nakamura, T. Cofilin phosphorylation and actin cytoskeletal dynamics regulated by rho- and Cdc42-activated LIM-kinase 2. *J. Cell Biol* 1999. 147: 1519–1532.
- Takasu, M. A., M. B. Dalva, R. E. Zigmond and M. E. Greenberg. Modulation of NMDA receptor-dependent calcium influx and gene expression through EphB receptors. *Science*(2002) 295(5554): 491-5.
- Takeichi, M. 1991. Cadherin cell adhesion receptors as a morphogenetic regulator. *Science*. 251:1451D1455.

Takeichi, M. 1995. Morphogenetic roles of classic cadherins. *Curr. Opin. CellBiol.* 7:619-627.

Tashiro A, Minden A, Yuste R: Regulation of dendritic spine morphology by the rho family of small GTPases: antagonistic roles of Rac and Rho. *Cereb Cortex* 2000, 10:927-938.

Tashiro, A. and Yuste, R. Regulation of dendritic spine motility and stability by Rac1 and Rho kinase: Evidence for two forms of spine motility. *Mol. Cell. Neurosci* 2004. 26: 429-440.

Tashiro, A., Minden, A., and Yuste, R. Regulation of dendritic spine morphology by the rho family of small GTPases: Antagonistic roles of Rac and Rho. *Cereb. Cortex* 2000 10: 927-938.

Tepass, U., D. Godt and R. Winklbauer. Cell sorting in animal development: signalling and adhesive mechanisms in the formation of tissue boundaries. *Curr Opin Genet Dev* (2002)12(5): 572-82.

Thomas, S. M. and J. S. Brugge. Cellular functions regulated by Src family kinases. *Annu Rev Cell Dev Biol* (1997)13: 513-609.

Torres, R., B. L. Firestein, H. Dong, J. Staudinger, E. N. Olson, R. L. Huganir, D. S. Bredt, N. W. Gale and G. D. Yancopoulos. PDZ proteins bind, cluster and synaptically co-localize with Eph receptors and their ephrin ligands. *Neuron*(1998) 21: 1453-1463.

Tu, J.C., Xiao, B., Naisbitt, S., Yuan, J.P., Petralia, R.S., Brakeman, P., Doan, A., Aakalu, V.K., Lanahan, A.A., Sheng, M., et al. Coupling of mGluR/Homer and PSD-95 complexes by the Shank family of postsynaptic density proteins. *Neuron* 1999 23: 583-592.

Uchida N, Honjo Y, Johnson KR, Wheelock MJ, Takeichi M. 1996. The catenin/cadherin adhesion system is localized in synaptic junctions bordering transmitter release zones. *J Cell Biol* 135:767-779.

Van Aelst L, Cline HT. Rho GTPases and activity-dependent dendrite development. *Curr Opin Neurobiol.* 2004 Jun;14(3):297-304.

Van Etten RA. 1999. Cycling, stressed-out and nervous: cellular functions of c-Abl. *Trends Cell Biol* 9:179-186.

- Wahl, S., H. Barth, T. Ciossek, K. Aktories and B. K. Mueller. Ephrin-A5 induces collapse of growth cones by activating Rho and Rho kinase. *J Cell Biol*(2000) 149(2): 263-70.
- Wang, H. U., Z.-F. Chen and D. J. Anderson. Molecular Distinction and Angiogenic Interaction between Embryonic Arteries and Veins Revealed by ephrin-B2 and Its Receptor Eph-B4. *Cell* (1998) 93: 741-753.
- Wang, H. U., Z.-F. Chen and D. J. Anderson. Molecular Distinction and Angiogenic Interaction between Embryonic Arteries and Veins Revealed by ephrin-B2 and Its Receptor Eph-B4. *Cell*(1998) 93: 741-753.
- Weaver, A.M., A.V. Karginow, A.W. Kinley, S.A. Weed, Y. Li, J.T. Parsons, and J.A. Cooper.
2001. Cortactin promotes and stabilizes Arp2/3-induced actin filament network formation.
Curr. Biol. 11:370–374.
- Weaver, A.M., J.E. Heuser, A.V. Karginov, W.L. Lee, J.T. Parsons, and J.A. Cooper. 2002.
Interaction of cortactin and N-WASp with Arp2/3 complex. *Curr. Biol.* 12:1270–1278
- Weed, S.A., and J.T. Parsons. 2001. Cortactin: coupling membrane dynamics to cortical actin assembly. *Oncogene.* 20:6418–6434.
- Wilkinson, D. G. Eph receptors and ephrins: regulators of guidance and assembly. *International Review of Cytology* (2000).: 196177-244.
- Wilkinson, D. G. Multiple roles of EPH receptors and ephrins in neural development. *Nat Rev.Neurosci*_(2001) 2(3): 155-64.
- Wilkinson, D. G. Multiple roles of EPH receptors and ephrins in neural development. *Nat Rev Neurosci* (2001). 2(3): 155-64.
- Wilkinson, D. G. Topographic mapping: organising by repulsion and competition? *Curr Biol* (2000). 10(12): R447-51.
- Wilkinson, D. G.. Eph receptors and ephrins: regulators of guidance and assembly. *International Review of Cytology*(2000) 196: 177-244.
- Wilkinson, D. G.. Topographic mapping: organising by repulsion and competition? *Curr Biol*(2000) 10(12): R447-51.

- Wong P, Zheng H, Chen H, Becher M, Sirinathsinghji D, Trumbauer M, Chen H, Price D, Van
 fer Ploeg L, Sisodia S. 1997. Presenilin 1 is required for Notch 1 and D11 1
 expression in
 the paraxial mesoderm. *Nature* 387:288–292.
- Wong WT, Faulkner-Jones BE, Sanes JR, Wong RO: Rapid dendritic remodeling in the
 developing retina: dependence on neurotransmission and reciprocal regulation by
 Rac and
 Rho. *J Neurosci* 2000, 20:5024-5036.
- Xu, Q., G. Mellitzer, V. Robinson and D. G. Wilkinson. In vivo cell sorting in
 complementary segmental domains mediated by Eph receptors and ephrins.
Nature (1999)399(6733): 267-71.
- Yamazaki, D., Suetsugu, S., Miki, H., Kataoka, Y., Nishikawa, S., Fujiwara, T., Yoshida,
 N., and
 Takenawa, T. WAVE2 is required for directed cell migration and cardiovascular
 development. *Nature* 2003 424: 452–456.
- Yan, C., Martinez-Quiles, N., Eden, S., Shibata, T., Takeshima, F., Shinkura, R.,
 Fujiwara, Y.,
 Bronson, R., Snapper, S.B., Kirschner, M.W., et al.. WAVE2 deficiency reveals
 distinct roles in embryogenesis and Rac-mediated actin-based motility. *EMBO J*
 2003. 22: 3602–3612
- Yang, N., Higuchi, O., Ohashi, K., Nagata, K., Wada, A., Kangawa, K., Nishida, E., and
 Mizuno,
 K. Cofilin phosphorylation by LIM-kinase 1 and its role in Rac-mediated actin
 reorganization. *Nature* 1998 393: 809–812.
- Yap, A.S., C.M. Niessen, and B.M. Gumbiner. 1998. The juxtamembrane region of the
 cadherin
 cytoplasmic tail supports lateral clustering, adhesive strengthening, and
 interaction with
 p120. *J. Cell Biol.* 141:779–789.
- Yap, A.S., W.M. Briehner, and B.M. Gumbiner. 1997. Molecular and functional analysis of
 of
 cadherin-based adherens junctions. *Annu. Rev. Cell Dev. Biol.* 13:119–146.
- Yu X, Malenka RC: Beta-catenin is critical for dendritic morphogenesis. *Nat Neurosci*
 2003,
 6:1169-1177.

- Yu, H. H., A. H. Zisch, V. C. Dodelet and E. B. Pasquale. Multiple signaling interactions of Abl and Arg kinases with the EphB2 receptor. *Oncogene*(2001) 20(30): 3995-4006.
- Yu, T. W. and C. I. Bargmann. Dynamic regulation of axon guidance. *Nat Neurosci* (2001) 4(Suppl): 1169-76.
- Yu, W., Ahmad, F. J. & Baas, P. W. Microtubule fragmentation and partitioning in the axon during collateral branch formation. *J. Neurosci.* 14, 5872–5884 (1994).
- Zhang, H., Webb, D.J., Asmussen, H., and Horwitz, A.F. Synapse formation is regulated by the signaling adaptor GIT1. *J. Cell Biol* 2003. 161: 131–142.
- Zhou J, Liyanage U, Medina M, Ho C, Simmons AD, Lovett M, Kosik KS.1997. Presenilin 1 interaction in the brain with a novel member of the armadillo family. *NeuroReport* 8:2085–2090.
- Zisch, A. H., M. S. Kalo, L. D. Chong and E. B. Pasquale. Complex formation between EphB2 and Src requires phosphorylation of tyrosine 611 in the EphB2 juxtamembrane region. *Oncogene*(1998) 16(20): 2657-70.
- Zou, J. X., B. Wang, M. S. Kalo, A. H. Zisch, E. B. Pasquale and E. Ruoslahti. An Eph receptor regulates integrin activity through R-Ras. *Proc Natl Acad Sci U S A*(1999) 96(24): 13813-8.
- Zukerberg LR, Patrick GN, Nikolic M, Humbert S, Wu CL, Lanier LM, Gertler FB, Vidal M, Van Etten RA, Tsai LH. 2000. Cables links Cdk5 and c-Abl and facilitates Cdk5 tyrosine phosphorylation, kinase upregulation, and neurite outgrowth. *Neuron* 26:633–646.

10. CURRICULUM VITAE

Last Name: Dolce
First Name: Luca
Date and Place of Birth: July 14th, 1975. Palermo, Italy

Education

- 01/08/01 to present: Continuation of **PhD.-studies** in the laboratory of Dr. Rüdiger Klein at Max-Planck Institute of Neurobiology, Munich, Germany.
- 07/02/01 to 31/07/01: Begin of **PhD.-studies** in the laboratory of Dr. Rüdiger Klein at European Molecular Biology Laboratories (EMBL), Heidelberg, Germany.
- 2000 - 2001: **Euro Community Fellowship in Transplant medicine,**
Istituto Mediterraneo per i Trapianti e Terapie ad Alta Specializzazione (ISMETT), Palermo, Italy.
- 1994 - 1999: **Master degree, Summa Cum Laude, in Biological Sciences.**
University of Palermo, Italy. Specialization in Molecular Biology and Genetic Engineering.
Thesis title: “Construction of a High Molecular Weight Genomic Library of *Streptomyces coelicolor* A3(2) in Artificial Chromosomes ”.
- Sept/1997 - Oct/1998: **Erasmus Scheme,**
University of Wales, Swansea, UK
- Sept/1989 - Jun/1994: Liceo Classico “G. Ugdulena”, Termini Imerese (PA), Italy.
High School with a specialization in humanistic subjects.
- Sept/1981- Jun/1989: Primary and Secondary Education completed in Caccamo (PA), Italy